Theses and Dissertations

8-2013

Characterization and Quantification of Monomers, Oligomers, and By-products from Switchgrass Hemicelluloses during Biomass Pretreatment

Kris Allan Bunnell
University of Arkansas, Fayetteville

Follow this and additional works at: http://scholarworks.uark.edu/etd

Part of the Biochemical and Biomolecular Engineering Commons, and the Bioresource and Agricultural Engineering Commons

Characterization and Quantification of Monomers, Oligomers, and By-products from Switchgrass Hemicelluloses during Biomass Pretreatment

Characterization and Quantification of Monomers, Oligomers, and By-products from
Switchgrass Hemicelluloses during Biomass Pretreatment

A dissertation submitted in partial fulfillment
of the requirements for the degree of
Doctor of Philosophy in Biological Engineering

by

Kris Bunnell
University of Arkansas
Bachelor of Science in Biological Engineering, 2009

August 2013
University of Arkansas

This dissertation is approved for recommendation to the Graduate Council.

_____

Dr. Danielle Julie Carrier

Dissertation Director

_____   _____

Dr. Edgar C. Clausen   Dr. Jackson O. Lay Jr.

Committee Member   Committee Member

_____   _____

Dr. Jin-Woo Kim   Dr. Greg J. Thoma

Committee Member   Committee Member

ABSTRACT

Production of fuels and chemicals from biomass is contingent upon economical release of carbohydrates from biomass. Carbohydrates can then be used for production of bio-based products using a biochemical conversion process. Pretreatment, the first step of the biochemical conversion process, has been suggested to be the most costly step of the conversion process. Thus, better understanding the behavior of biomass during pretreatment is imperative for an economically viable production of biofuels and chemicals. Elucidating the physicochemical properties of biomass and developing an understanding the depolymerization patterns of biomass during pretreatment will help progress towards this goal.

In this study, July- and February-harvested switchgrass hemicelluloses were extracted and characterized for monosaccharide constituents, glycosyl linkages, and molecular size using acid hydrolysis, per-O-methylation analysis, and size exclusion chromatography, respectively. The results revealed that the July hemicelluloses contained 13% glucose, 67% xylose, and 19% arabinose, and the February hemicelluloses contained 4.8% glucose, 79% xylose, and 16% arabinose. Glycosyl linkage analysis revealed both hemicelluloses to have similar linkages but in different proportions. Size exclusion chromatography showed that the July hemicelluloses had an average molecular weight of 30,000 g mol^{-1}, and the February hemicelluloses had an average molecular weight of 28,000 g mol^{-1}.

Once characterized, extracted hemicelluloses were used as feedstock for production of xylose oligomers that were then fractionated using centrifugal partition chromatography (CPC) with a butanol:methanol:water (5:1:4, V:V:V) solvent system. Xylose oligomers with a degree of polymerization (DP) from two to six were successfully produced via autohydrolysis and fractionated via CPC. Yields for xylobiose (DP2), xylotriose (DP3), xylotetraose (DP4),

xylopentose (DP5), and xylohexose (DP6) were 24, 34, 23, 19, and 38 mg, respectively, per g of hemicelluloses. Purities, as calculated by mass of a given oligomer divided by the total mass of detected oligomers and degradation products and then reported on a percent basis, were 75, 89, 87, 77, and 69% for DP2, DP3, DP4, DP5, and DP6, respectively.

Lastly, depolymerization patterns of CPC-fractionated xylose oligomers were investigated through pretreatment studies and subsequent kinetic modeling. DP6 was pretreated using water at 160 and 180 ^{o}C and 1.0 wt % sulfuric acid at 160 ^{o}C. Modeling results revealed that degradation rate constants increased with increasing temperature and acid concentrations, and that acid promotes cleavage of end bonds over interior bonds in xylose oligomers.

ACKNOWLEDGMENTS

TABLE OF CONTENTS

1.0 INTRODUCTION

The depletion of petroleum reserves, environmental impact concerns, and energy independence and security have contributed to resurgence in developing alternative energy sources (Himmel *et al.*, 2007). Although there are several alternative energy options available (solar, nuclear, geothermal, hydroelectric, wind, etc.), conversion of biomass to energy is the only option that can generate liquid transportation fuels in the short term. Being such, the Energy Independence and Security Act of 2007 (EISA, 2007) mandated that the United States produces 36 billion gallons of renewable fuel per year by 2022, of which 21 billion gallons must be from feedstocks other than corn starch and 16 billion gallons must be from cellulosic biomass. **Figure 1** displays the annual renewable fuel production mandates as outlined by EISA 2007.

Current first generation biomass to energy technologies rely on conversion of sugars, starches, or oils (Sims *et al.*, 2010). In the United States, the current bioethanol industry is reliant upon conversion of corn starch; the starch is enzymatically hydrolyzed to glucose before being fermented to ethanol. In Brazil, bioethanol is produced from sugarcane. Sugarcane is mechanically pressed, releasing a sucrose stream that is fermented to ethanol. These conversion technologies are relatively simple because of the nature of the feedstocks; however, both feedstocks are used for food and feed production, which generates the food/feed-for-fuel debate. Thus, there has been intensive research into the development of second generation biofuels, or biofuels that are generated using cellulosic or non-sugar/starch feedstocks.
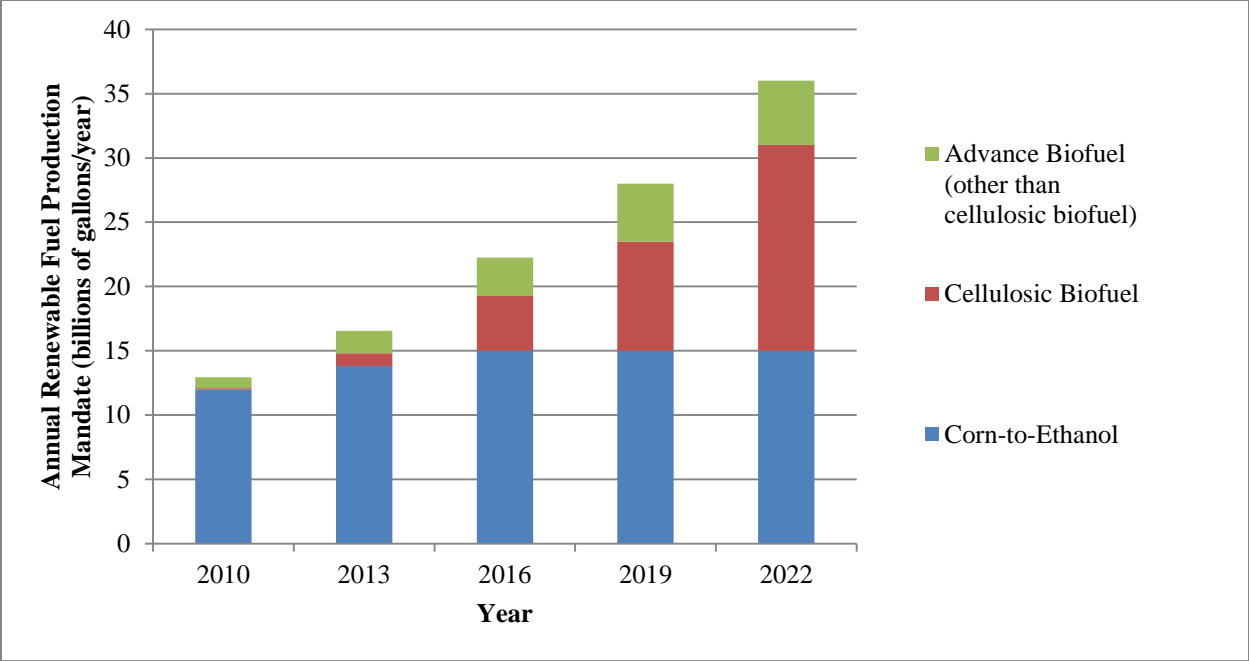
Figure 1: Annual renewable fuel production mandates as outlined in the Energy Independence and Security Act of 2007.

Biomass for second generation biofuels can originate from a plethora of sources, including municipal wastes, agricultural residues (corn stover, wheat straw, rice straw, sugarcane bagasse, etc.), or dedicated energy crops (switchgrass, miscanthus, sorghum, willow, poplar, etc.). The conversion of these feedstocks to fuels and chemicals is inherently more complicated because of their complex structure and composition. In the case of agricultural residues and dedicated energy crops, biomass is composed of primarily cellulose, hemicelluloses, and lignin. These natural polymers have been developed by nature to withstand environmental stresses and are therefore recalcitrant to degradation. To overcome this natural recalcitrance, it is necessary that a pretreatment step is incorporated into the conversion process (**Figure 2**). Original conventions for conversion were to utilize cellulose while essentially abandoning the hemicelluloses. However, like cellulose, hemicelluloses also contain valuable sugars that can be converted to products. Thus, in the attempt of achieving higher sugar yields, increased conversion efficiencies, and more favorable economics, all portions of the biomass must be used in a conscientious manner.

The goal of pretreatment is to render the biomass most susceptible to saccharification such that maximum amounts of fermentation substrates are released and utilized. There are several technologies being explored for pretreatment, including ammonia fiber explosion (AFEX), lime pretreatment, sulfur dioxide steam explosion, ionic liquids, hydrothermal pretreatment, and dilute acid hydrolysis. Each candidate technology has its inherent advantages and disadvantages. When weighing factors such as conversion efficiency, capital cost, operating cost, and scalability, hydrothermal and dilute acid pretreatments appear to be among the leading technologies for use in industry.
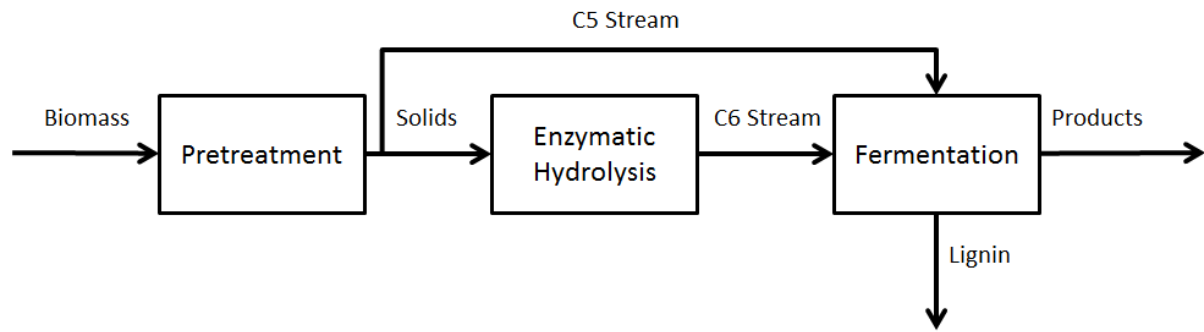
Figure 2: Process flow diagram of the biochemical conversion of biomass to fuels and chemicals.

During dilute acid pretreatment, a mineral acid (often sulfuric acid) and heat are used to hydrolyze the hemicelluloses, resulting in a sugar-rich hydrolysate and remaining solids. The remaining solids are cellulose and lignin, which will have structural alterations. The remaining solids will then be more amenable to saccharifying enzymes such that the cellulose can be hydrolyzed into glucose for fermentation. The lignin remaining after enzymatic hydrolysis can then be used to generate process heat or as a raw materials source for the production of other chemicals.

However, pretreatment is not as simple as hydrolyzing hemicelluloses and rendering cellulose ready for enzymatic saccharification. The harsh reaction conditions required to overcome cell wall recalcitrance lead to the degradation of monosaccharides released during the process. The degradation products not only reduce conversion efficiencies by lowering the amount of substrates available for conversion, but also wreak havoc in subsequent processes by inhibiting hydrolytic enzymes and fermentation microorganisms. The major inhibitory compounds produced from the degradation of monosaccharides are furfural, hydroxymethylfurfural (HMF), formic acid, and levulinic acid and degradation of lignin produces phenolics (Kim *et al*., 2013a; Palmqvist *et al.*, 2000; Ximenes *et al.*, 2010). Although milder pretreatment conditions could minimize the production of these inhibitory compounds, severe conditions are necessary to overcome the recalcitrant nature of the cell wall. Milder pretreatment conditions can also result in incomplete hydrolysis of hemicelluloses, leaving xylose oligomers that can also inhibit hydrolytic enzymes (Qing *et al.*, 2010). Therefore pretreatment must occur at a 'sweet spot' of conditions that result in maximum product yield. To determine this sweet spot of conditions, the rates and mechanisms involved during pretreatment must be further developed and understood.

Deconstruction of hemicelluloses is important to the economic viability of the lignocellulosics-to-biobased products industry because these five carbon sugars represent 20 to 30 % of the mass of the plant cell wall. Because hemicelluloses do not instantaneously depolymerize into xylose, but rather into a series of oligomers that hinder hydrolyzing enzymes, it is critical to understand the kinetics of hemicelluloses depolymerization. Birchwood xylan-derived oligomers and reference standard oligomers were studied in terms of their depolymerization. Results showed that their corresponding bonds were cleaved differently at different processing conditions, leading to the production of additional oligomers and degradation products. Switchgrass, an important bioenergy crop, has never been studied through the lens of hemicelluloses-derived oligomers depolymerization. This study is providing a first incursion into switchgrass hemicelluloses-derived oligomers depolymerization.

2.0 OBJECTIVES

Although milder pretreatment conditions could minimize the production of inhibitory compounds, severe conditions are necessary to overcome the recalcitrant nature of the cell wall. Therefore pretreatment must occur at a 'sweet spot' of conditions that result in maximum product yield. There is a knowledge gap that relates pretreatment processing parameters to inhibitor product generation. It is hypothesized that by understanding the effects that temperature, acid concentration, and time have on hemicelluloses, including its derived oligomers, depolymerization into xylose, processing conditions that minimize degradation product formation can be designed. To determine these optimized pretreatment conditions, the rates and mechanisms of hemicelluloses depolymerization must be further characterized. In an attempt to achieve our overall goal, the objectives of this project are:

Objective 1: Extract and characterize switchgrass hemicelluloses.

Objective 2: Produce and purify switchgrass hemicelluloses-derived oligomers.

Objective 3: Develop an understanding of depolymerization patterns of switchgrass hemicelluloses and xylose oligomers undergoing pretreatment at various temperatures and acid concentrations**.**

The proposed work is creative and original because it seeks to provide molecular-level information as to how hemicelluloses depolymerize into oligomers, xylose, and inhibitory compounds. This work is the first report on in-house purified switchgrass-derived hemicelluloses and switchgrass hemicelluloses-derived oligomers.

3.0 LITERATURE REVIEW

3.1 Biofuels from lignocellulosic biomass

Production of biofuels from lignocellulosic biomass offers many advantages over petroleum-based fuels, including reduced greenhouse gas emissions, revitalization of rural economies, and improvements in energy security and independence (Sanchez and Cardona, 2008; Sims *et al*., 2010). Lignocellulosic biomass is globally available and in large supply, with approximately 10 to 50 billion tons produced annually (Claassen *et al*., 1999). Lignocellulosic biomass is available from sources such as municipal wastes, agricultural residues (corn stover, wheat straw, rice straw, rice hulls, and sugarcane bagasse), and dedicated bioenergy crops (switchgrass, miscanthus, sorghum, willow, poplar, and pine) (Sanchez and Cardona, 2008; Sims *et al*., 2010). Of these sources, switchgrass (*Panicum virgatum,* L.) is considered to be an important candidate as a dedicated bioenergy crop because it requires low inputs, produces high yields of biomass, provides good carbon sequestration, prevents erosion, and has a wide geographic distribution throughout North America (Sanderson *et al*., 1996). The composition of switchgrass varies among cultivars, levels of plant maturity, and even within different regions of the plant, but is roughly 30-40% cellulose, 20-35% hemicelluloses, and 10-20% lignin, with the remaining mass being comprised of extractives, protein, and ash (Adler *et al.*, 2006; Ragauskas, 2010; Dien *et al*., 2006).

Many strategies are being explored to help biofuels progress towards commercialization, including genetic engineering of biomass and fermentation microorganisms, further understanding of biomass physicochemical properties, and better understanding of conversion processes (Sanchez and Cardona, 2008; Sims *et al*., 2010). Thus, one of the objectives of this work was to characterize the physicochemical properties of hemicelluloses extracted from mid-

growing season (July) and weathered, post-frost (February) switchgrass. Elucidating the physicochemical properties of hemicelluloses would improve the understanding of the production of monosaccharides and degradation products formed during pretreatment so that the "sweet spot" of high monosaccharide and low inhibitor yields could be attained. Elucidating the physicochemical properties could also provide more insight into the physiological role of hemicelluloses. A second objective of this work seeks to better understand the underlying rates and mechanisms of pretreatment during the conversion process.

3.2 Composition of lignocellulosic biomass

Lignocellulosic biomass is composed of three main components, cellulose, hemicelluloses, and lignin, accounting for 30-50, 20-40, and 10-25 wt % of biomass, respectively (McKendry, 2002; Saha, 2003). Cellulose is the most abundant polysaccharide occurring in biomass and is comprised of glucose subunits connected through β-1,4 glycosidic bonds (Fan *et al*., 1982, Jorgensen *et al*., 2007; McKendry, 2002). Cellulose forms both highly organized crystalline structures and amorphous structures in the plant, and together these form cellulose microfibrils that exhibit intermolecular hydrogen bonding (Jorgensen *et al*., 2007; Laureano-Perez *et al*., 2005).

Hemicelluloses are the second most abundant polysaccharides occurring in biomass. Unlike cellulose, which is a homogeneous polymer, hemicelluloses are heterogeneous polymers consisting of pentoses, hexoses, and sugar acids (Ebringerova *et al*., 2005; Puls and Schuseil, 1993; Saha, 2003). Whereas cellulose varies little among different biomass sources, hemicelluloses are completely dependent upon the source from which they originate. Hemicelluloses from hardwoods, softwoods, and herbaceous feedstocks all differ in composition and structure (Ebringerova *et al*., 2005; Puls and Schuseil, 1993; Saha, 2003). However, the most abundant hemicelluloses are xylans, consisting of a β-1,4-linked xylose backbone substituted with pentoses, hexoses, and sugar acids (Ebringerova *et al*., 2005; Puls and Schuseil, 1993; Saha, 2003).

Lignin is a high molecular weight, amorphous heteropolymer consisting of the phenylpropane units *p*-coumaryl alcohol, coniferyl alcohol, and sinapyl alcohol (Hendriks and Zeeman, 2009; Kumar *et al*., 2009; McKendry, 2002). Like hemicelluloses, lignin properties are

also dependent upon biomass source, with proportion of the phenylpropane units differing among softwoods, hardwoods, and herbaceous biomass (McKendry, 2002).

Together, these components form a complex matrix in the cell wall that is a network of cellulose microfibrils that are covered and protected by the hemicelluloses and lignin as shown in **Figure 3** (Hendriks and Zeeman, 2009; Hoch, 2007; Saha, 2003). This cellulose-hemicelluloses-lignin network provides rigidity and support to the cell wall and resistance to chemical and microbial attack (Jorgensen *et al.*, 2007; McKendry, 2002). Thus, the cell wall structure is recalcitrant when trying to breakdown biomass to its substituent molecules (Himmel *et al.*, 2007). This recalcitrant nature requires that biomass must undergo a series of unit operations, including pretreatment and enzymatic hydrolysis, before substrates can be effectively generated for conversion to fuels and chemicals.
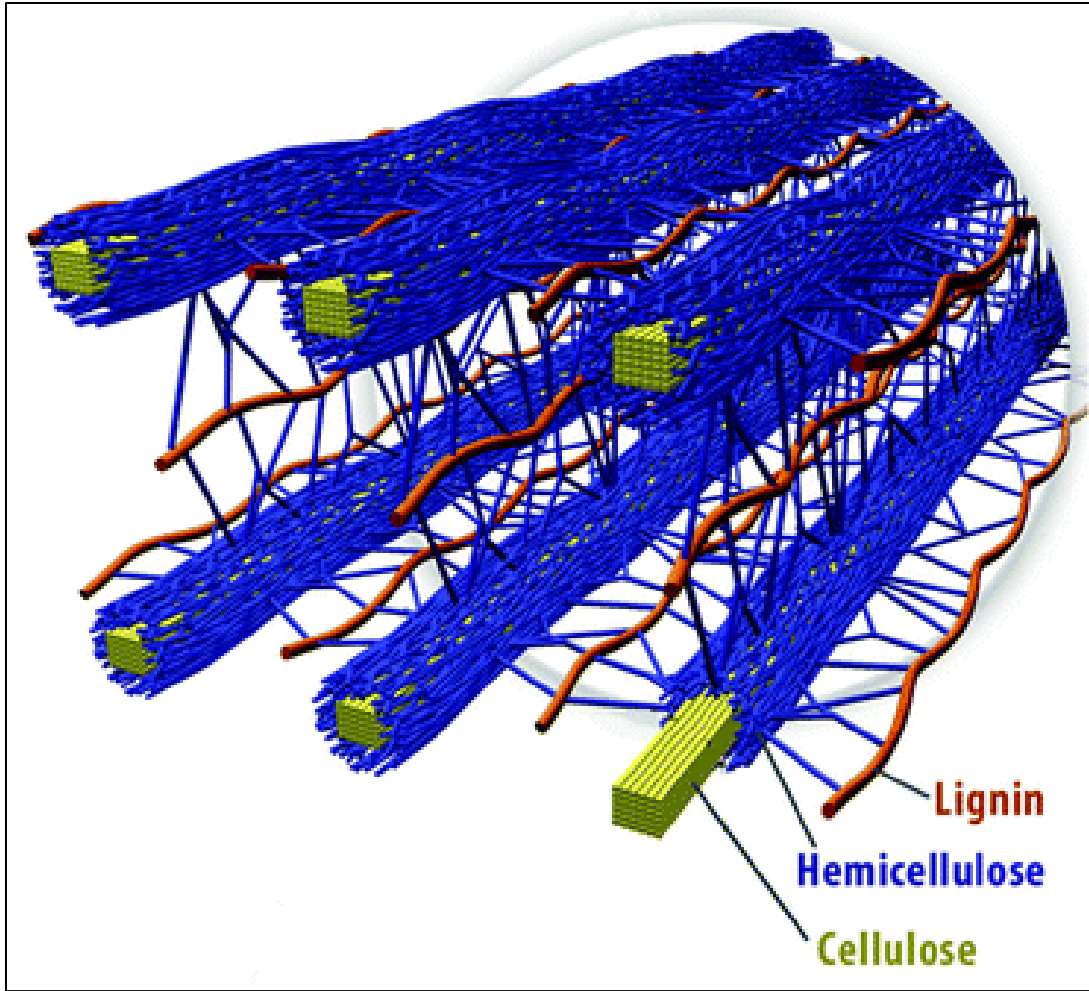
Figure 3: Arrangement of cellulose, hemicelluloses, and lignin in the cell wall of plants (Source: United States Department of Energy).

3.3 Pretreatment technologies for biochemical conversion

Pretreatments can be classified as biological, physical, chemical, and physico-chemical (Alvira *et al*., 2010; Hendriks and Zeeman, 2009). The goal of pretreatment is to overcome the natural recalcitrance of biomass and make it amenable to release of substrates for conversion to fuels and chemicals. For biochemical conversion, the biomass must first be pretreated to render the cellulose more accessible to enzymes for saccharification to fermentable sugars (Garlock *et al*., 2011). After pretreatment, the cellulose is enzymatically hydrolysed to glucose, before monomeric sugars from pretreatment and enzymatic hydrolysis are used for conversion to products (Wyman *et al*., 2005). Pretreatment cost has been suggested to be second only to feedstock cost in the conversion of biomass to biofuels, and overcoming biomass recalcitrance such that sugars can be economically produced from biomass is crucial for commercialization (Lynd *et al*., 2008; Mosier *et al*., 2005).

There are many pretreatment technologies available, and the pretreatment technology chosen will affect many factors, including how the biomass is handled prior to pretreatment, how the generated liquid stream and solids are processed, treatment of waste, and potential of co-product generation (Yang and Wyman, 2008). Each of these factors affects costs and the overall economics of the conversion process. Possible pretreatment technologies include ammonia fiber explosion (AFEX), organosolv, ozonolysis, ionic liquids, steam explosion, liquid hot water, ammonia recycle percolation, lime, CO_2 explosion, liquid hot water, dilute acid, wet oxidation, and microwave pretreatment (Alvira *et al*., 2010; Hendriks and Zeeman, 2009). Among these, the leading pretreatment technologies for consideration in industrial use include AFEX, lime, ammonia recycle percolation, liquid hot water, and dilute acid hydrolysis (Alvira, *et al*., 2010; Garlock *et al*., 2011; Yang and Wyman, 2008). **Figure 4** presents a schematic for the

generalized effect that these pretreatments, which occur over a range of pH values, have on the cellulose, hemicelluloses, and lignin in the cell wall. As can be seen, pH is affects how the recalcitrance of the cell wall is overcome as well as the range of products that are produced during pretreatment.
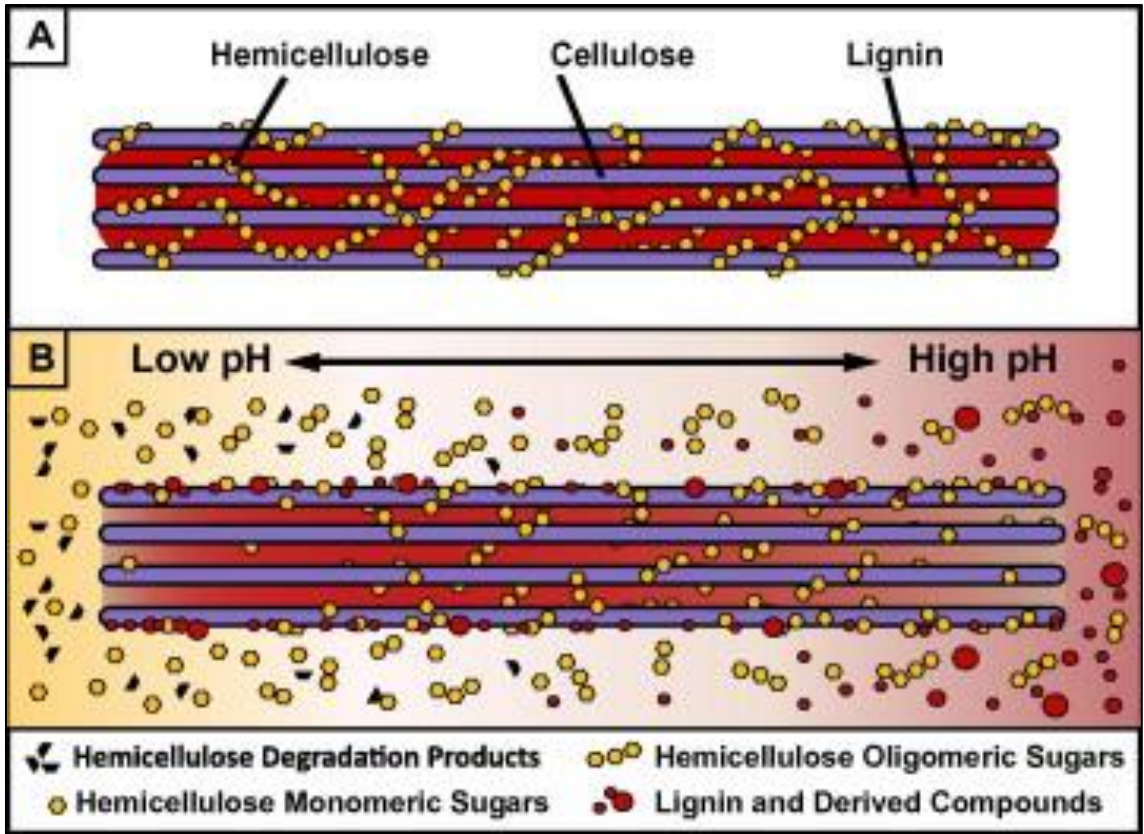
Figure 4: Cellulose, hemicelluloses, and lignin in the plant cell wall at untreated conditions (A) and during different pretreatment conditions (B) (Source: Garlock *et al.*, 2011).

During AFEX pretreatment, liquid anhydrous ammonia is mixed with biomass at ratios from 0.6:1 to 2:1 at temperatures ranging from 60 to 200 ^{o}C is mixed with biomass and pressurized anywhere from 1.4 to 4.8 MPa for 5 to 45 min (Alvira *et al*., 2010; Sharara *et al*., 2012). The AFEX process disrupts lignin-carbohydrate ester linkages, alters lignin structure, decrystallizes cellulose, and physically disrupts biomass fibers (Alvira *et al*., 2010; Laureano-Perez *et al*., 2005; Yang and Wyman, 2008). This results in a pretreated solid that almost quantitatively retains the cellulose, hemicelluloses, and lignin fractions (Wyman *et al*., 2005b). Although AFEX has been effective on agricultural residues and herbaceous biomass, wood and other high lignin containing feedstocks do not perform as well during AFEX pretreatment (Wyman *et al*., 2005b). AFEX pretreated biomass also requires additional xylanase enzymes to hydrolyze oligomeric hemicellulose to monomeric sugars (Mosier *et al*., 2005).

Lime pretreatment is another alkali-based pretreatment technology. Lime pretreatment uses approximately 0.1 g CaO or Ca(OH)$_2$ per g biomass with 5 to 15 g water per g biomass at temperatures ranging from 85 to 150 ^{o}C for 1 to 13 h (Alvira *et al*., 2010; Hendriks and Zeeman, 2009; Yang and Wyman, 2008). Similarly to AFEX, lime removes lignin and acetyl groups while opening up the structure for increased enzymatic access to cellulose and hemicelluloses (Alvira *et al*., 2010; Hendriks and Zeeman, 2009; Yang and Wyman, 2008). Lime is relatively safe, inexpensive, and available globally; however, like AFEX, it is not effective on wood and other high lignin biomass (Hendriks and Zeeman, 2009; Yang and Wyman, 2008).

Another alkali pretreatment technology is ammonia recycle percolation. During ammonia recycle percolation, 5 to 15 wt % aqueous ammonia, at temperatures from 80 to 210 ^{o}C, passes through biomass at a rate of approximately 5 mL per min for up to 90 min (Alvira *et al*., 2010; Yang and Wyman, 2008). Ammonia recycle percolation solubilizes hemicelluloses and produces

low-lignin, short-chained pretreated solids that are rich in glucan content (Yang and Wyman, 2008). The resulting glucan-rich solids are susceptive to hydrolytic enzymes. Ammonia recycle percolation does suffer from high energy costs because of high liquid loadings (Alvira *et al.*, 2010; Yang and Wyman, 2008).

Liquid hot water pretreatment uses water at temperatures from 160 to 240 ^{o}C at elevated pressures to solubilize hemicelluloses, partially depolymerize lignin, and render cellulose accessible for enzymatic hydrolysis (Alvira *et al.*, 2010; Hendriks and Zeeman, 2009). To minimize inhibitor formation, pH is maintained between pH 4 and 7 (Alvira *et al.*, 2010; Hendriks and Zeeman, 2009; Yang and Wyman, 2008). As a result, solubilized hemicelluloses primarily remain as xylose oligomers, which will require additional enzymes for hydrolysis to monomeric sugars (Mosier *et al.*, 2005).

Dilute acid hydrolysis uses an acid, most often aqueous sulfuric acid, at concentrations from 0.2 to 2 wt % at temperatures from 140 to 200 ^{o}C for residence times of 1 min to 2 hours (Sharara *et al.*, 2012; Yang and Wyman, 2008). The aqueous sulfuric acid hydrolyzes hemicelluloses to mostly monosaccharides, disrupts lignin, and produces cellulose that is amenable to enzymatic hydrolysis (Schell *et al.*, 2003; Wyman *et al.*, 2005; Yang and Wyman, 2008). A disadvantage of dilute acid hydrolysis is the production of degradation products that are inhibitory to hydrolytic enzymes and fermentation microorganisms (Alvira *et al.*, 2010; Fenske *et al.*, 1998; Palmqvist and Hahn-Hagerdal, 2000a,b; Yang and Wyman, 2008). However, when milder pretreatment conditions are used, xylose oligomers can result as products from the hydrolysis of hemicelluloses (Kamiyama and Sakai, 1979; Lloyd and Wyman, 2003). Resulting xylose oligomers require additional enzymes for further hydrolysis into xylose, which can then be fermented to ethanol (Mosier *et al.*, 2005; Saha, 2003). Xylose oligomers have also been

found to decrease hydrolysis rates and reduce glucan conversion by competitively inhibiting cellulases (Qing *et al*., 2010). An important feature of dilute acid hydrolysis is that it has been found to be applicable to a wide range of feedstocks (Mosier *et al*., 2005).

Although each of the pretreatment technologies has its advantages and disadvantages, there still remains no best option. When comparing the economic performance of dilute acid, hot water, AFEX, ammonia recycle percolation, and lime pretreatments on a consistent basis in a 50 MMgal per year ethanol production facility, corresponding to a corn stover feed rate of 2000 metric dry tons per day, little differentiation in the economic performances was seen when all soluble sugars, both oligomeric and monomeric, were taken into account (Eggeman and Elander, 2005). However, without accounting for oligomeric sugars as well, dilute acid produced the lowest minimum ethanol selling price (Eggeman and Elander, 2005). Also, of the competing technologies, dilute acid hydrolysis is considered to be closest to commercialization and is favored by the National Renewable Energy Laboratory (Alvira *et al*., 2010; Sims *et al*., 2010; Yang and Wyman, 2008). It is also worth noting that Eggeman and Elander (2005) found the key cost drivers of pretreatment to be yield of both pentoses and hexoses, solids concentration, enzyme loading, and hemicellulase activity. To minimize cost of conversion, it is important to understand how acid concentration and temperature affect oligomer, monomer, and degradation product formation during dilute acid hydrolysis.

3.4 Inhibitors produced during pretreatment

Pretreatment hydrolysates often contain compounds that are inhibitory to enzymatic hydrolysis and fermentation (Du *et al.*, 2010; Fenske *et al.*, 1998; Kim *et al.*, 2013a; Kim *et al.*, 2013b; Kothari and Lee, 2011; Palmqvist and Hahn-Hagerdal, 2000). This inhibition is caused by compounds that can be grouped into four categories: furan derivatives, organic acids, lignin derivatives, and sugars (Kim *et al.*, 2013a; Palmqvist and Hahn-Hagerdal, 2000; Qing *et al.*, 2010; Ximenes *et al.*, 2011, 2010). Many studies have investigated the inhibition effects of these compounds as stand-alone components as well as a consortium of compounds mimicking a pretreatment hydrolysate. Results show that these compounds work synergistically to inhibit enzymatic hydrolysis and fermentation, and even the consortium of compounds is not as harmful as the real pretreatment hydrolysate (Kothari and Lee, 2011; Larsson *et al.*, 1999).

During dilute acid hydrolysis, the harsh environment of acidic media and high temperatures can degrade six-carbon sugars such as glucose into hydroxymethylfurfural (HMF), which can further degrade into levulinic acid, formic acid, and humin (Ulbricht *et al.*, 1984). Similarly, five-carbon sugars, such as xylose and arabinose, can degrade into furfural and formic acid (either through degradation of furfural or directly from five-carbon sugars) (Nimlos *et al.*, 2006; Williams and Dunlop, 1948). These degradation products are inhibitory to saccharifying enzymes and fermentation microorganisms (Arora *et al.*, 2013; Hodge *et al.*, 2008; Klinke *et al.*, 2004; Larsson *et al.*, 1999; Palmqvist and Hahn-Hagerdal, 2000). However, all compounds are not equal in regards to strength of inhibition, and some even increase ethanol production when in dilute concentrations (Larsson *et al.*, 1999). This complex nature of inhibitors requires an understanding of the starting material such that reaction conditions can be optimized for selective production of monosaccharides and enzyme- and microorganism-enhancing compounds.

Phenolic compounds from lignin degradation also play a key role in enzymatic hydrolysis and fermentation inhibition. Phenols such as vanillin, syringaldehyde, trans-cinnamic acid, and hydroxybenzoic acid have been reported to inhibit cellulose and hemicelluloses hydrolysis and fermentation (Kim *et al*., 2013a; Panagiotou and Olsson, 2007; Ximenes *et al*., 2011, 2010). Kim *et al*. (2013a) reported that less polar phenolic compounds are more inhibitory than are more polar phenolic compounds. The use of adsorbents and a 90 ^{o}C water wash were found to benefit enzymatic hydrolysis and fermentation via the removal of phenolic compounds and xylose oligomers (Kim *et al*., 2013a).

Xylose oligomers have also received attention for inhibiting processes downstream of pretreatment (Qing *et al*., 2010; Kim *et al*., 2013a). Xylose oligomers inhibit cellulase enzymes, resulting in lower hydrolysis rates and glucose yields (Qing *et al*., 2010). In fact, Qing *et al.* (2010) reported xylose oligomers to be more inhibitory to cellulase enzymes than xylose, xylan, glucose, and cellobiose. Because xylose oligomers were partially hydrolyzed by the cellulase enzymes, it is believed that xylose oligomers compete with cellulose for active sites on the enzymes (i.e. competitive inhibition) (Qing *et al*., 2010). Kim *et al*. (2013a) also reported xylose oligomers, which are present in steam pretreated mixed hardwood, inhibit cellulase enzyme activity. Towards overcoming this inhibition, Kumar and Wyman (2009) reported that addition of β-xylosidase and xylanase to cellulase and β-glucosidase mixtures improved enzymatic hydrolysis of xylan and cellulose in pretreated corn stover solids, especially for solids that retained much of the xylose in the solids. Work reported by Kothari and Lee (2011) also demonstrated the inhibitory effects of xylose oligomers. However, Kothari and Lee (2011) reported that xylose oligomers were more inhibitory to xylan digestibility than glucan digestibility, and, on the contrary to Kumar and Wyman's results, cellulase enzymes did not

hydrolyze xylose oligomers. Clearly the role of xylose oligomers as potential enzymatic

hydrolysis inhibitors warrants further research and investigation.

3.5 Xylose oligomers during pretreatment

As seen in the previous section, oligomers are important intermediate products in hemicelluloses hydrolysis. In a study conducted by Kumar and Wyman (2008), commercially purchased xylo-oligomers (xylose – DP1, xylobiose – DP2, xylotriose – DP3, xylotetrose – DP4, and xylopentose – DP5) were subjected to hydrolysis at 160 ^{o}C at five pH values (1.45, 2.75, 3.75, 4.75, and 7.0) for times varying from 0 to 90 min. Concentrations of monomer and oligomers were monitored post-hydrolysis, and rate constants were determined by minimizing the sum of squares between experimental and model-predicted data. The model proposed by Kumar and Wyman (**Figure 5**) allowed for the depolymerization of oligomers into lower oligomers as well as the direct degradation of oligomers (i.e. it was not necessary for oligomers to depolymerize to xylose before degradation products could be formed). All reactions were assumed to be first-order, irreversible reactions.

Results revealed that xylose formation increased with increased acid; however, xylose degradation becomes significant if acid is overly increased. Results also showed that the DP of oligomers had a positive correlation on the overall disappearance rate constants, with increased DP oligomers exhibiting higher rate constants, and a negative correlation on the formation of xylose, with xylose production decreasing with increasing oligomer DP. The study showed that as acid increased, direct degradation of oligomers decreased. Only DP2 and DP3 experienced losses to degradation under non-acidic conditions. Thus, increased acid decreased direct degradation of oligomers as well.

22
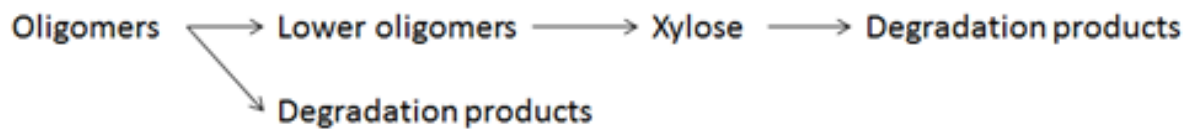
Figure 5: Xylo-oligomer depolymerization model proposed by Kumar and Wyman (2008).

Although the model developed by Kumar and Wyman (2008) allowed for direct degradation of oligomers, quantum mechanical modeling by Qian and Nimlos (2009) suggests that oligomers should preferentially hydrolyze into lower oligomers rather than undergo dehydration to form degradation products. Recent work by Lau (2012) looked to build upon the work undergone by Kumar and Wyman in three distinct areas. Firstly, Lau proposed a model similar to Kumar and Wyman, except that it incorporated the results of Qian and Nimlos and did not allow for direct degradation of oligomers (**Figure 6**). Secondly, Lau monitored and quantified furfural and formic acid as specific degradation products of xylose rather than using a generic degradation products term. This is of particular interest to industry as these products are inhibitory to saccharification enzymes and fermentation microorganisms and thus need to be quantified. And thirdly, Lau investigated the depolymerization of xylose oligomers over a range of temperatures and acid conditions, allowing for the development of a model that accounts for rate constant dependence on these parameters. Also worth noting is that Lau used xylose oligomers that were produced in-house rather than purchased commercially.

Lau examined the degradation of DP1, DP2, DP3, and DP4 at 120, 160, and 200 $^{\circ}$C at 0.0, 0.1, and 1.0 % (V/V) sulfuric acid for 0 to 60 min. Monomer, oligomer, furfural, and formic acid concentrations were monitored, and rate constants were calculated by maximizing the coefficient of correlation (R^2) using a Microsoft Excel Solver routine. The resulting model was very sensitive to formic acid concentrations, thus potentially skewing results. Lau also found that acid increased dissociation of the external bonds of DP4 versus the internal bond, which was contrary to the results found by Kumar and Wyman.
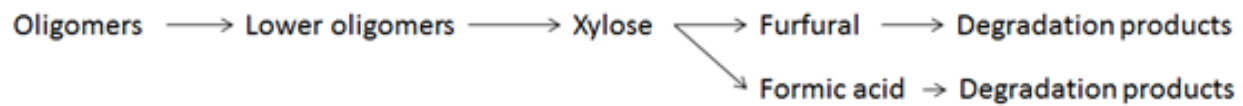
Figure 6: Xylose oligomer depolymerization model proposed by Lau (2012).

Based on the discrepancy of the results of the previous studies, the effect of acid on the cleavage of different bonds within oligomers needs to be investigated further. Investigating the degradation of DP5 would provide further information on the comparison of cleavage rates for internal versus external bonds. Perhaps even more interesting will be investigating the degradation of DP6, which has three different bonds – two external bonds, two intermediate bonds, and one middle bond. Thus, this study will build upon Lau's work by investigating the depolymerization of DP5 and DP6 at varying acid concentrations, temperatures, and hydrolysis times such that a model that accounts for these parameters can be developed, as well as offering more insight into the effect of acid on preferential bond cleavage.

The distribution of oligomers would be of great importance when considering using the oligomers for applications such as prebiotics or as soluble dietary fiber, as well as understanding their role in degradation products formation. Understanding which processing conditions minimize hemicelluloses degradation products formation while allowing for depolymerization into monomercic sugars that can be fermented to products is critical for the field to advance.

3.6 Hemicelluloses during pretreatment

There have been many studies on hemicelluloses decomposition during pretreatment. Early models described the hydrolysis of hemicelluloses to proceed in two linear steps (**Figure 7A**). In this model, hemicelluloses first hydrolyze to xylose before degrading into degradation products. Later models expand upon this initial model by including oligomers as intermediates between hemicelluloses and xylose, as well as degradation of xylose into furfural (**Figure 7B**).

Morinelly *et al.* (2009) studied the degradation of xylan hemicelluloses in switchgrass, aspen, and balsam at 150, 160, and 175 $^{\circ}$C and sulfuric acid concentrations of 0.25, 0.50, and 0.75 wt %. Xylose and furfural concentrations were monitored using high performance liquid chromatography (HPLC), and total oligomers were quantified based on the National Renewal Energy Laboratory's (NREL) total sugar analysis procedure (Sluiter *et al.*, 2008c). In this procedure, an aliquot of hydrolysate is analyzed for monomers using HPLC, and a separate aliquot is adjusted to 4 wt % acid before being hydrolysed at 121 $^{\circ}$C for 1 h. The re-hydrolysed aliquot is then analyzed for monomers using HPLC, and the increase in monomer content is attributed to oligomer fractions that were originally present in the hydrolysate. Based upon the monomer, oligomer, and furfural concentration data and the degradation model shown in Figure 3, Morinelly *et al*. generated rate constants and Arrhenius parameters using a least squares curve fitting method. The resulting model successfully described xylose throughout hydrolysis; however, furfural and oligomer data were not predicted as successfully as xylose data. Oligomers were predicted well at shorter reaction times, but not at longer times. Furfural was overestimated at early reaction times and underestimated at later reaction times. The group also acknowledged the neutralizing effect of ash and protein in the biomass samples, which can effectively lower the acid concentration.

$$(A) \ Hemicelluloses \rightarrow Xylose \rightarrow Degradation \ products$$

$$(B) \ Hemicelluloses \rightarrow Oligomers \rightarrow Xylose \rightarrow Furfural \rightarrow Degradation \ products$$

Figure 7: (A) Two step linear model for the hydrolysis of hemicelluloses (B) Four step linear model used by Morinelly *et al.* (2009) for the hydrolysis of hemicelluloses.

Additional hemicelluloses degradation models describe the reaction pathway similarly to that seen in Figure 3 except that the hemicelluloses are divided into two distinct fractions, a fast reacting portion and a slow reacting portion. In a study by Nabarlatz *et al*. (2004), the autohydrolysis of corncobs was carried out at temperatures ranging from 150 to 190 $^{\circ}$C and reaction times of 0 to 330 min. Resulting hydrolysates were monitored for xylose, arabinose, acetic acid, and furfural using HPLC; oligomers were monitored using methods similar to those used by Morinelly *et al*. (i.e. hydrolysis of oligomers to monomers before quantifying). Rate constants and Arrhenius parameters were estimated using a least-squares objective function. The resulting model was able to accurately predict product concentration profiles. However, this study did not investigate the effects of acid on the degradation of hemicelluloses, and the distribution of oligomers produced was not modeled.

Studying the effects of pretreatment on extracted hemicelluloses will provide further insight into exhibited bimodal kinetic behavior. Because the extracted hemicelluloses are free of other cell wall components, transport limitations should be minimized, as well as the buffering effects of ash and protein seen by Morinelly *et al.* (2008). Nabarlatz *et al*. noted that the two distinct fractions of hemicelluloses are likely caused by varying degrees of association of the hemicelluloses with cellulose and lignin in the cell wall. With hemicelluloses composition and linkage data in-hand, it can be tested to see if a correlation exists between these data and degradation rates, ultimately providing insight into whether or not two distinct fractions of hemicellulose exist to explain the bimodal behavior, or if it is a result of transport limitations and cell wall matrix interactions. Arabinose and degradation products will also be monitored. Arabinose is of particular interest because, similarly to xylose, it will degrade into furfural and

29

formic acid (Nabarlatz *et al.*, 2004). Degradation of arabinose could help account for the

discrepancies between Morinelly *et al.*'s experimental and model-predicted furfural data.

3.7 Production of xylose oligomers feedstock

As previously noted, the behavior of xylose oligomers during pretreatment needs to be further investigated, as well as the inhibitory role these compounds play. It is worth noting that xylose oligomers are not only of interest to the biofuels industry, but also to industries such as agriculture, nutraceuticals, and functional foods (Moure *et al*., 2006; Vazquez *et al*., 2000). As part of the biorefinery process, the pretreatment hydrolysate could be removed and used as a source of xylose oligomers for applications such as prebiotics, ripening agents, and animal feeds. The remaining pretreated solids could go on to enzymatic hydrolysis to produce fermentable glucose and ultimately ethanol or other desired products (Kumar *et al*., 2012). With this approach, the need for additional xylanases and cellulase inhibition caused by xylose oligomers could be avoided while at the same time producing a valuable co-product stream from the hydrolysate. All of which could help the overall economics of the biorefinery process (Sims *et al*., 2010).

Current and proposed methods for purification of xylose oligomers include solvent extraction, precipitation, membrane filtration, anion-exchange chromatography, size-exclusion chromatography, and simulated moving bed chromatography (Moure *et al*., 2006; Swennen *et al*., 2005; Yuan *et al*., 2004; Kabel *et al*., 2002; Katapodis *et al*., 2003; Oshaki *et al*., 2003). For example, Swennen *et al*. (2005) isolated oligosaccharides from wheat flour using ethanol precipitation and ultrafiltration with 5, 10, and 30 kDa molecular mass cut-off membranes. Yuan *et al*. (2004) produced and purified a xylobiose- and xylotriose-rich syrup from corncob meal using dilute acid pretreatment, steam extraction, and enzymatic hydrolysis followed by filtration, flocculation, ion-exchange desalination, nanofiltration, and vacuum evaporation. Taking a different approach, Kabel *et al*. (2002) and Katapodis et al. (2003) used anion-exchange

chromatography in combination with size-exclusion chromatography, the former to purify xylo-oligosaccharides from *Eucalyptus* wood and spent brewer's grain whereas the latter isolated feruloylated oligosaccharides from wheat flour. However, these processes only removed undesired compounds and/or monosaccharides from oligosaccharide pools without further separation into oligosaccharide fractions of a targeted, singular DP.

One process that has demonstrated the ability to separate oligosaccharide pools to narrowly-focused DP oligosaccharide fractions is CPC (Lau *et al*., 2011; Lau *et al*., 2013). CPC possesses the advantage of no irreversible solute retention because there is no solid support, but rather an exchangeable liquid stationary phase held in place by centrifugal force (Cazes and Nunogaki, 1987; Chevolot *et al*., 1998). Thus, the stationary phase can be regenerated or replaced at a cost that is much less than conventional solid support systems (Chevolot *et al*., 1998).

Using CPC for fractionation would allow production of a feedstock of xylose oligomers for use in studies to examine the behavior of xylose oligomers during pretreatment and the inhibitory role of these compounds. Specifically, the effects of pretreatment parameters such as temperature, time, and acid concentration could be observed for oligomers of different DP, providing useful information on bond cleavage preferences. The inhibitory effects of different DP oligomers could also be observed with respect to individual hydrolytic enzymes.

3.8 Relevance and implications of study objectives

The objectives of this study will provide more clarity to the depolymerization of xylose oligomers during dilute acid hydrolysis and autohydrolysis. This will include more information as to how acid concentration and temperature affect the rates of cleavage at different bonds within the xylose oligomers. Understanding how these cleavage rates react to different processing conditions will be important to control production of xylose oligomers, monomer, and degradation products during pretreatment at the commercial scale. Lastly, studying this with authentic material that has been isolated from a bioenergy-destined plant can provide crucial information for real-world application.

4.0 MATERIALS AND METHODS

4.1 Materials

4.1.1 Switchgrass samples

Alamo switchgrass plots were planted July 3, 2008 at the University of Arkansas Agricultural Research and Extension Center in Fayetteville, AR (36.0625° N, 94.1572° W). Plots were established by drilling seed cultivar Alamo in 18-cm wide rows into a prepared seedbed with a 12-row drill. Switchgrass samples were harvested on either July 4, 2009 (pre-anthesis) or February 18, 2010 (weathered, post-frost). From the 0.1 ha plots, approximately 10 kg of biomass were air dried at 55 °C; 100 g samples were ground to a size 20 mesh, and stored in a 4 °C cold room until being used.

4.1.2 Chemicals and standard reference compounds

Dimethyl sulfoxide (DMSO), xylose (DP1), glucose, arabinose, furfural, hydroxymethylfurfural (HMF), and deuterium oxide were purchased from Sigma-Aldrich (St. Louis, MO). Xylobiose (DP2), xylotriose (DP3), xylotetraose (DP4), xylopentose (DP5), and xylohexose (DP6) were purchase from Megazyme (Wicklow, Ireland). Dextran standards were purchased from Polymer Standards Service – USA (Silver Spring, MD). Formic acid was purchased from Amresco (Solon, OH). Water was purified to 18.2 MΩ using a Millipore (Billerica, MA) Direct-Q 3 unit. Sulfuric acid, methanol, and acetone were purchased from EMD (Gibbstown, NJ). Chloroform was purchased from BDH (West Chester, PA). Glacial acetic acid was purchased from Mallinckrodt Chemicals (Hazelwood, MO). Sodium chlorite, sodium borohydride, acetic anhydride, methyl iodide, and trifluoroacetic acid were purchased from Alfa Aesar (Ward Hill, MA). Potassium hydroxide, sodium hydroxide, and butanol were purchased from Macron Fine Chemicals (Center Valley, PA). Ethanol was purchased from Koptec (King of

Prussia, PA). Calcium carbonate was purchased from J.T. Baker (Phillipsburg, NJ). Sodium acetate was purchased from Thermo Fisher Scientific (Sunnyvale, CA). All solvents were of HPLC grade.

4.2 Methods

4.2.1 Switchgrass characterization

4.2.1.1 Compositional analysis of switchgrass

Switchgrass samples were characterized using the National Renewable Energy Laboratory's (NREL) suite of laboratory analytical procedures (LAP) (Sluiter *et al*., 2008a; Sluiter *et al*., 2008b; Sluiter *et al*., 2008c) as described below. Moisture content was measured using an Ohaus infrared moisture analyzer (Nanikon, Switzerland). Ash content was determined by first igniting 2 g of switchgrass; the switchgrass was then loaded into a furnace (Thermolyne, Dubuque, IA) set at 575 ^{o}C and ashed to constant weight over 24 h. Extractives were quantified by successive water and ethanol Soxhlet extractions. First, 190 mL of water were refluxed through 5 g of switchgrass for 8 h. Next, 190 mL of 190-proof ethanol were refluxed through the material for 8 h. The difference between the initial weight of switchgrass and the weight of the extracted switchgrass was considered as extractives. Extractives-free switchgrass was then used to determine the structural carbohydrates and lignin in the biomass. One hundred milligrams of biomass were mixed with 1.0 mL of 72% (w/w) aqueous sulfuric acid and agitated at 100 rpm in a 30 ^{o}C water bath for 1 h. Mixtures were then diluted to 4% (w/w) aqueous sulfuric acid by addition of water. Samples were hydrolyzed at 121 ^{o}C for 1 h in an autoclave. An aliquot from each of the samples was then neutralized to pH 7 with calcium carbonate before being filtered through a 0.2-µm nylon syringe filter (Thermo Scientific, Rockwood, TN) and analyzed via high performance liquid chromatography (HPLC) for monomeric sugar content, as described by Sluiter *et al*. (2008c). Acid insoluble lignin (Klason lignin) was determined by recovering, drying, and weighing the solids remaining after hydrolysis. Klason lignin was corrected for ash

36

by heating the recovered solids in the furnace at 575 ^{o}C after drying. Protein was determined by first determining combustible nitrogen using an Elementar Rapid N instrument (Mt. Laurel, NJ). Crude protein was then calculated as N x 6.25 (Padmore, 1990).

4.2.1.2 Scanning electron microscopy (SEM)

Switchgrass fibers were examined using scanning electron microscopy (SEM). Internode samples were collected 10 cm above harvest height using forceps. Internode samples were then mounted on stubs and sputter-coated with 1-2 nm of gold. Scanning electron micrographs were obtained using an FEI Nova Nanolab duo-beam SEM/FIB (Hillsboro, OR).

4.2.2 Switchgrass hemicelluloses extraction

An alkali extraction method, modified from Methacanon *et al.* (2003) and Bowman *et al.* (2011), was used to extract and purify switchgrass hemicelluloses. First, extractives were removed by means of a water wash and Soxhlet extraction. Five grams of ground switchgrass were mixed with 100 mL of water and stirred for 2 h at ambient temperature. The water-washed switchgrass was then extracted using a Soxhlet apparatus with 180 mL of chloroform:methanol (2:1, V/V) for 4 h. The extracted switchgrass was then de-lignified by mixing the biomass with 100 mL of water and stirring at ambient temperature while adding 1 mL of glacial acetic acid and 2 g of sodium chlorite. After 1 h, an additional 1 mL of glacial acetic acid and 2 g of sodium chlorite were added. After 2 h, the mixture was filtered through four layers of commercially available cheesecloth. The holocellulose (remaining solids) was washed with water until near neutral pH, washed again with 50 mL of acetone, and air dried. Next, the cellulose and hemicelluloses were separated by mixing the holocellulose with 100 mL of 4 M potassium hydroxide (KOH). The holocellulose-KOH mixture was stirred overnight at ambient temperature. The solution was then filtered through four layers of cheesecloth. The cellulose (remaining solids) was washed with 50 mL of 4 M KOH, followed by 50 mL of water. The filtrate (hemicelluloses) was adjusted to pH 5 with the addition of acetic acid and stirred at ambient temperature for 4 h. Then 1000 mL (4:1, V/V) of 100% ethanol was added and briefly stirred. The mixture was then stored in a 4 $^{\circ}$C cold room overnight. Then the mixture was filtered using Miracloth (Calbiochem, La Jolla, CA), and the precipitate was dialyzed for 96 h in 18.2 MΩ water using 10,000 molecular weight cut off (MWCO) SpectraPor 7 dialysis tubing (Spectrum Laboratories, Rancho Dominguez, CA). The dialyzed precipitate was then lyophilized (Labconocon Freezone 18, Kansas City, MO) and stored in a -20 $^{\circ}$C freezer until being used.

4.2.3 Hemicelluloses characterization

4.2.3.1 Compositional analysis of hemicelluloses

One hundred milligrams of hemicelluloses were mixed with 1.0 mL of 72% (w/w) aqueous sulfuric acid and agitated at 100 rpm in a 30 $^{\circ}$C water bath for 1 h. Mixtures were then diluted to 4% (w/w) aqueous sulfuric acid by addition of water. Samples were hydrolyzed at 121 $^{\circ}$C for 1 h in an autoclave. An aliquot from each of the samples was then neutralized to pH 7 with calcium carbonate before being filtered through a 0.2-µm nylon syringe filter and analyzed via HPLC for monomeric sugar content.

4.2.3.2 Molecular weight analysis

Extracted hemicelluloses were dissolved in dimethylsulfoxide (DMSO) and separated using Phenomenex Phenogel (Torrance, CA) 10^5 Å and 100 Å columns in tandem with a Phenomenex Phenogel guard column. Eluent was 100% DMSO at a flow rate of 0.4 mL min^{-1} provided by a Waters 515 HPLC pump. Eluted compounds were monitored using a Waters 2410 refractive index detector. Molecular weight was determined using a calibration curve built with dextran standards and glucose.

4.2.3.3 Glycosyl linkage analysis

For glycosyl linkage analysis, hemicelluloses were permethylated, depolymerized, reduced, and acetylated; and the resulting partially methylated alditol acetates (PMAAs) analyzed by gas chromatography-mass spectrometry (GC-MS) as described by York *et al.* (1985).

Initially, dry hemicelluloses were suspended in 200 µL of DMSO and placed on a magnetic stirrer for 2 weeks. The sample was then permethylated by the method of Ciukanu and Kerek

(1984) (treatment with sodium hydroxide and methyl iodide in dry DMSO). The sample was subjected to the sodium hydroxide base for 10 min then methyl iodide was added and left for 40 min. The base was then added for 10 min and finally more methyl iodide was added for 40 min. This addition of more methyl iodide and sodium hydroxide base was to insure complete methylation of the polymer. Following sample workup, the permethylated material was hydrolyzed using 2 M trifluoroacetic acid (2 h in sealed tube at 121°C), reduced with sodium borohydride, and acetylated using acetic anhydride/trifluoroacetic acid. The resulting PMAAs were analyzed on a Hewlett Packard 5975C GC (Palo Alto, CA) interfaced to a 7890A MSD (mass selective detector, electron impact ionization mode) (Toulouse, France); separation was performed on a 30 m Supelco 2330 (Bellefonte, PA) bonded phase fused silica capillary column.

4.2.3.4 Scanning electron microscopy (SEM)

Similarly to switchgrass fibers, extracted hemicelluloses were mounted on stubs and sputter-coated with 1-2 nm of gold. Scanning electron micrographs were obtained using an FEI Nova Nanolab duo-beam SEM/FIB.

4.2.4 Production of switchgrass hemicelluloses-derived oligomers

To produce oligomers, 800 mg of switchgrass hemicelluloses were loaded into a stainless steel reactor (20 cm in length, 1.4 cm ID, 2.5 cm OD, 32-mL capacity) with 20 mL of water and hydrolyzed at 160 $^{\circ}$C for 60 min in a fluidized sand bath (Techne Ltd., Burlington, NJ). After hydrolysis, the reactors were immediately cooled by submersion in cold tap water. The hydrolysate was then collected, filtered through a 0.45-μm syringe filter (VWR International, Radnor, PA), and neutralized using 50% sodium hydroxide and a Mettler-Toledo SevenEasy pH-meter (Columbus, OH). Neutralized hydrolysate was then dried using a rotary vacuum dryer (Savant, Farmingdale, NY).

4.2.5 Switchgrass hemicelluloses-derived oligomers fractionation

The hydrolysate produced via autohydrolysis at 160 ^{o}C for 60 min contained oligomers with a wide range in DP. Centrifugal partition chromatography (CPC) was used to fractionate this oligomer pool into individual DP oligomer fractions as subsequently described.

4.2.5.1 Centrifugal partition chromatography (CPC) setup and operation

The solvent system used was butanol:methanol:water (5:1:4, V:V:V) (Lau *et al.,* 2013). Solvent was prepared in a separatory funnel, well mixed, and allowed to settle into two distinct phases overnight before each phase was collected into separate reservoirs. The CPC used was an Armen Instrument (Saint Ave, France) Spot CPC controlled with Cherry Instruments (Chicago, IL) Cherry 1 software. The water-rich lower phase was loaded into the 250-mL column for 30 min at a flow rate of 10 mL min^{-1} while the column rotated at 500 rpm; this was the loading of the stationary phase. The column speed was then increased to 2300 rpm before the butanol-rich upper phase (mobile phase) was introduced into the column at a flow rate of 8 mL min^{-1}. Once the column had achieved equilibrium, the stationary volume inside the column could be calculated. Rotary-vacuum -dried hydrolysates that were reconstituted in 20 mL of the lower phase and 10 mL of the upper phase were then injected into the 30-mL sample loop. The sample was then injected into the column with the mobile phase flowing at 8 mL min^{-1}. After 424 min of separation, extrusion began by switching the mobile phase from the butanol-rich upper phase to the water-rich lower phase; extrusion lasted 44 min. Eluting compounds were monitored using an evaporative light scattering detector (SofTA Model 300S ELSD, Westminster, CO) with settings the same as used by Lau *et al.* (2013). Fractions were collected using a Teledyne Isco (Lincoln, NE) Foxy R1 fraction collector and Waters (Milford, MA) Fraction Collector III, which were

arranged in series to expand collection time. Each fraction was collected over a 1-min period, and collection began after 60 min of run time.

4.2.6 Switchgrass hemicelluloses-derived oligomers characterization

Collected CPC fractions were dried using a rotary vacuum drier and reconstituted in water before being analyzed using high performance anion exchange chromatography with pulsed amperometric detection (HPAEC-PAD), electrospray ionization mass spectrometry (ESI-MS), and high performance liquid chromatography (HPLC) as described in the following sections.

4.2.6.1 High performance anion exchange chromatography with pulsed amperometric detection (HPAEC-PAD) analysis of oligomers

Oligomers were identified using an HPAEC-PAD system (Dionex ICS-5000, Sunnyvale, CA) equipped with an ICS 3/5 electrochemical detector, a CarboPac PA200 guard column, and a CarboPac PA200 analytical column (Dionex, Sunnyvale, CA). Separation was achieved using a two solvent gradient system. Solvent A was 100 mM sodium hydroxide, and solvent B was 100 mM sodium hydroxide with 320 mM sodium acetate. Both solvents were padded under helium gas. Elution began with 100% solvent A for 15 min, followed by a linear increase of solvent B to 50% over the next 40 min. Solvent B was then increased to 100% over 1 min and held constant for 4 min before returning to 100% solvent A over 1 min. Solvent A was then held at 100% for 9 min. Flow rate was a constant 0.5 mL min^{-1}, and the compartment and columns were operated at 35 $^{\circ}$C. Oligomers were quantified based on peak area using calibration curves built using purchased xylose oligomers ranging in DP from two to six.

4.2.6.2 Electrospray ionization mass spectrometry (ESI-MS) analysis of oligomers

Samples were analyzed using ESI-MS using a Bruker ultrOTOF-Q (Bruker Daltonic GmbH, Bremen, Germany) quadrupole/time-of-flight (qQ-TOF) mass spectrometer equipped

with an ESI source. The samples were mixed with 0.1% formic acid in methanol and introduced into the ion source via syringe pump operating at 3 μL min^{-1}. The source temperature was 180 ^{o}C, the drying gas flow was 5 L min^{-1}, and the nebulizing gas pressure was 1 bar. Remaining instrument parameters were adjusted to obtain optimal signal between m/z 300-1000.

4.2.6.3 Total sugar analysis

CPC fractions were tested for monosaccharide composition using a total sugar analysis (Sluiter *et al.*, 2008c). Fractions were brought to a 4% (w/w) sulfuric acid concentration by addition of 72% (w/w) sulfuric acid. Samples were then hydrolyzed at 121 ^{o}C for 60 min before being neutralized with calcium carbonate, filtered using a 0.2-μm syringe filter, and analyzed for monomeric sugars via HPLC.

4.2.7 High performance liquid chromatography (HPLC) identification and quantification

4.2.7.1 HPLC analysis for monomeric sugars

HPLC analyses for monomeric sugars were carried out using a Waters 2695 Separations Module (Milford, MA) equipped with a Shodex SP-G guard column (New York, NY) and SP0810 column operated at 85 ^{o}C. Water was used eluent at a flow rate of 0.6 mL min^{-1}. Compounds were monitored using a Waters 2414 refractive index detector, and monomers were quantified using calibration curves built using purchased arabinose, glucose and xylose standards.

4.2.7.2 HPLC analysis for degradation products

HPLC analyses for degradation products were carried out using a Waters 2695 Separations Module equipped with a Micro-Guard Cation H precolumn (Biorad, Hercules, CA) and Biorad Aminex HPX-87H (Biorad, Hercules, CA) column operated at 55 ^{o}C. Eluent was 5 mM sulfuric acid at a flow rate of 0.6 mL min^{-1}. Compounds were monitored using a Waters 2996 photodiode array detector, and degradation products were quantified using calibration curves built using purchased formic acid, furfural, and HMF standards.

4.2.8 Pretreatment experiments

4.2.8.1 Dilute acid hydrolysis of switchgrass hemicelluloses

Twenty milligrams of switchgrass hemicelluloses were hydrolysed in stainless steel reactors (4.9 cm in length, 0.56 cm ID, 0.79 cm OD, 1.21 mL capacity) using 1 mL of 0.5 or 1.0 % (w/w) aqueous sulfuric acid at 140, 160, or 180 ^{o}C in an industrial fluidized sand bath. When the predetermined reaction time had elapsed, the reactors were cooled by submersion in cold tap water. The hydrolysate was then collected, centrifuged at 7500 g (Eppendorf MiniSpin Plus, Hamburg, Germany), and separated into two aliquots. One aliquot was directly filtered using a 0.2-µm nylon syringe filter and analyzed for degradation products via HPLC, and the other aliquot was neutralized with calcium carbonate, filtered with a 0.2-µm nylon syringe filter, and analyzed for monomeric sugars via HPLC.

4.2.8.2 Hydrothermal pretreatment (autohydrolysis) of switchgrass hemicelluloses

Twenty milligrams of switchgrass hemicelluloses were hydrolysed in 1.21-mL capacity stainless steel reactors using 1 mL of water at 140, 160, or 180 ^{o}C in an industrial fluidized sand bath. When the predetermined reaction time had elapsed, the reactors were cooled by submersion in cold tap water. The hydrolysate was then collected, centrifuged at 7500 g, and separated into two aliquots. One aliquot was directly filtered using a 0.2-µm nylon syringe filter and analyzed for degradation products via HPLC, and the other aliquot was neutralized with calcium carbonate, filtered with a 0.2-µm nylon syringe filter, and analyzed for monomeric sugars via HPLC.

4.2.8.3 Dilute acid hydrolysis of switchgrass hemicelluloses-derived oligomers

Oligomers were hydrolysed in 1.21-mL capacity stainless steel reactors using 1 mL of 0.5 or 1.0 % (w/w) aqueous sulfuric acid at 140, 160, or 180 ^{o}C in an industrial fluidized sand bath. When the predetermined reaction time had elapsed, the reactors were cooled by submersion in cold tap water. The hydrolysate was then collected and separated into two aliquots. One aliquot was directly filtered using a 0.2-µm nylon syringe filter and analyzed for degradation products via HPLC, and the other aliquot was filtered with a 0.2 µm nylon syringe filter and analyzed for oligomers via HPAEC-PAD as described in section 4.2.6.1.

4.2.8.4 Hydrothermal pretreatment (autohydrolysis) of switchgrass hemicelluloses-derived oligomers

Oligomers were hydrolysed in 1.21-mL capacity stainless steel reactors using 1 mL of water at 140, 160, or 180 ^{o}C in an industrial fluidized sand bath. When the predetermined reaction time had elapsed, the reactors were cooled by submersion in cold tap water. The hydrolysate was then collected and separated into two aliquots. One aliquot was directly filtered using a 0.2-µm nylon syringe filter and analyzed for degradation products via HPLC, and the other aliquot was filtered with a 0.2-µm nylon syringe filter, and analyzed for oligomers via HPAEC-PAD as described in section 4.2.6.1.

4.2.9 Kinetic modeling

4.2.9.1 Model assumptions

Based on literature, all reactions are assumed to be first order, irreversible reactions with Arrhenius-type temperature and acid concentration dependence. Degradation products were assumed to be generated only from the degradation of monomeric sugars and not from direct degradation of oligomers. Based on these assumptions, the reaction pathway for oligomers can be seen in **Figure 8**. Based on the reaction pathway in **Figure 8**, the kinetic equations can be derived as shown in **Equations 1-8**:

$$\frac{dX_6}{dt} = -k_6 X_6 \tag{1}$$

$$\frac{dX_5}{dt} = -k_5 X_5 + k_{61} X_6 \tag{2}$$

$$\frac{dX_4}{dt} = -k_4 X_4 + k_{62} X_6 + k_{51} X_5 \tag{3}$$

$$\frac{dX_3}{dt} = -k_3 X_3 + 2k_{63} X_6 + k_{52} X_5 + k_{41} X_4 \tag{4}$$

$$\frac{dX_2}{dt} = -k_2 X_2 + k_{62} X_6 + k_{52} X_5 + 2k_{42} X_4 + k_{31} X_3 \tag{5}$$

$$\frac{dX_1}{dt} = -k_1 X_1 + k_{61} X_6 + k_{51} X_5 + k_{41} X_4 + k_{31} X_3 + 2k_{21} X_2 \tag{6}$$

$$\frac{dF}{dt} = -k_F F + k_{1F} X_1 \tag{7}$$

$$\frac{dA}{dt} = -k_A A + k_{1A} X_1 + k_{FA} F \tag{8}$$

where X_6, X_5, X_4, X_3, X_2, X_1, F, and A are concentrations of DP6, DP5, DP4, DP3, DP2, DP1, furfural, and formic acid, respectively, in mmol/L. k_{61}, k_{62}, k_{63}, k_{51}, k_{52}, k_{41}, k_{42}, k_{31}, k_{21}, k_{1F}, k_{1A}, and k_{FA} are the rate constants for the formation of DP1 from DP6, DP2 from DP6, DP3 from DP6, DP1 from DP5, DP2 from DP5, DP1 from DP4, DP2 from DP4, DP1 from DP3, DP1 from DP2, furfural from DP1, formic acid from DP1, and formic acid from furfural, respectively, in min^{-1}. k_{FL} and k_{AL} are the rate constants for the degradation of furfural and formic acid, respectively, into unaccounted degradation products in min^{-1}.

The overall degradation rates for DP6, DP5, DP4, DP3, DP2, DP1, furfural, and formic acid are k_6, k_5, k_4, k_3, k_2, k_1, k_F, and k_A, respectively, and can be described as shown in **Equations 9-16**:

$$k_6 = k_{61} + k_{62} + k_{63} \qquad \textbf{(9)}$$

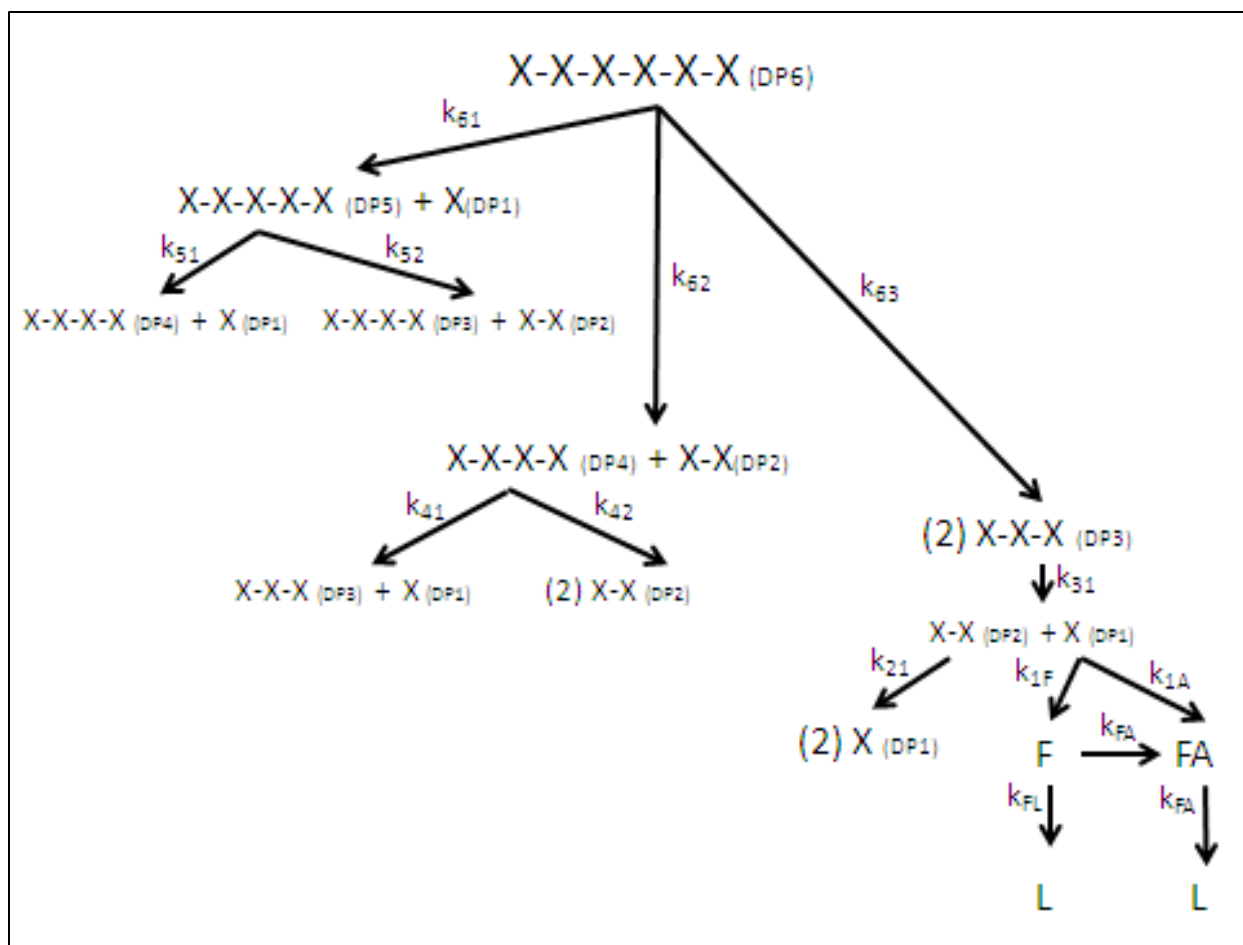$$k_5 = k_{51} + k_{52} \qquad \textbf{(10)}$$

$$k_4 = k_{41} + k_{42} \qquad \textbf{(11)}$$

$$k_3 = k_{31} \qquad \textbf{(12)}$$

$$k_2 = k_{21} \qquad \textbf{(13)}$$

$$k_1 = k_{1F} + k_{1A} \qquad \textbf{(14)}$$

$$k_F = k_{FA} + k_{FL} \qquad \textbf{(15)}$$

$$k_A = k_{AL} \qquad \textbf{(16)}$$

Figure 8: Reaction pathway for degradation of xylose oligomers. k_{61}, k_{62}, k_{63}, k_{51}, k_{52}, k_{41}, k_{42}, k_{31}, k_{21}, k_{1F}, k_{1A}, and k_{FA} are the rate constants for the formation of DP1 from DP6, DP2 from DP6, DP3 from DP6, DP1 from DP5, DP2 from DP5, DP1 from DP4, DP2 from DP4, DP1 from DP3, DP1 from DP2, furfural from DP1, formic acid from DP1, and formic acid from furfural, respectively, in min^{-1}. k_{FL} and k_{AL} are the rate constants for the degradation of furfural and formic acid, respectively, into unaccounted degradation products in min^{-1}.

4.2.9.2 Modeling temperature and acid concentration effects

Rate constants for DP6, DP5, DP4, DP3, DP2, DP1, furfural, and formic acid were assumed to be affected by temperature and acid concentration, thus warranting the need for the Arrhenius equation for modeling these parameter effects on degradation rates. Because some pretreatment experiments were carried out without acid, the Arrhenius-type equation shown in **Equation 17** was used for modeling temperature and acid concentration effects:

$$k_i = k_o(H^+)^m EXP(-E_a/RT) \qquad\qquad (17)$$

where k_i is the rate constant of a given compound in min^{-1}, k_o is the pre-exponential factor in min^{-1}, (H^+) is the hydrogen ion concentration in $mol\ L^{-1}$, m is the unitless acid concentration exponent, E_a is the activation energy in $J\ mol^{-1}$, R is the gas constant in $J\ mol^{-1}\ K^{-1}$ (8.314), and T is the reaction temperature in K.

4.2.9.3 Parameter estimation

Expressions for DP6, DP5, DP4, DP3, DP2, DP1, furfural, and formic acid concentrations, in mmol/L, were generated using normal integration of **Equations 1-8**. Rate constants were estimated by a normalized least-squares method using the Excel Solver routine. This approach minimized the difference between the model-predicted and experimental data. Once rate constants were determined, Arrhenius parameters were also estimated by least-square method using the Excel Solver Routine.

5.0 RESULTS AND DISCUSSION

5.1 High performance liquid chromatography (HPLC) identification and quantification

5.1.1 HPLC analysis for monomeric sugars

Arabinose, glucose, and xylose were analyzed using an HPLC equipped with a Shodex SP-G guard column, SP-0810 column, and refractive index detector. Sample chromatograms are shown in **Figure 9**. Glucose had a retention time of 15.7 min; xylose had a retention time of 16.8 min; and arabinose had a retention time of 19.3 min. These monomers were quantified using calibration curves (**Figure 10**) that were built by plotting peak area versus concentration over a range of 0 to 25 g L^{-1}. As can be seen in **Figure 10**, calibration curves were linear over the considered range with high R^2 values.
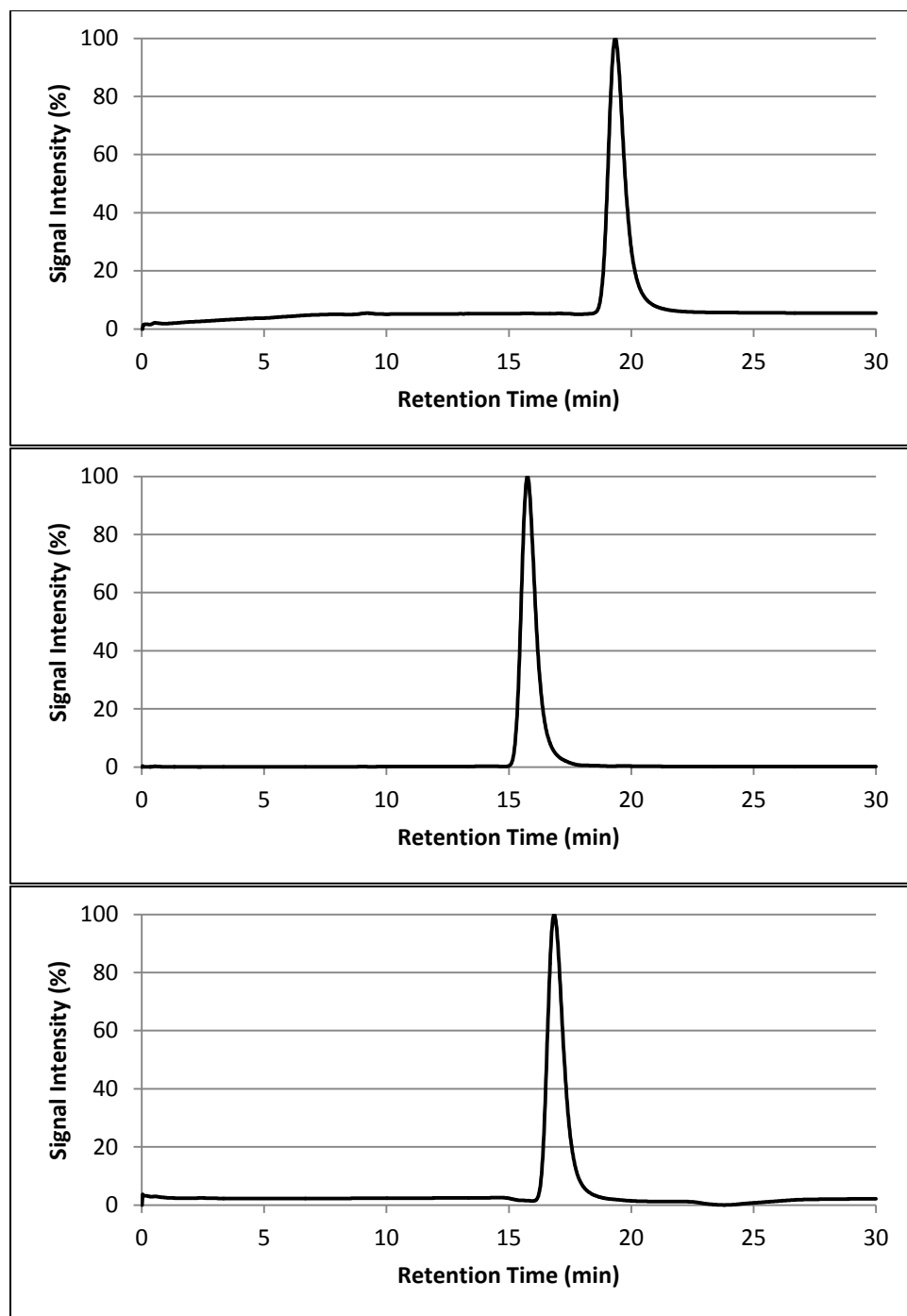
Figure 9: HPLC chromatograms of arabinose (top), glucose (middle), and xylose (bottom)

standards. Compounds were analyzed using an HPLC equipped with a Shodex AP-0810 column

and refractive index detector.
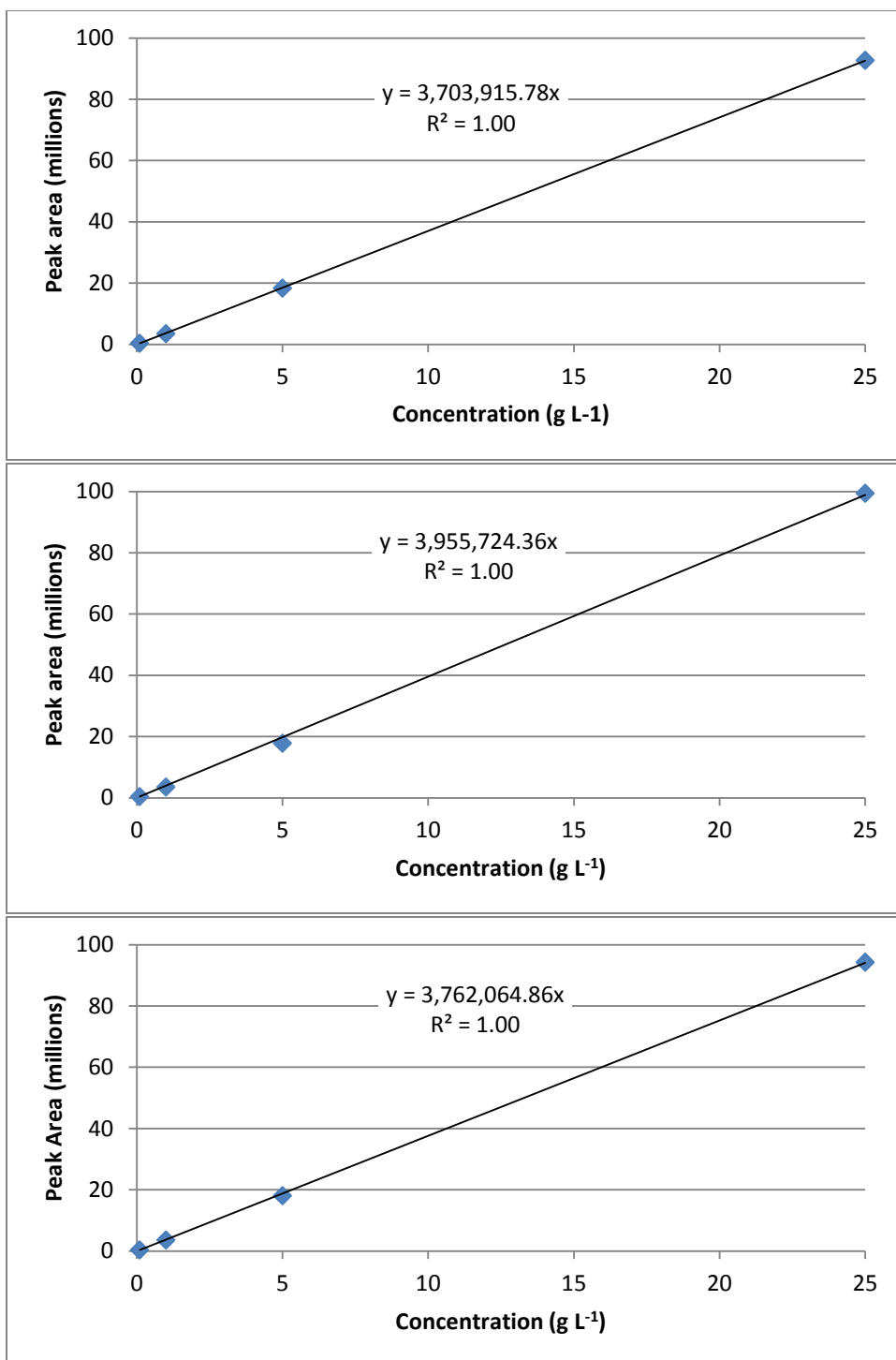
Figure 10: Calibration curves for arabinose (top), glucose (middle), and xylose (bottom) standards as determined using peak area versus concentration. Compounds were analyzed using an HPLC equipped with a Shodex AP-0810 column and refractive index detector.

5.1.2 HPLC analysis for degradation products

Furfural, hydroxymethylfurfural (HMF), and formic acid were analyzed using an HPLC equipped with a Micro-Guard Cation H precolumn, Biorad Aminex HPX-87H column, and photodiode array detector. Furfural and HMF were monitored at 280 nm, and formic acid was monitored at 210 nm. Sample chromatograms are shown in **Figure 11**. Formic acid had a retention time of 13.7 min; HMF had a retention time of 29.2 min; and furfural had a retention time of 44.3 min. These compounds were quantified using calibration curves (**Figure 12**) that were built by plotting peak area versus concentration over a range of 0 to 2.5 g L^{-1} for furfural, 0 to 2.5 g L^{-1} for HMF, and 0 to 10 g L^{-1} for formic acid. As can be seen in **Figure 12**, calibration curves were linear over the considered range with high R^2 values. However, because an unknown compound was co-eluting with formic acid (**Figure 13**), formic acid concentrations were not included in experimental data or kinetic modeling. Formic acid had a retention time of 13.7 min, and the unknown compound had a retention time of 13.4 min.
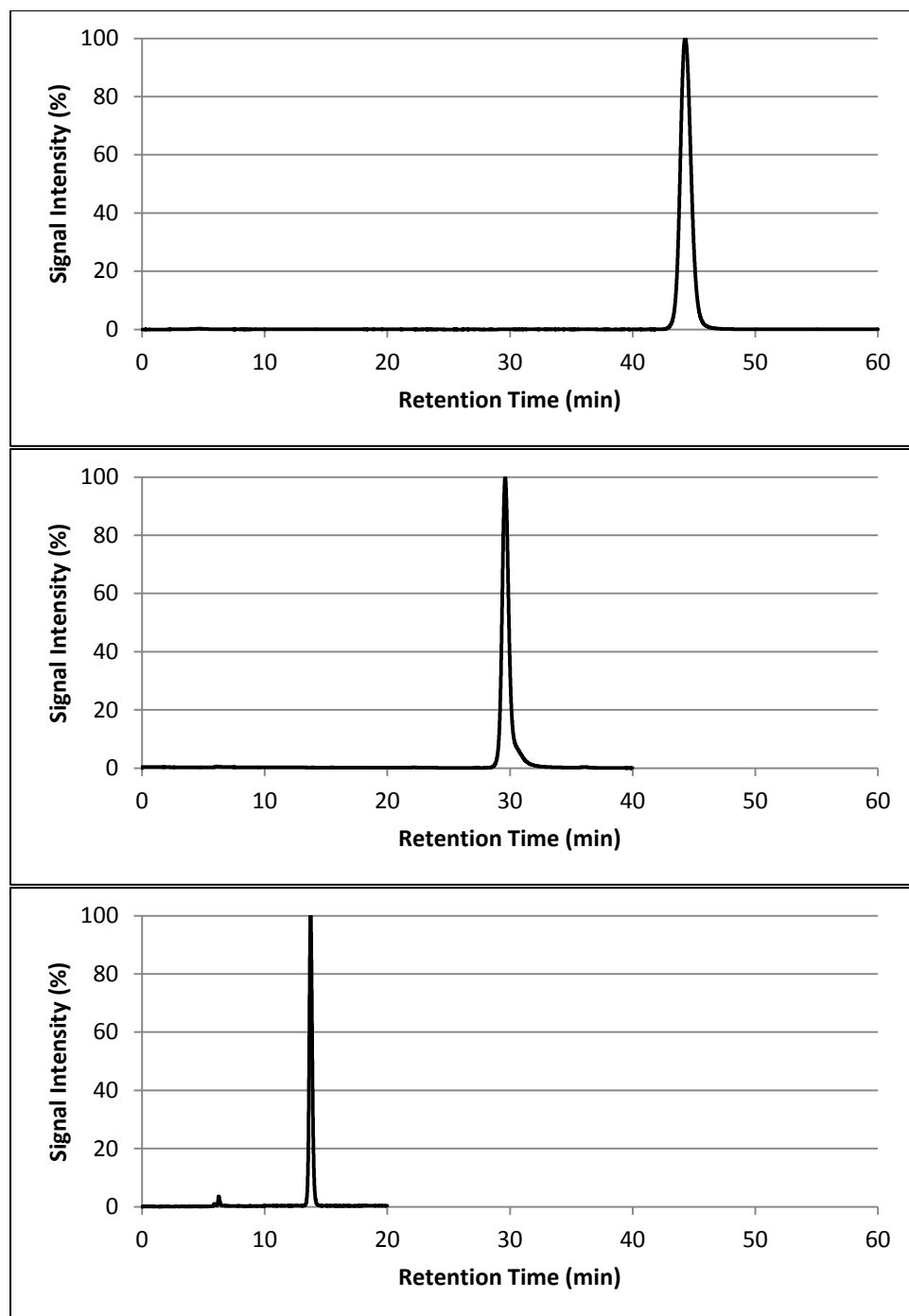
Figure 11: HPLC chromatograms for furfural (top), hydroxymethylfurfural (HMF) (middle), and formic acid (bottom) standards. Compounds were analyzed using an HPLC equipped with a Biorad HPX-87H column and photodiode array detector. Furfural and HMF were monitored at 280 nm, and formic acid was monitored at 210 nm.
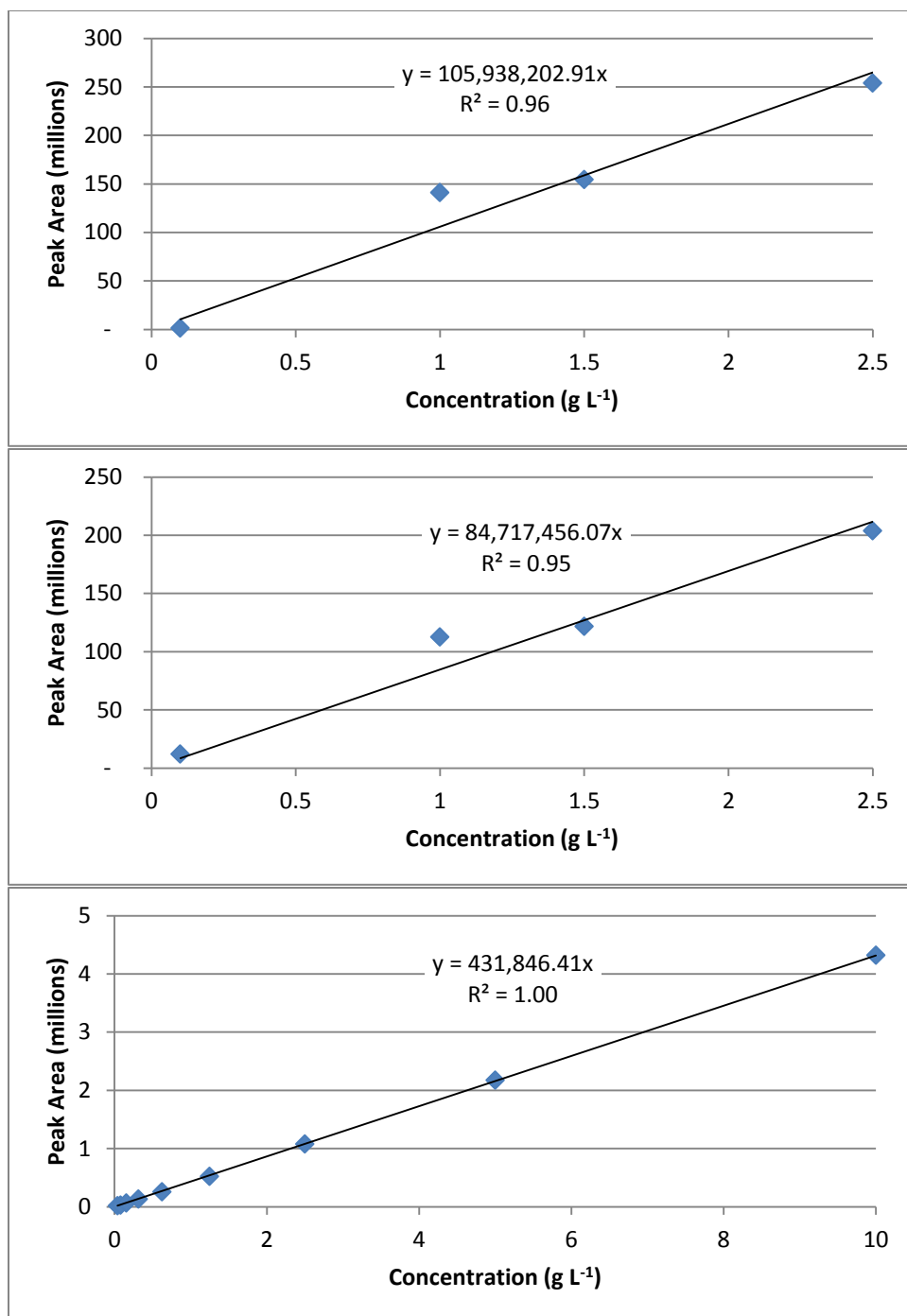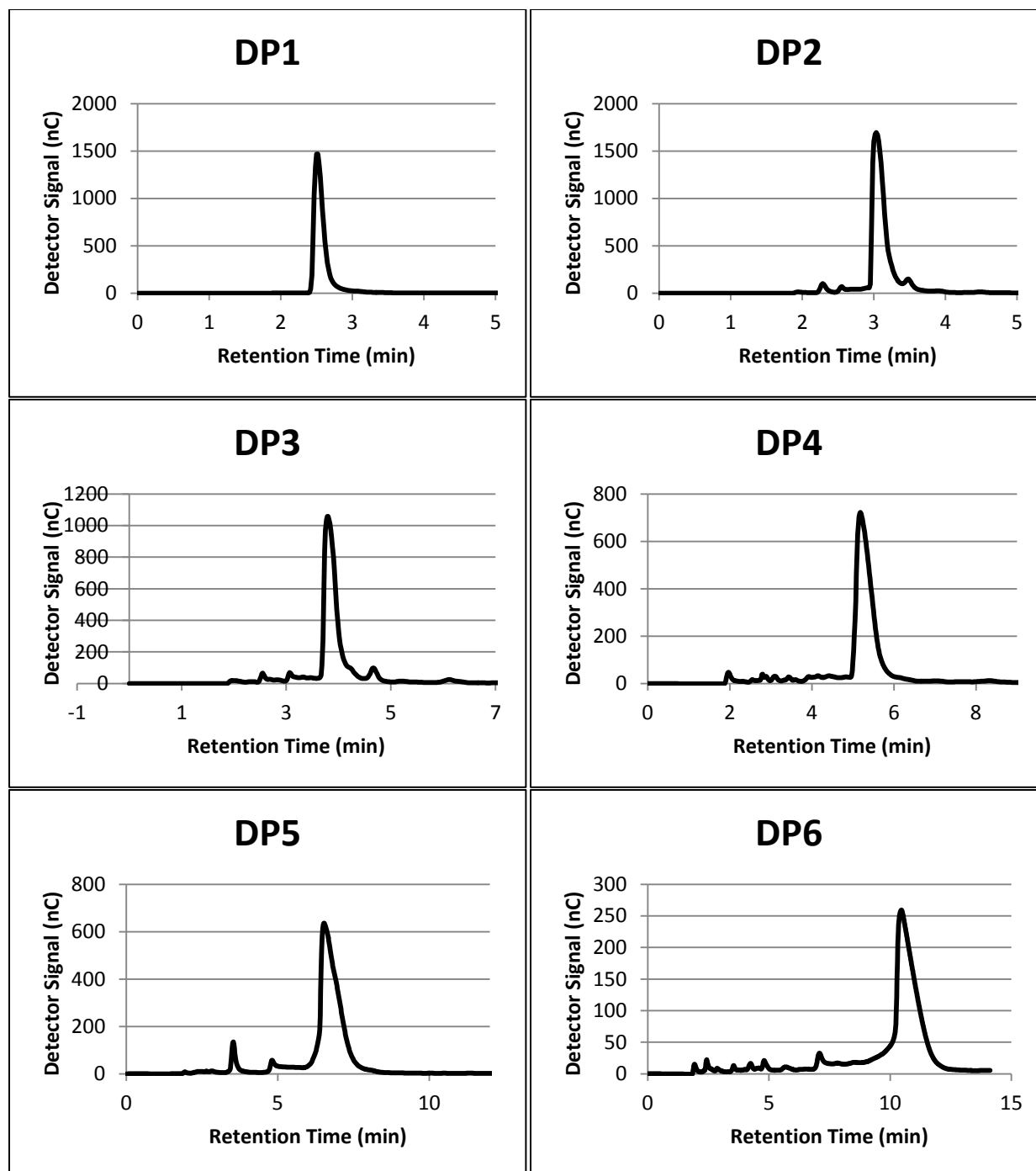
Figure 12: Calibration curves for furfural (top), hydroxymethylfurfural (HMF) (middle), and formic acid (bottom) standards as determined using peak area versus concentration. Compounds were analyzed using an HPLC equipped with a Biorad HPX-87H column and photodiode array detector.
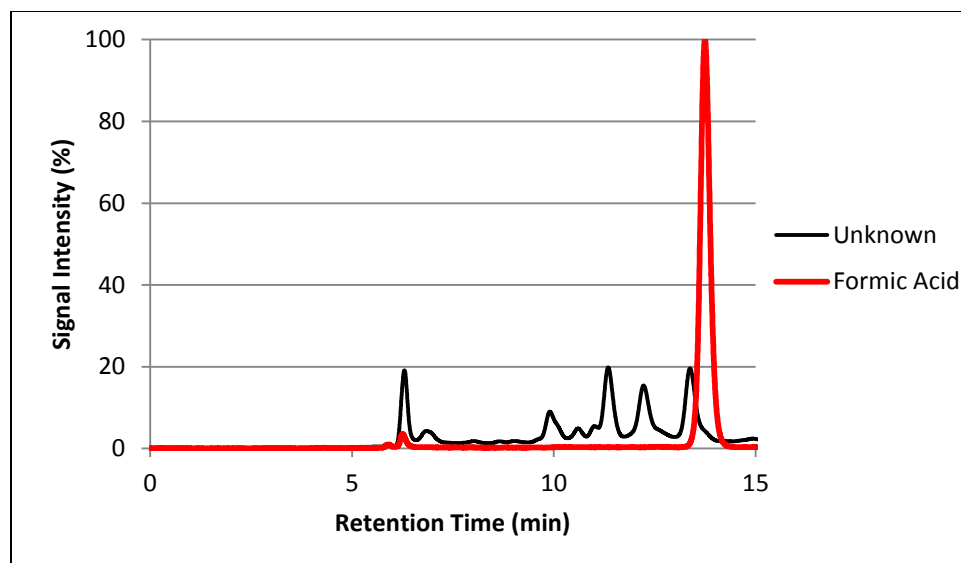
Figure 13: HPLC chromatogram showing the co-elution of an unknown compound with formic acid. Formic acid had a retention time of 13.7 min, and the unknown compound had a retention time of 13.4 min. Both compounds were analyzed using an HPLC equipped with a Biorad HPX-87H column and photodiode array detector at 210 nm.

5.1.3 High performance anion exchange chromatography with pulsed amperometric

detection (HPAEC-PAD) analysis of oligomers

Xylose oligomers were analyzed using an HPAEC-PAD system equipped with a CarboPac PA200 guard column, CarboPac PA200 analytical column, and electrochemical detector. Sample chromatograms are shown in **Figure 14**. DP6, DP5, DP4, DP3, DP2, and DP1 were quantified using calibration curves (**Figure 15**) that were built by plotting peak area versus concentration over a range of 0 to 2.0 g L^{-1}. As can be seen in **Figure 15**, calibration curves were linear over the considered range with high R^2 values.

Figure 15: HPAEC-PAD chromatograms for DP1 (top left), DP2 (top right), DP3 (middle left), DP4 (middle right), DP5 (bottom left), and DP6 (bottom right) standards. Compounds were analyzed using a HPAEC-PAD system equipped with a CarboPac PA200 analytical column and electrochemical detector.
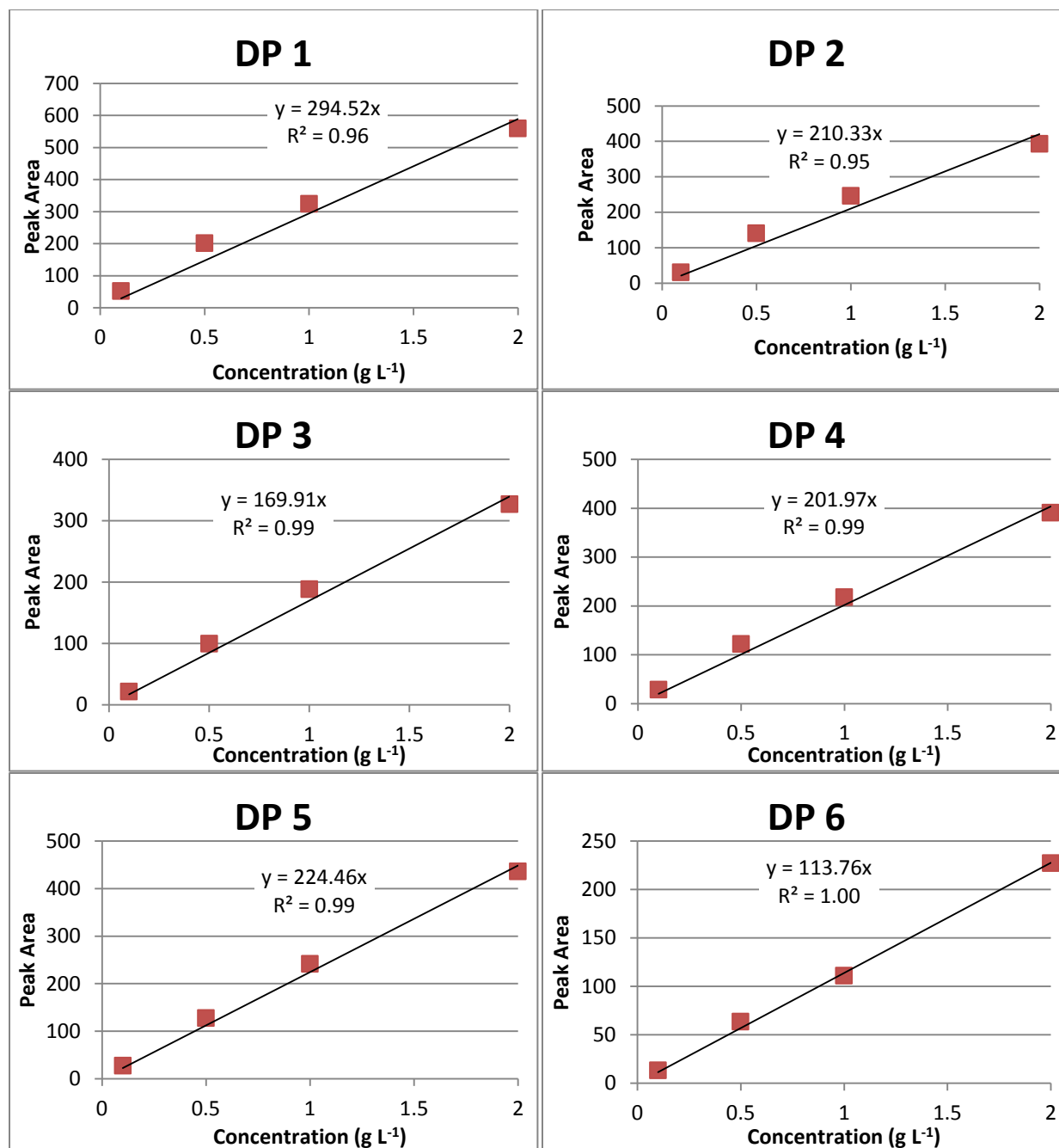
Figure 15: Calibration curves for DP1 (top left), DP2 (top right), DP3 (middle left), DP4 (middle right), DP5 (bottom left), and DP6 (bottom right) standards as determined using peak area versus concentration. Compounds were analyzed using a HPAEC-PAD system equipped with a CarboPac PA200 analytical column and electrochemical detector.

5.2 Switchgrass characterization

5.2.1 Compositional analysis of switchgrass

Table 1 reports the composition of the switchgrass samples obtained from the University of Arkansas Agricultural Research and Extension Center in Fayetteville, AR. Statistical analysis revealed significant differences in the extractives, ash, Klason lignin, and protein contents between the February- and July-harvested samples at the $\alpha = 0.05$ level. No significant differences were observed among polysaccharide contents. These results are in general agreement with other literature values for switchgrass components (Adler *et al*., 2006; David and Ragauskas, 2010; Dien *et al*., 2006; Yan *et al*., 2010). As mentioned by Adler *et al*. (2006), these characteristics will affect the quality of the biomass for biofuels production. Although the lower ash content of February-harvested switchgrass is desirable, this could be offset by the increased lignin content. Protein content could also play a key role if generation of co-products is considered. There are many other factors that must be considered as well, including farm operations management, conversion facility need, and transportation and harvesting logistics to name a few (Adler *et al*., 2006).

Table 1: Switchgrass composition by percent mass on dry basis (n=6).

| Component	July[A,B]	February[A,B]
Cellulose	37.01 ± 1.51A	36.7 ± 1.34A
Hemicelluloses	28.10 ± 3.60A	28.90 ± 1.50A
Ash	4.91 ± 0.17A	2.60 ± 0.13B
Extractives	15.6 ± 0.15A	12.2 ± 0.18B
Klason lignin	6.74 ± 2.14B	13.6 ± 1.05A
Protein	5.38 ± 0.05A	2.13 ± 0.04B

[A]Numbers represent mean ± standard deviation.
[B]Values in the same row with different letters are significantly different at the $\alpha = 0.05$ level.

5.2.2 Scanning electron microscopy (SEM)

Micrographs of the February- and July-harvested switchgrass internode samples and extracted hemicelluloses are shown in **Figure 16**. July internode samples appeared to have smoother fibers compared to those of the February samples, as noted by the numerous trichomes occurring along the internode area of the blade. No observable differences could be seen between the extracted hemicelluloses.
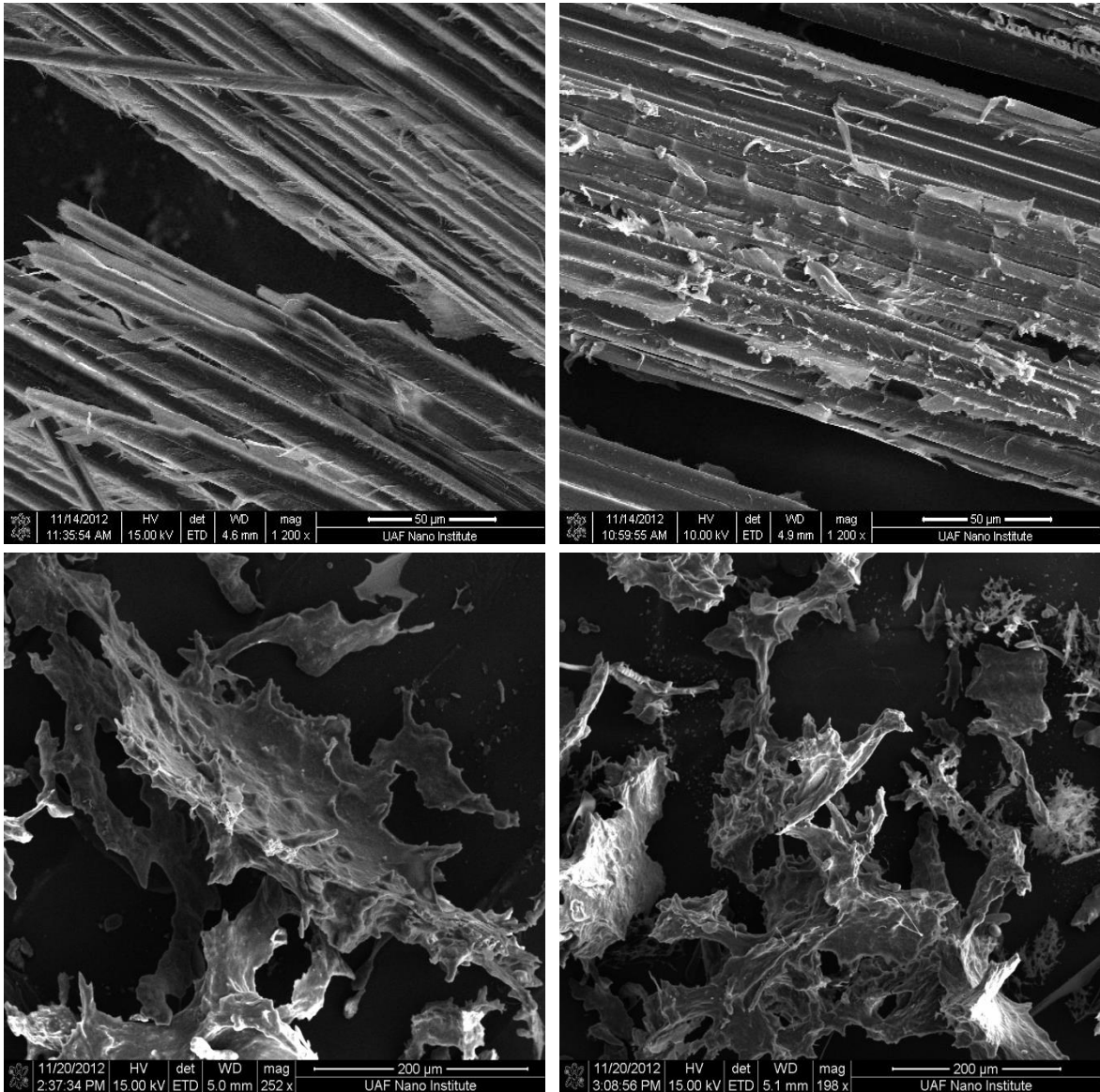
Figure 16: Scanning electron micrographs of July- (top left) and February-harvested (top right) switchgrass internode samples and extracted July- (bottom left) and February-harvested (bottom right) switchgrass hemicelluloses.
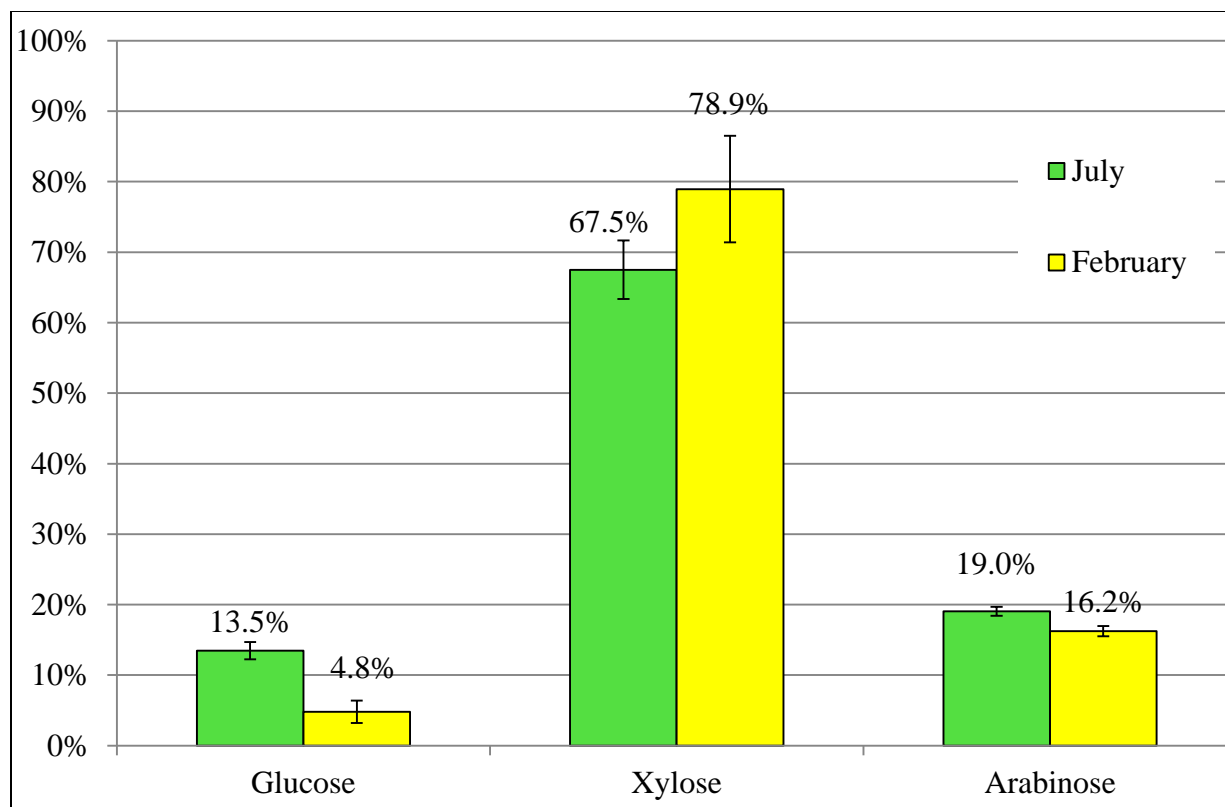
5.3 Switchgrass hemicelluloses extraction

Alkali extraction methods modified from Methacanon *et al*. (2003) and Bowman *et al*. (2011) were used to successfully extract hemicelluloses from July- and February-harvested switchgrass samples. Extraction of July- and February-harvested switchgrass samples yielded 22 and 25 % (dry basis) hemicelluloses from starting biomass, respectively, corresponding to 79 and 85 % of available hemicelluloses according to compositional analysis results of the switchgrass samples reported in **Table 1**. These results are comparable with those obtained by Bowman *et al*. (2011), who obtained 27 % (dry basis) hemicelluloses from the extraction of Alamo switchgrass.

5.4 Hemicelluloses characterization

### 5.4.1 Compositional analysis of hemicelluloses

The extracted switchgrass hemicelluloses were characterized in terms of their monomeric composition, which consisted of xylose, glucose, and arabinose as shown in **Figure 17**. July hemicelluloses were 14, 68, and 19 wt % glucose, xylose, and arabinose, respectively; and February hemicelluloses were 5, 79, and 16 wt % glucose, xylose, and arabinose, respectively. The differences in xylose, glucose, and arabinose contents between July and February hemicelluloses were 11.4, 8.7, and 2.8 %, respectively, which were significantly different at the $\alpha = 0.05$ level. Minor amounts of galactose were also detected in some samples; however, quantities detected were below the level of quantification of the HPLC system used.

Figure 17: Carbohydrate composition of extracted switchgrass hemicelluloses. Differences were significantly different at the α = 0.05 level (n=6).

5.4.2 Molecular weight analysis

Figure 18 presents the results of size exclusion chromatography experiments. July hemicelluloses started eluting at 8.5 mL compared to February hemicelluloses starting elution at 9.75 mL, suggesting that July hemicelluloses contained a broader distribution of molecular weights than February hemicelluloses. Average molecular weights of 30,000 and 28,000 g mol^{-1} were calculated for July and February hemicelluloses, respectively. Based on the compositional analysis results, these molecular weights correspond to average degrees of polymerization of 219 for July hemicelluloses and 205 for February hemicelluloses.
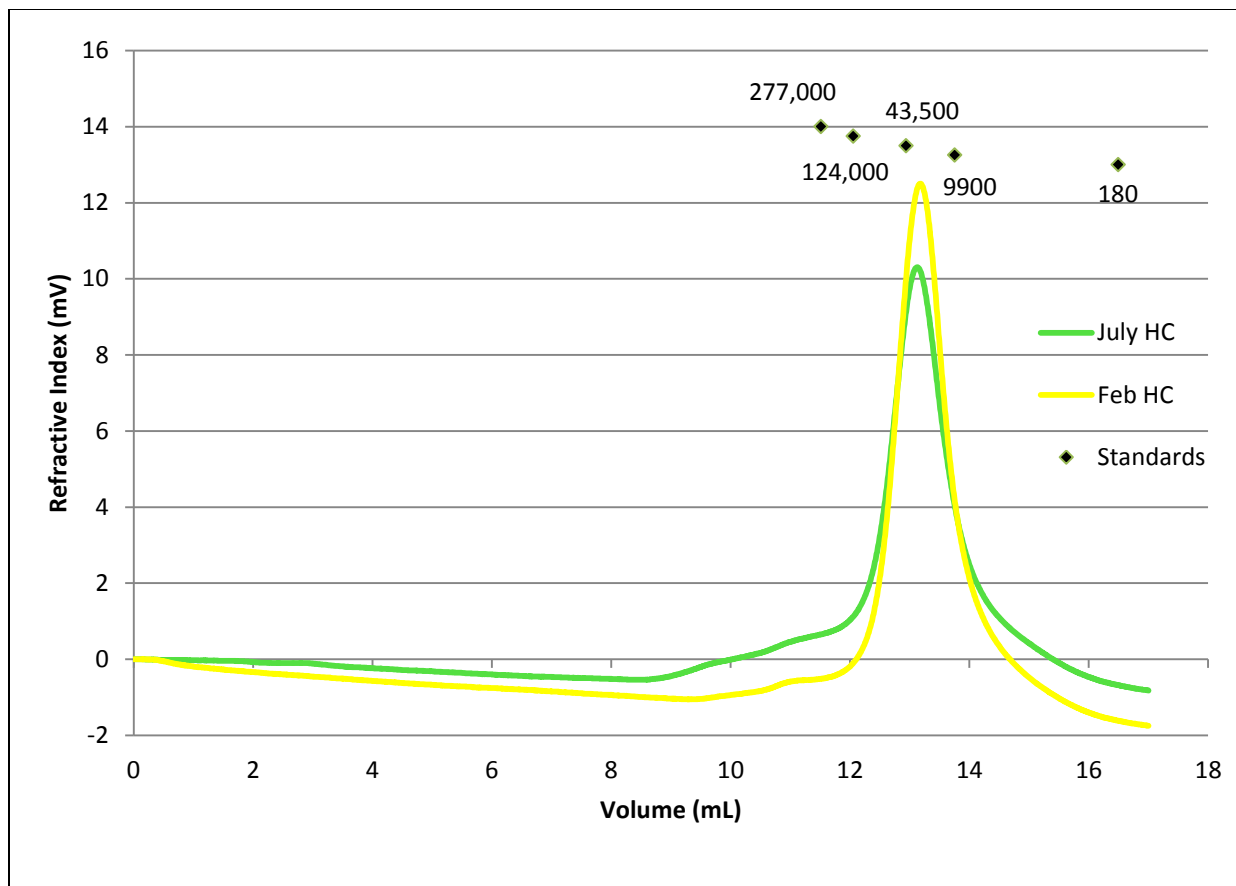
Figure 18: High performance size exclusion chromatograms of July (green line) and February (yellow line) switchgrass hemicelluloses and dextran standards (diamonds).

5.4.3 Glycosyl linkage analysis

Linkage analysis data showed both hemicelluloses to contain structurally identical glycosyl residues (**Table 2**). The main residue in both samples was 1,4-linked xylose (53% for July and 67% for February), with additional 1,3,4-linked xylose residues accounting for 12 and 11% of July and February hemicelluloses, respectively. July hemicelluloses contained 8.3% more 1,4-linked glucose residues than February hemicelluloses. Terminally linked arabinose and 1,2-linked arabinose residues were also present in both samples. Based upon these results, hemicelluloses are arabinoxylans, which are common to grasses and mixed-linkage glucans, which are associated with cell wall growth (Mazumder and York, 2010; Buckeridge *et al*., 2004).

Table 2: Glycosyl linkages of July and February switchgrass hemicelluloses.

| Glycosyl residue	Linkages	Peak area (%)	
		July	February
4 linked Xylopyranose	→4)-Xyl*p*-(1→	52.7	66.7
3,4 linked Xylopyranose	→3,4)-Xyl*p*-(1→	12.1	10.8
Terminally linked Xylopyranose	Xyl*p*-(1→	3.6	3.7
Terminally linked Arabinofuranose	Ara*f*-(1→	9.9	8.4
3 linked Arabinofuranose	→3)-Ara*f*-(1→	0.5	0.3
2 linked Arabinopyranose	→2)-Ara*p*-(1→	1.6	1.1
4 linked Arabinopyranose or 5 linked Arabinofuranose	→4)-Ara*p*-(1→ or →5)-Ara*f*-(1→	0.1	0.1
4 linked Glucopyranose	→4)-Glc*p*-(1→	14.1	5.8
3 linked Glucopyranose	→3)-Glc*p*-(1→	1.3	0.8
Terminally linked Glucopyranose	Glc*p*-(1→	0.8	0.3

5.5 Summary on switchgrass hemicelluloses

In summary, hemicelluloses were successfully extracted from July- and February-harvested switchgrass samples and subsequently characterized for monomeric composition, size, and glycosyl linkages and published in Bunnell *et al*. (2013a). Results showed that changes do occur in the physicochemical properties of the hemicelluloses as switchgrass senesces. Using the methods reported here, the physicochemical properties of other bioenergy-destined feedstocks could be examined. It would be interesting to see if the physicochemical properties of other feedstocks such as crop residues, hardwoods, and softwoods change in a manner similar to switchgrass. These results could have major implications for converting biomass into fuels and chemicals, as well as providing insight on the physiological role of hemicelluloses.

5.6 Production of switchgrass hemicelluloses-derived oligomers

Switchgrass hemicelluloses were hydrolyzed at 160 ^{o}C for 60 min in water. The resulting hydrolysate oligomer, monomer, and degradation products profiles can be seen in **Figure 19**. Yields of 43, 25, 24, 34, 23, 19, and 38 mg of arabinose, xylose, xylobiose (DP2), xyolotriose (DP3), xylotetraose (DP4), xylopentose (DP5), and xylohexose (DP6), respectively, were generated per g of hemicelluloses. These yields are lower than those obtained by Lau *et al*. using birchwood xylan hydrolyzed at 200 ^{o}C for 60 min in water; however, formation of degradation products such as furfural and formic acid were minimized (Lau *et al*., 2013).

These yields could possibly be increased through the refining of processing parameters or by modifying the process itself. Increasing the reaction temperature has been shown to favor oligomer production but care must be taken to avoid production of degradation products (Nabarlatz *et al*., 2004). Multi-stage reactions are also a consideration for autohydrolysis production. Another process that could be employed is enzymatic hydrolysis, which offers a route for more targeted fractions dependent upon the enzyme selected. For example, Yuan *et al*. (2004) were able to produce primarily DP2 and DP3 using *Aspergilllus niger* AN-1.15 xylanases.
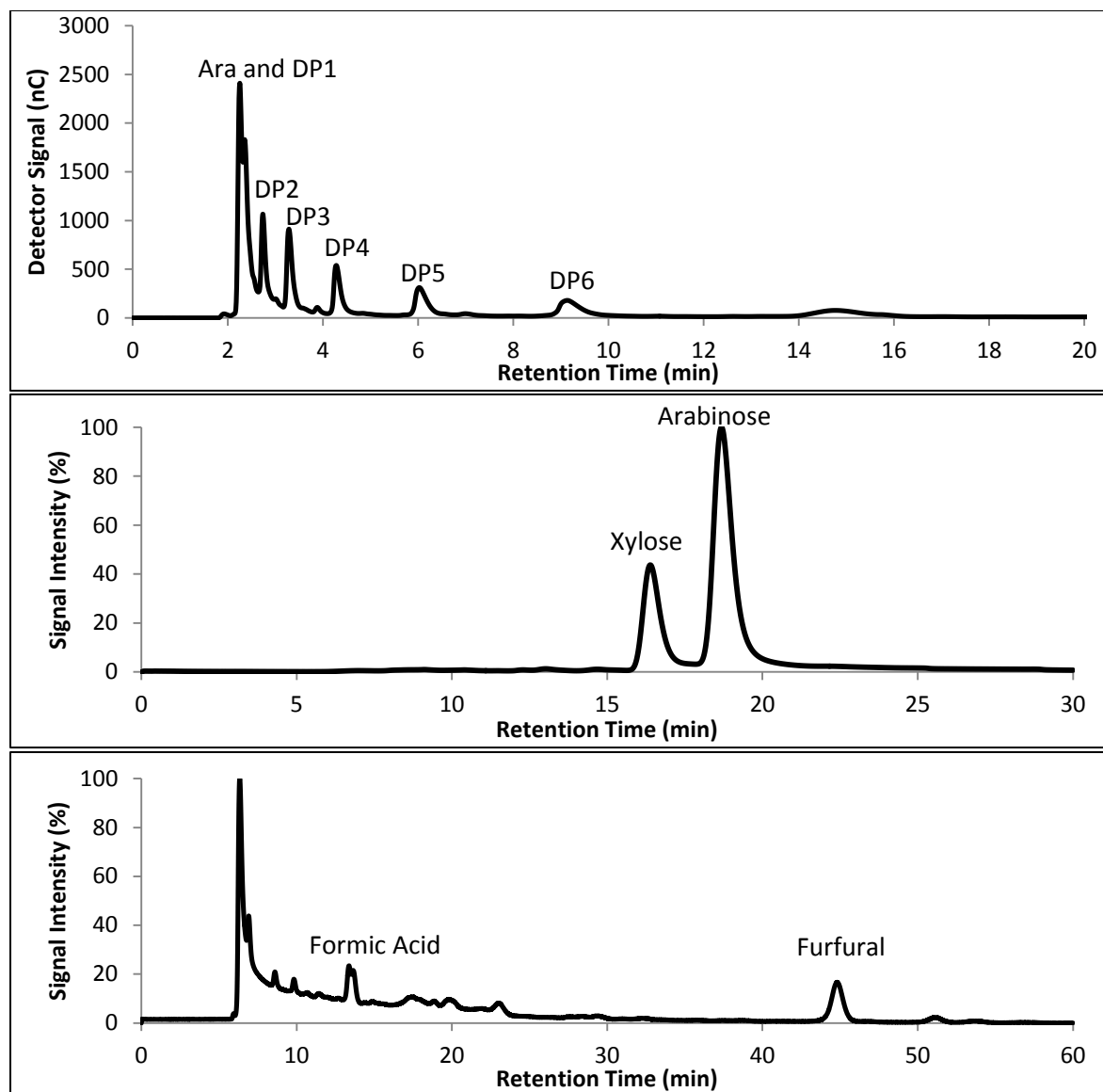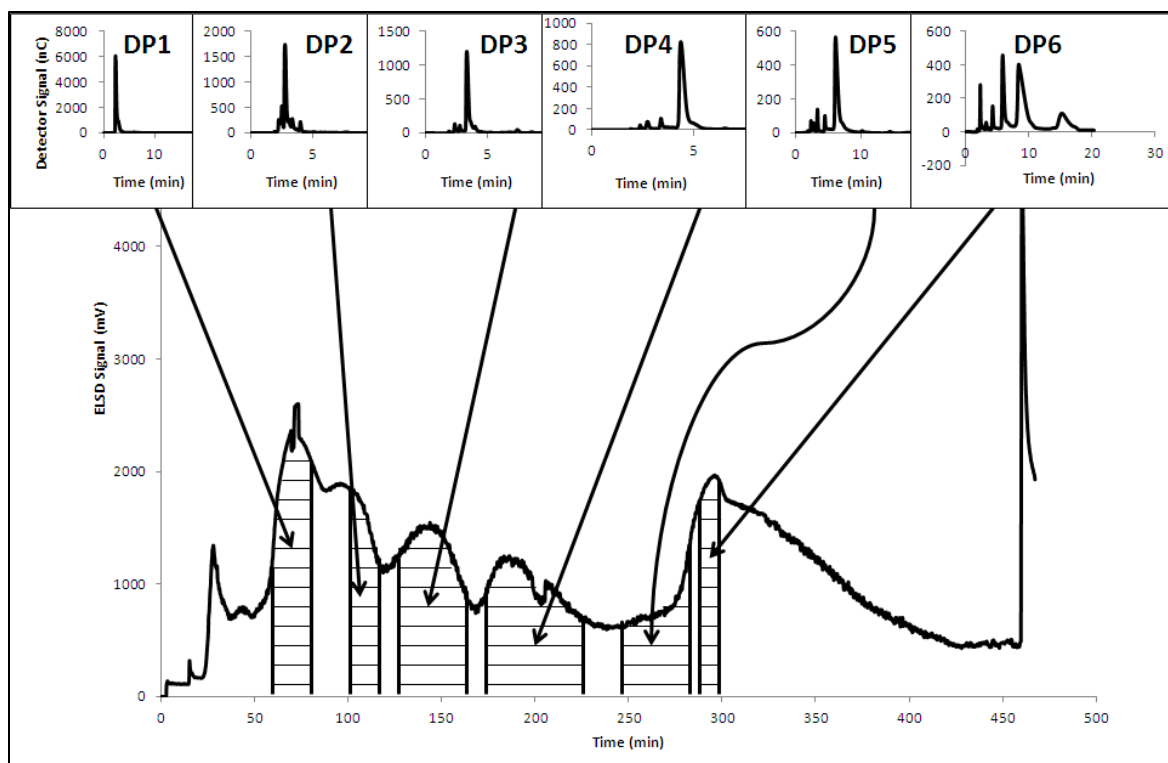
Figure 19: High performance anion-exchange chromatography with pulsed amperometric detection (HPAEC-PAD) chromatogram (top) [Ara and DP1 – arabinose and xylose (2.4 min), DP2 – xylobiose (2.7 min), DP3 – xylotriose (3.3 min), DP4 – xylotetraose (4.3 min), DP5 – xylopentose (6.0 min), DP6 – xylohexose (9.0 min)], high performance liquid chromatography (HPLC) chromatogram for monomers (middle) [xylose (16.8 min), arabinose (19.3 min)], and HPLC chromatogram for degradation products (bottom) [formic acid (13.7 min), furfural (44.8 min)] for switchgrass hemicelluloses autohydrolysed at 160 $^{\circ}$C for 60 min.

5.7 Switchgrass hemicelluloses-derived oligomers fractionation

Arabinose and xylose, DP2, DP3, DP4, DP5, and DP6 eluted the column at 61-80, 105-114, 130-165, 175-228, 245-285, and 291-299 min, respectively, as shown in **Figure 20**. Fractions were consolidated based upon the HPAEC-PAD results for the composition of the fractions, and high and low purity consolidated fractions were obtained. High purity consolidated fractions contained primarily the designated oligomer, whereas low purity consolidated fractions contained the fractions that were a transition of elution from a lower DP oligomer to a higher DP oligomer. **Table 3** lists the consolidated fractions of oligomers with corresponding yields and purities. With commercially available xylose oligomers in the range of 75-95% purity, this method provides satisfactory results up to DP5 (Moure *et al.*, 2006). For a tradeoff in yield, DP6 could also be produced within this purity range. DP2-DP5 could also be attained at higher purities if greater purity was preferential over greater yields.

Beyond 299 min of separation, DP6 and higher DP oligomers were either not separated with satisfactory resolution or the elution volumes were too close for the volume of each collected fraction (8 mL), resulting in a wide range of DPs as shown in **Figure 21**. However, because no there are no commercially available oligomer standards with a DP greater than six, these compounds cannot be quantified. Nonetheless, if these higher range DP oligomers were targeted for fractionation, the authors would recommend exploring additional solvent systems.

Figure 20: Evaporative light scattering detector (ELSD) signal for centrifugal partition chromatography (CPC) separation of switchgrass hemicelluloses-derived oligomers with inserts of high performance anion-exchange chromatography with pulsed amperometric detection (HPAEC-PAD) chromatograms for consolidated fractions. DP1 – arabinose and xylose, 61-81 min; DP2 – xylobiose, 105-114 min; DP3 – xylotriose, 130-165 min; DP4 – xylotetraose, 175-228 min; DP5 – xylopentose, 245-285 min; DP6 – xylohexose, 291-299 min.

Table 3: Xylose oligomer elution times, yields, and purities.

Compound[A]	Elution time (min)	Yield (mg/g)[B]	Purity (%)[C]
High purity consolidated fractions			
Xylobiose (DP2)	105-114	2.4 ± 0.7	75 ± 7
Xylotriose (DP3)	130-165	12.1 ± 5.0	89 ± 1
Xylotetraose (DP4)	175-228	11.0 ± 2.9	87 ± 2
Xylopentose (DP5)	245-285	6.8 ± 1.6	77 ± 6
Xylohexose (DP6)	291-299	11.6 ± 3.5	69 ± 12
Low purity consolidated fractions			
Arabinose and xylose (DP1)	61-80	30.0 and 17.4	62 and 36
Xylobiose (DP2) and xylotriose (DP3)	115-129	4.2 and 5.1	45 and 55
Xylotriose (DP3) and xylotetraose (DP4)	166-174	1.3 and 1.0	53 and 41
Xylotetraose (DP4) and xylopentose (DP5)	229-244	4.6 and 2.2	63 and 30
Xylopentose (DP5) and xylohexose (DP6)	286-290	7.4 and 1.5	74 and 15

[A] Degree of polymerization (DP) [B] mg xylose oligomer per g autohydrolyzed hemicelluloses [C]

Purity calculated as mass of xylose oligomer divided by the total mass of detected compounds

(xylose oligomers and degradation products).
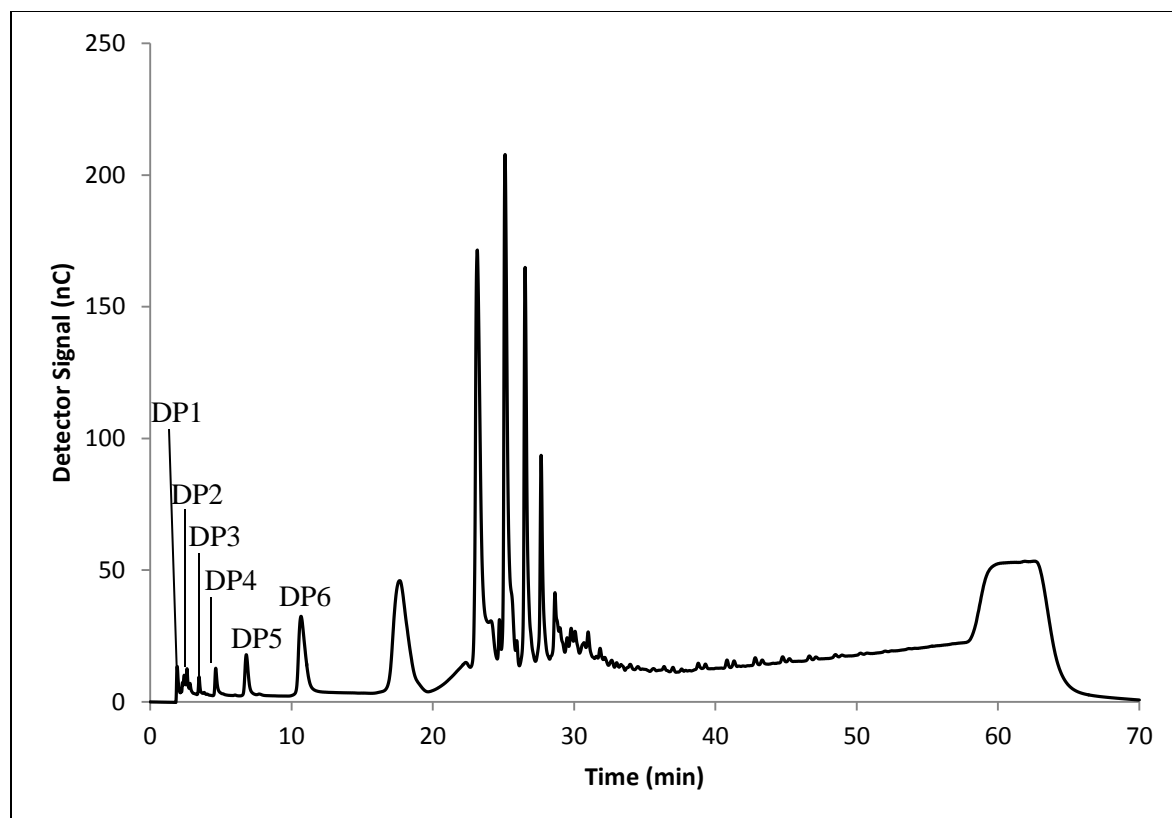
Figure 21: High performance anion-exchange chromatography with pulsed amperometric detection (HPAEC-PAD) chromatogram for consolidated fractions of 300-460 min of separation using centrifugal partition chromatography (CPC). At 300 min of separation and beyond, xylohexose (DP6) and higher degree of polymerization (DP) oligomers were comingled in collected 8-mL (1 min of separation) fractions, resulting in a wide range of DPs being detected.

## 5.8 Switchgrass hemicelluloses-derived oligomers characterization

5.8.1 Electrospray ionization mass spectrometry (ESI-MS) analysis of oligomers

ESI-MS results are shown in **Figures 22-26**. DP2, DP3, DP4, DP5, and DP6 were detected at mass-to-charge ratios of 305, 437, 569, 701, and 833, respectively, corresponding to oligomers with sodium ions. Oligomers were also detected at mass-to-charge ratios corresponding to oligomers with potassium ions; these sodium and potassium ions are residual from the processing of the switchgrass hemicelluloses. **Table 4** displays the mass-to-charge ratios assigned for each of the xylose oligomers. Mass spectra for the fractions produced in this work were cleaner than the mass spectra for the fractions obtained by Lau *et al.* (2013). However, the purities calculated in this work were lower than those obtained by Lau *et al*. (2013), likely because different methods were used for calculating purities. In Lau *et al*. (2013), purities were calculated as the peak area of a given xylose oligomer divided by the sum of peak areas for all of the xylose oligomers (DP1-DP12) as determined by HPLC. In this work, purities were calculated as mass of a given xylose oligomer divided by the total mass of detected compounds (DP1-DP6 and degradation products) as calculated using HPAEC-PAD and HPLC calibration curves. Purities were reported on a percent basis in both studies.

Table 4: Mass-to-charge ratios for xylose oligomers analyzed using electrospray ionization-mass spectrometry (ESI-MS).

Compound	m/z		
	Neutral	+ Na$^+$	+ K$^+$
Xylobiose (DP2)	282.0	305.0	321.1
Xylotriose (DP3)	414.0	437.1	453.2
Xylotetraose (DP4)	546.0	569.1	585.2
Xylopentose (DP5)	678.0	701.2	717.3
Xylohexose (DP6)	810.0	833.2	849.3
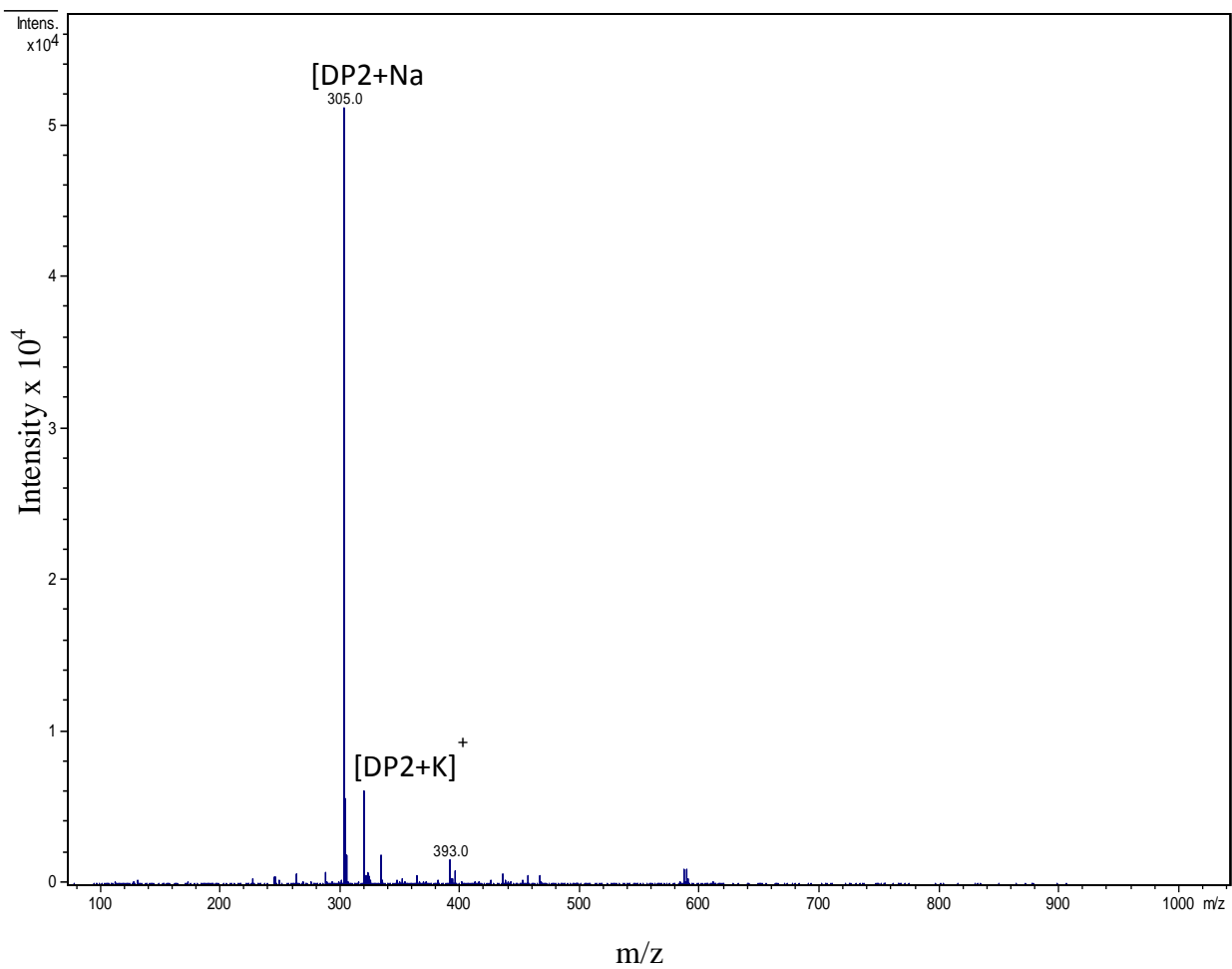
Figure 22: Electrospray ionization mass spectra (ESI-MS) of fractionated xylobiose (DP2).
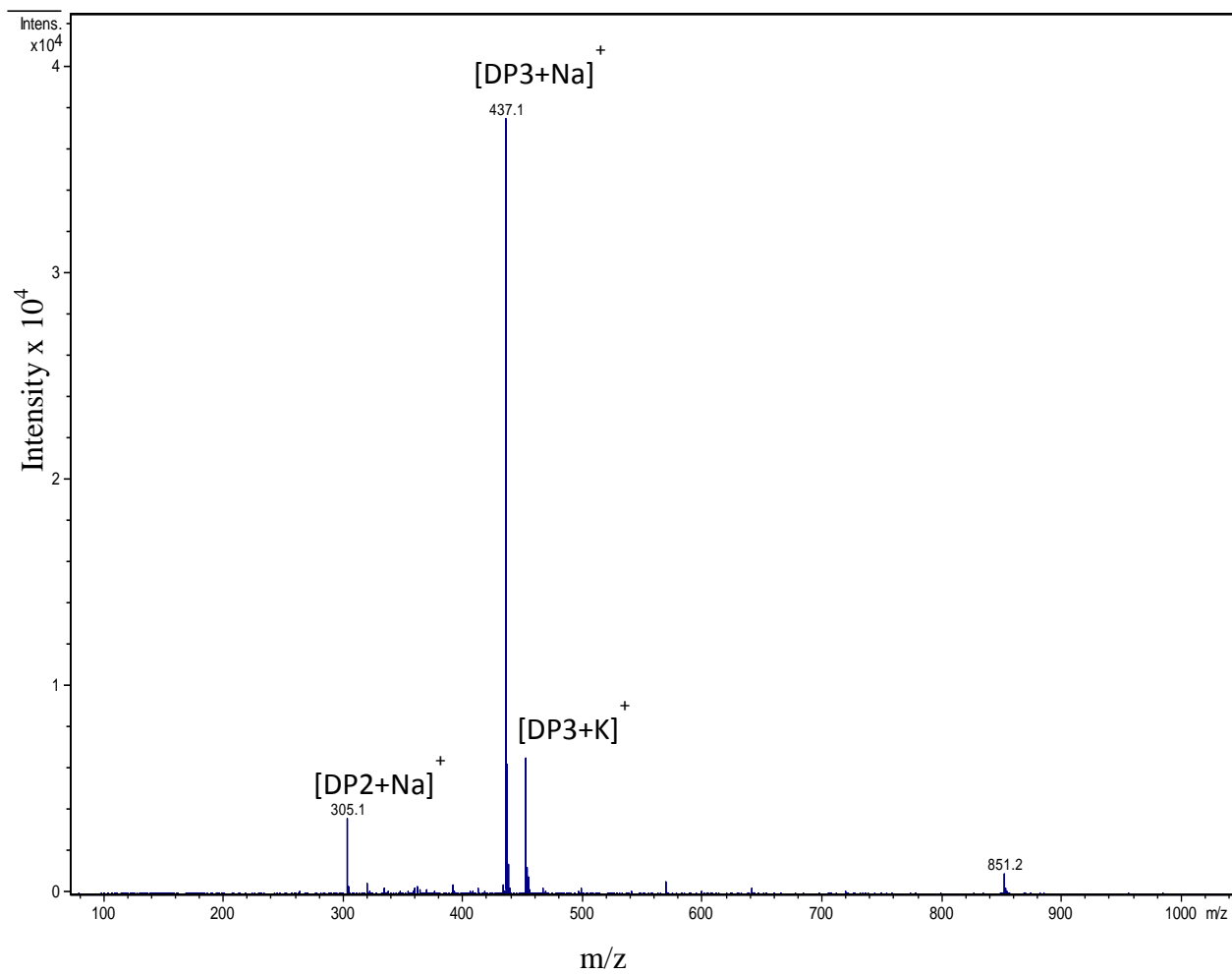
Figure 23: Electrospray ionization mass spectra (ESI-MS) of fractionated xylotriose (DP3).
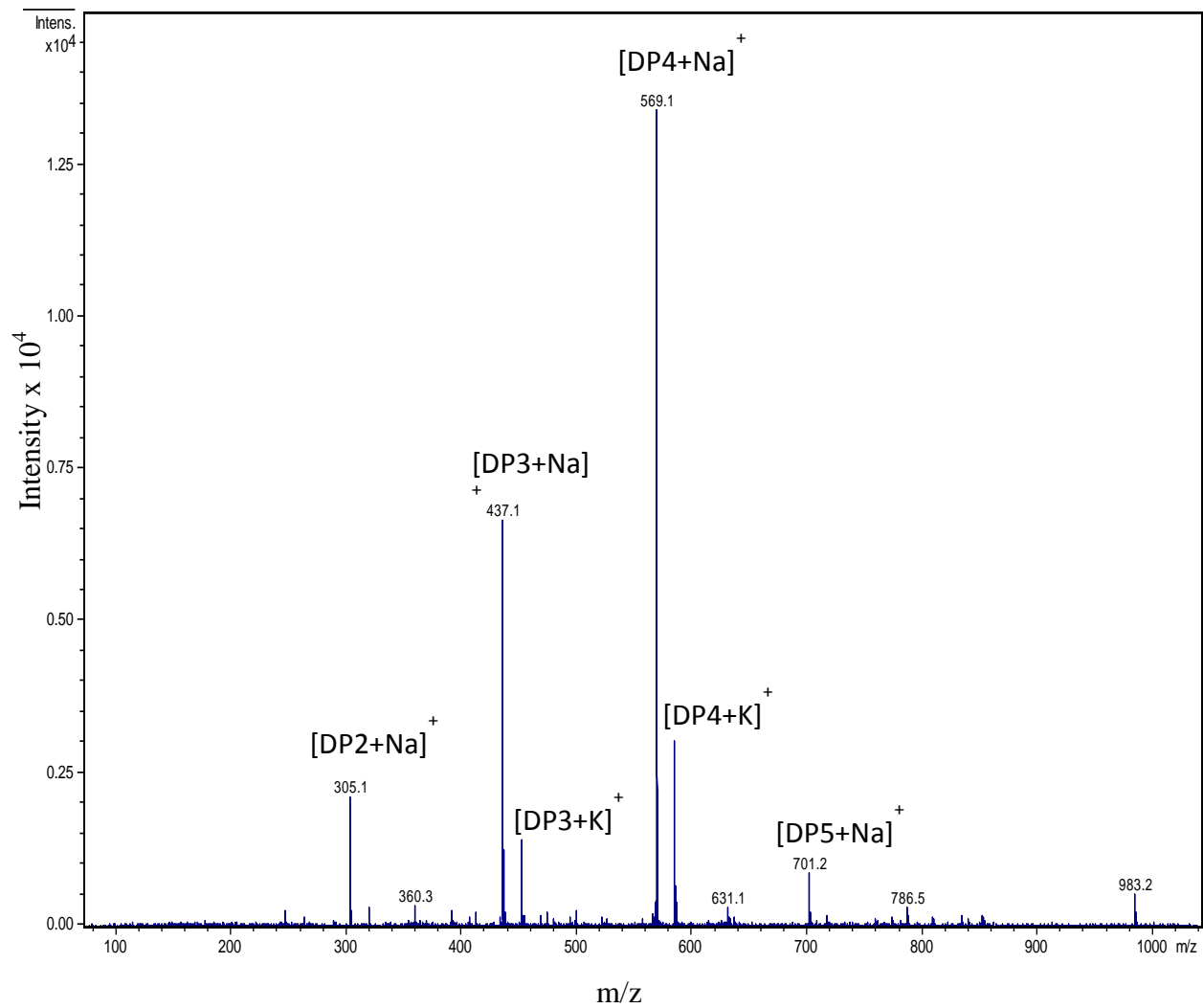
Figure 24: Electrospray ionization mass spectra (ESI-MS) of fractionated xylotetraose (DP4).
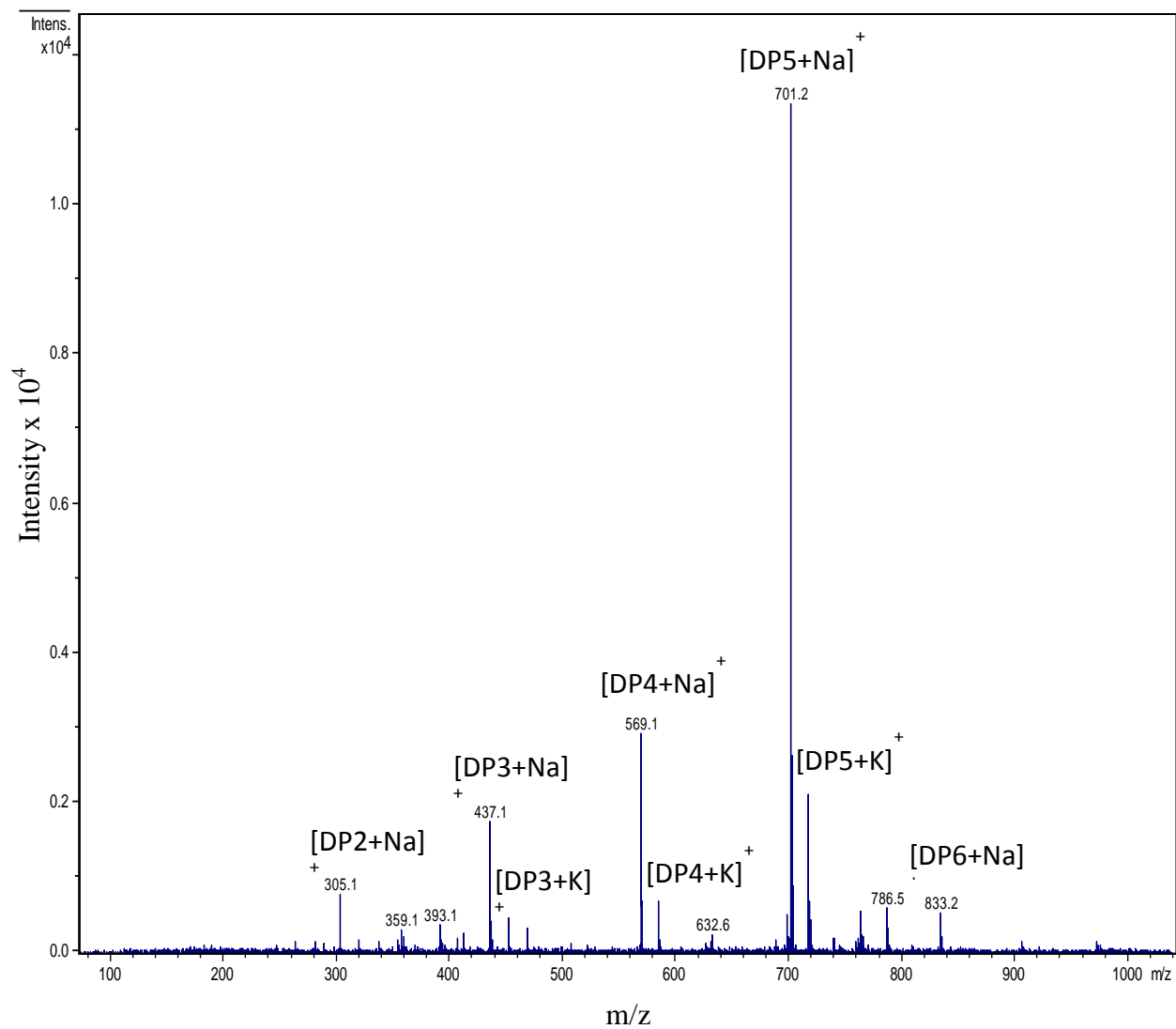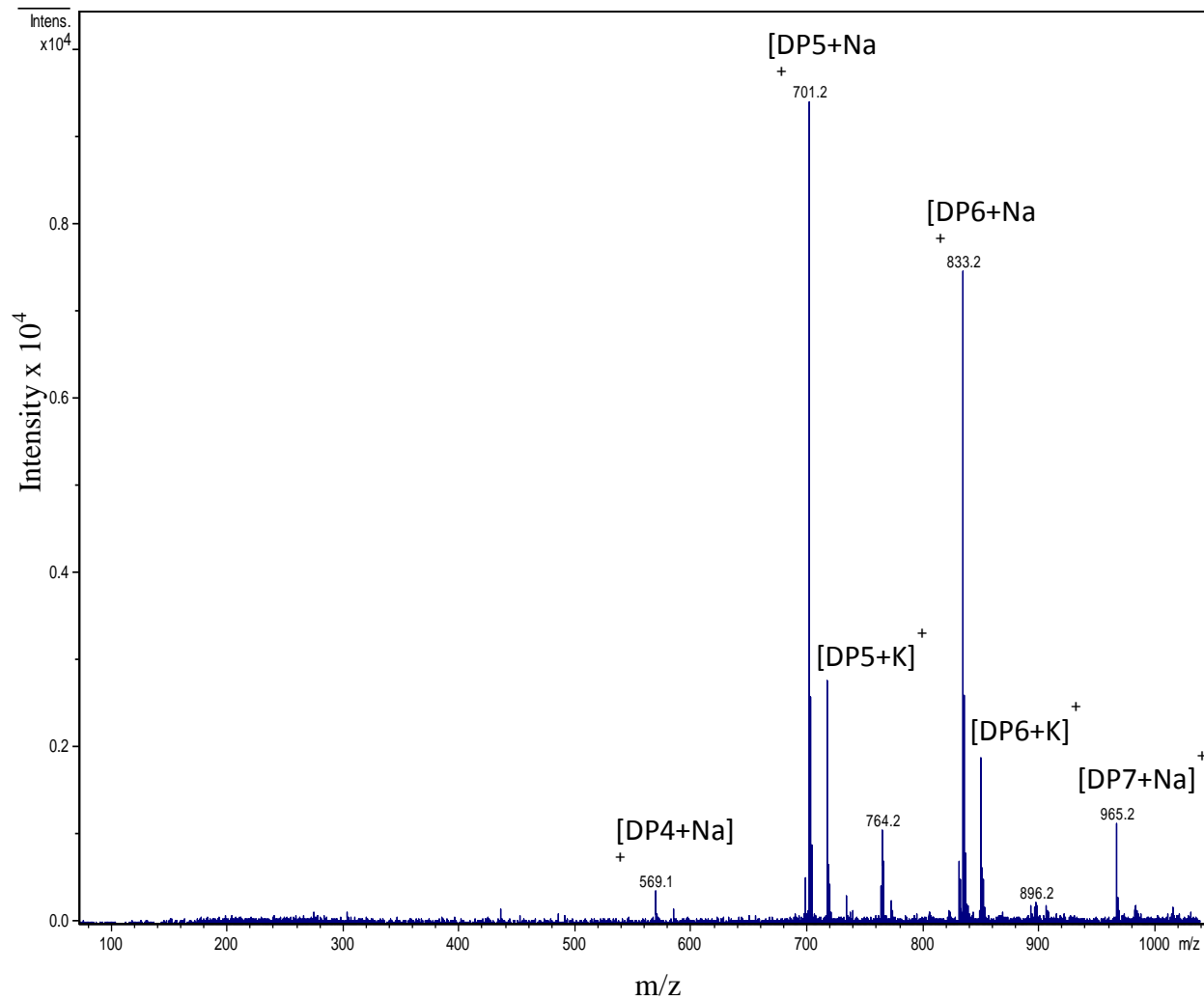
Figure 25: Electrospray ionization mass spectra (ESI-MS) of fractionated xylopentose (DP5).

Figure 26: Electrospray ionization mass spectra (ESI-MS) of fractionated xylohexose (DP6).

5.8.2 Total sugar analysis

Consolidated oligomer fractions were analyzed for monomeric sugar substituents using the NREL total sugar analysis (Sluiter *et al.*, 2008c). Total sugar analysis results of consolidated oligomer fractions revealed xylose as the only monosaccharide after 60 min of hydrolysis with 4 wt % sulfuric acid at 121 ^{o}C. Thus, the oligomers produced are believed to be constituted solely of xylose. This conclusion is further supported by the fact that CPC-fractionated oligomers and purchased xylose oligomers had identical retention times when analyzed using HPAEC-PAD. It has also been reported that during thermochemical pretreatment, the side groups of hemicelluloses react before the backbone of hemicelluloses (Sweet and Winandy, 1999). Bowman *et al.* (2011) also reported that arabinose branches are preferentially cleaved before the xylose backbone.

5.9 Summary on switchgrass-hemicelluloses-derived oligomers

Extracted switchgrass hemicelluloses were partially hydrolyzed in water at 160 $^{\circ}$C to produce a range of oligomers. These oligomers were then fractionated using CPC with a butanol:methanol:water solvent system, and resulted are being published (Bunnell *et al*., 2013b). Although the consolidated oligomer fractions obtained via CPC were not as pure as commercially available oligomers, these CPC-fractionated oligomers are still useful as feedstock for future studies. Because the oligomers eluted the CPC rotor in order of increasing DP, from smallest to largest, these fractions can be tailored such that they do not contain oligomers over a given DP. Thus, the consolidated fractions are suitable feedstock for pretreatment experiments that examine oligomer depolymerization. Also worth noting, the xylose oligomers fractionated in this work did not contain formic acid, which was observed in the xylobiose and xylotetraose samples in Lau *et al.* (2013). This is the first time xylose oligomers have been fractionated from switchgrass or any other bioenergy-destined feedstock using CPC.

5.10 Pretreatment experiments

5.10.1 Pretreatment of switchgrass hemicelluloses

Extracted switchgrass hemicelluloses were pretreated at 140, 160, and 180 $^{\circ}$C at sulfuric acid concentrations of 0.0, 0.5, and 1.0 wt %. Hydrolysis times varied from 0 to 120 min, depending on the hydrolysis conditions, and all experiments were performed in duplicate. Hydrolysis data for xylose, arabinose, and glucose yields can be seen in **Figure 27-29**. For February samples, initial concentrations of xylose, arabinose, and glucose in the hemicelluloses were 16.0, 1.0, and 3.3 g L^{-1}, respectively. For July samples, initial concentrations of xylose, arabinose, and glucose in the hemicelluloses were 13.5, 2.7, and 3.8 g L^{-1}, respectively. Hydrolysis data for furfural and HMF concentrations can be seen in **Figure 30-32**. Neither sample contained furfural or HMF prior to hydrolysis.

Figure 27 illustrates the effect of acid concentration on the yield of monomeric sugars for hydrolysis at 160 $^{\circ}$C. Maximum xylose yields were 18.6, 87.2, and 75.2 % of theoretical xylose for 0.0, 0.5, and 1.0 % acid, respectively, corresponding to hydrolysis times of 120, 5, and 2.5 min. Maximum arabinose yields were 21.0, 73.8, and 74.6 % of theoretical arabinose for 0.0, 0.5, and 1.0 % acid, respectively, corresponding to hydrolysis times of 30, 30, and 5 min. Maximum glucose yields were 38.4 and 55.6 % of theoretical glucose for 0.5 and 1.0 % acid, respectively, corresponding to hydrolysis times of 10 and 30 min. No glucose was released for water-only hydrolysis at 160 $^{\circ}$C. Thus, it can be seen that increasing the acid concentration accelerates the reaction, especially in the case of glucose.
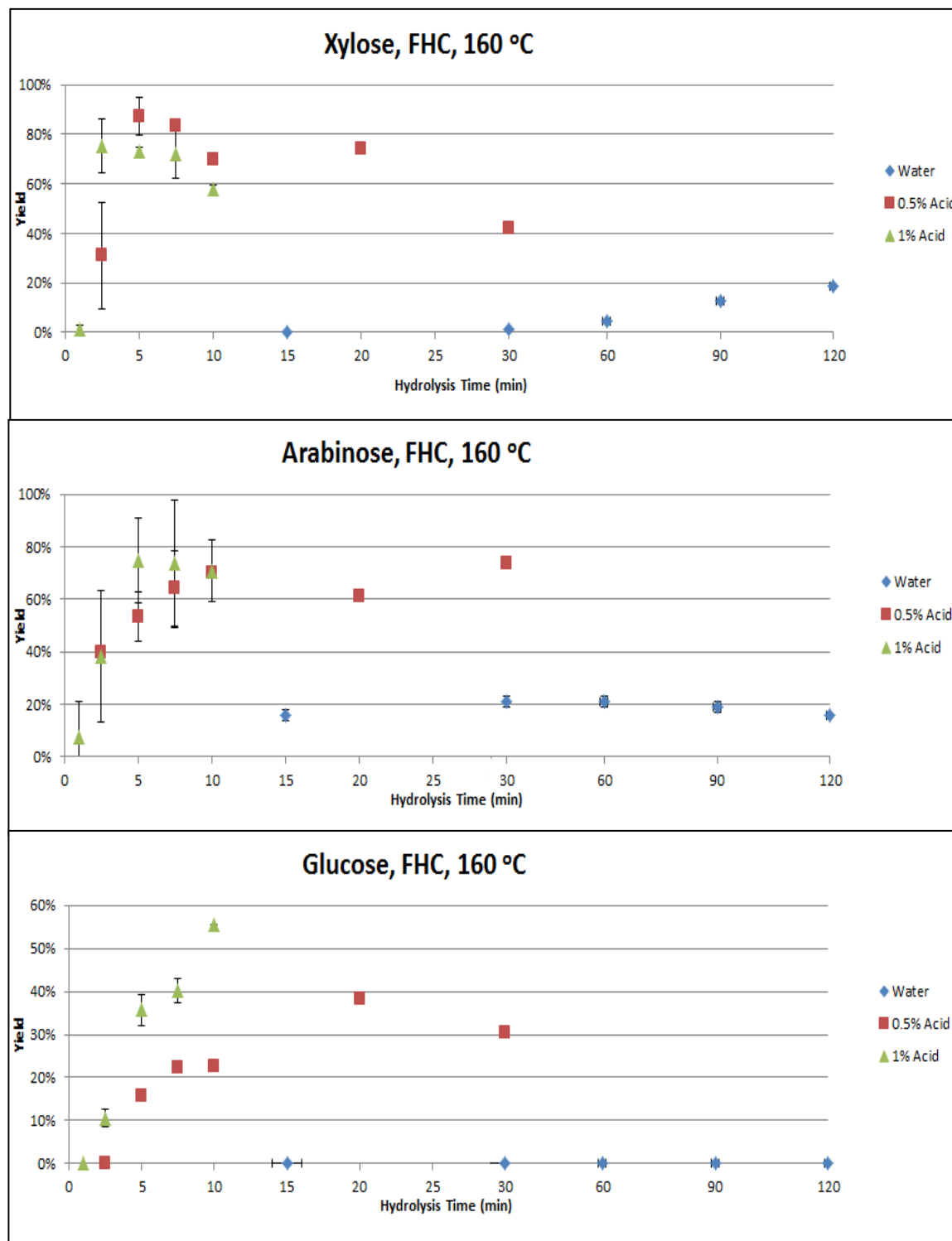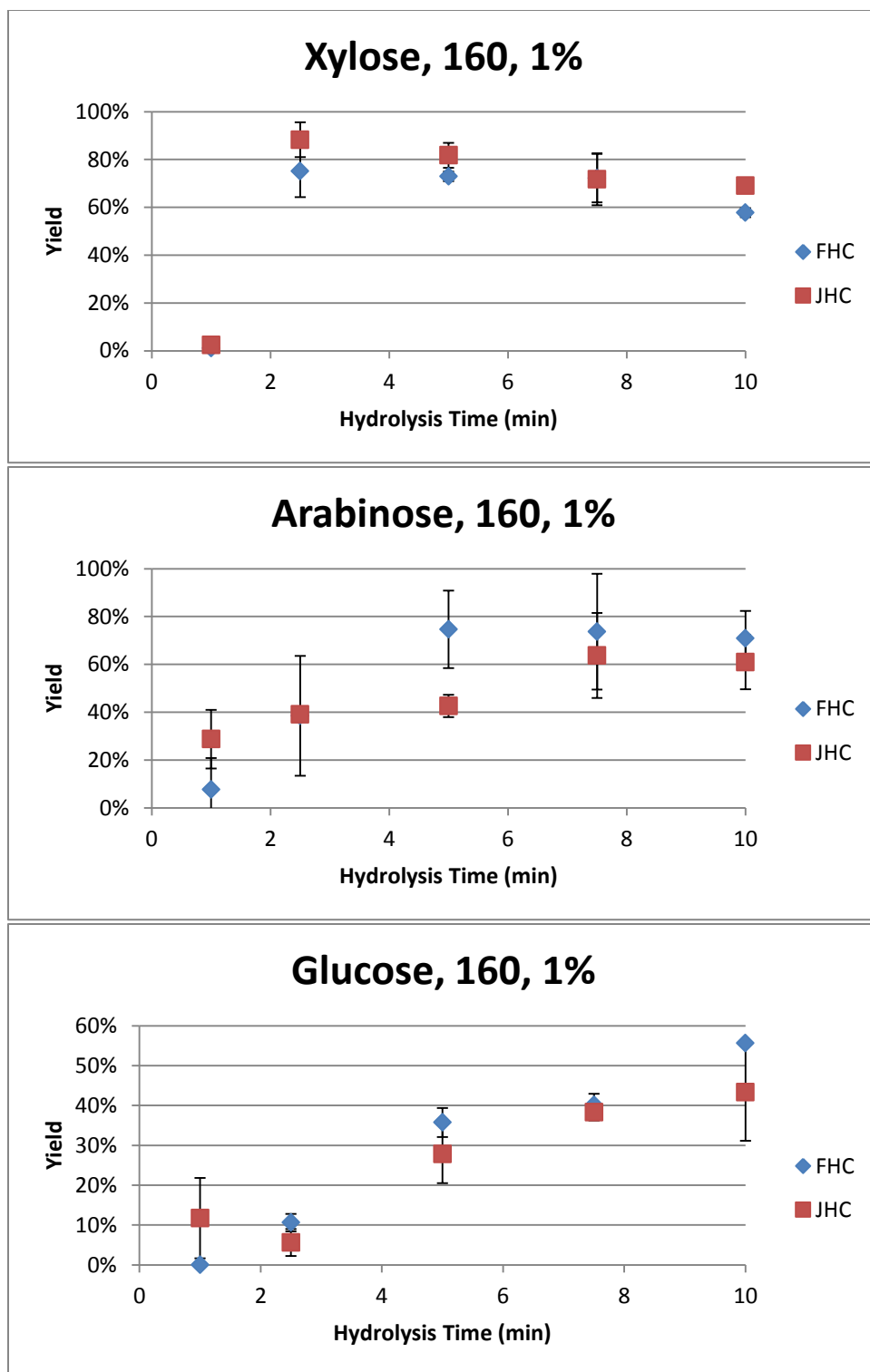
Figure 27: Experimental data for xylose (top), arabinose (middle), and glucose (bottom) yields from the hydrolysis of February hemicelluloses (FHC) at 160 °C at 0.0, 0.5, and 1.0 % acid.

Figure 28 illustrates the effect of temperature on the yield of monomeric sugars for hydrolysis using 1.0 % acid. Maximum xylose yields were 83.7, 75.2, and 73.3 % of theoretical xylose for 140, 160, and 180 ^{o}C, respectively, corresponding to hydrolysis times of 10, 2.5, and 2.5 min. Maximum arabinose yields were 42.1, 74.6, and 22.7 % of theoretical arabinose for 140, 160, and 180 ^{o}C, respectively, corresponding to hydrolysis times of 2.5, 5, and 1 min. Maximum glucose yields were 5.5, 55.6, and 12.3 % of theoretical glucose for 140, 160, and 180 ^{o}C, respectively, corresponding to hydrolysis times of 10, 10, and 1.5 min. For xylose, the main component of the hemicelluloses, maximum yields were obtained during longer hydrolysis times at lower temperatures. On the other hand, maximum arabinose and glucose yields were realized at 160 ^{o}C.

Figure 29 illustrates the effect harvest date on the yield of monomeric sugars for hydrolysis at 160 ^{o}C using 1.0 % acid. Maximum xylose yields were 88.3 and 75.2 % of theoretical xylose for July and February hemicelluloses, respectively, corresponding to hydrolysis times of 2.5 min for both samples. Maximum arabinose yields were 63.7 and 74.6 % of theoretical arabinose for July and February hemicelluloses, respectively, corresponding to hydrolysis times of 7.5 and 5 min. Maximum glucose yields were 43.3 and 55.6 % of theoretical glucose for July and February hemicelluloses, respectively, corresponding to hydrolysis times of 10 min for both samples. As seen in **Figure 29**, July and February hemicelluloses produced similar yield profiles for monomeric sugars. However, as discussed in **Section 5.4.1**, the composition of the two hemicelluloses does differ, thus resulting in different concentrations of monomeric sugars.
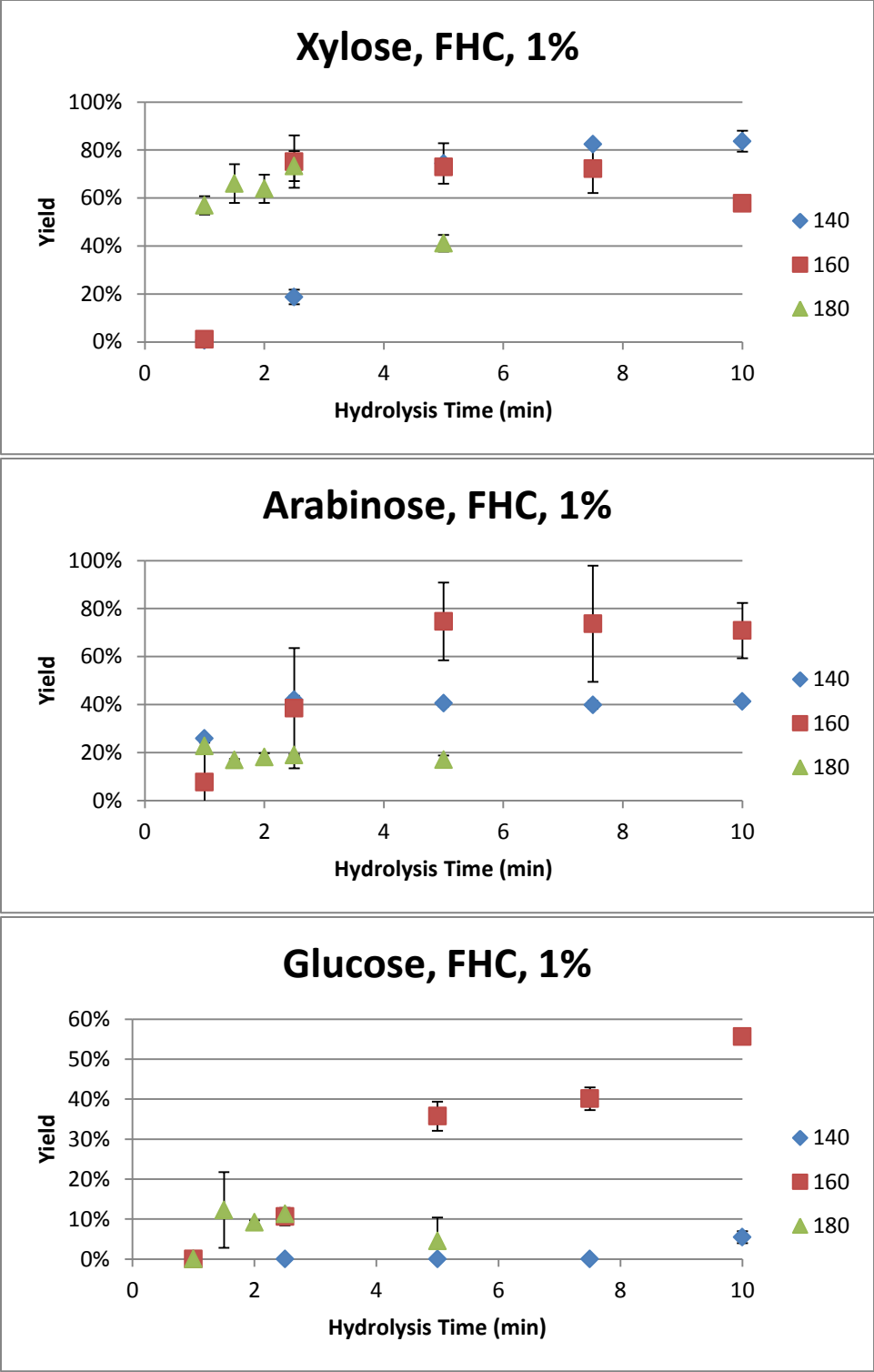
Figure 28: Experimental data for xylose (top), arabinose (middle), and glucose (bottom) yields

from the hydrolysis of February hemicelluloses (FHC) using 1.0 % acid at 140, 160, and 180 ^{o}C.
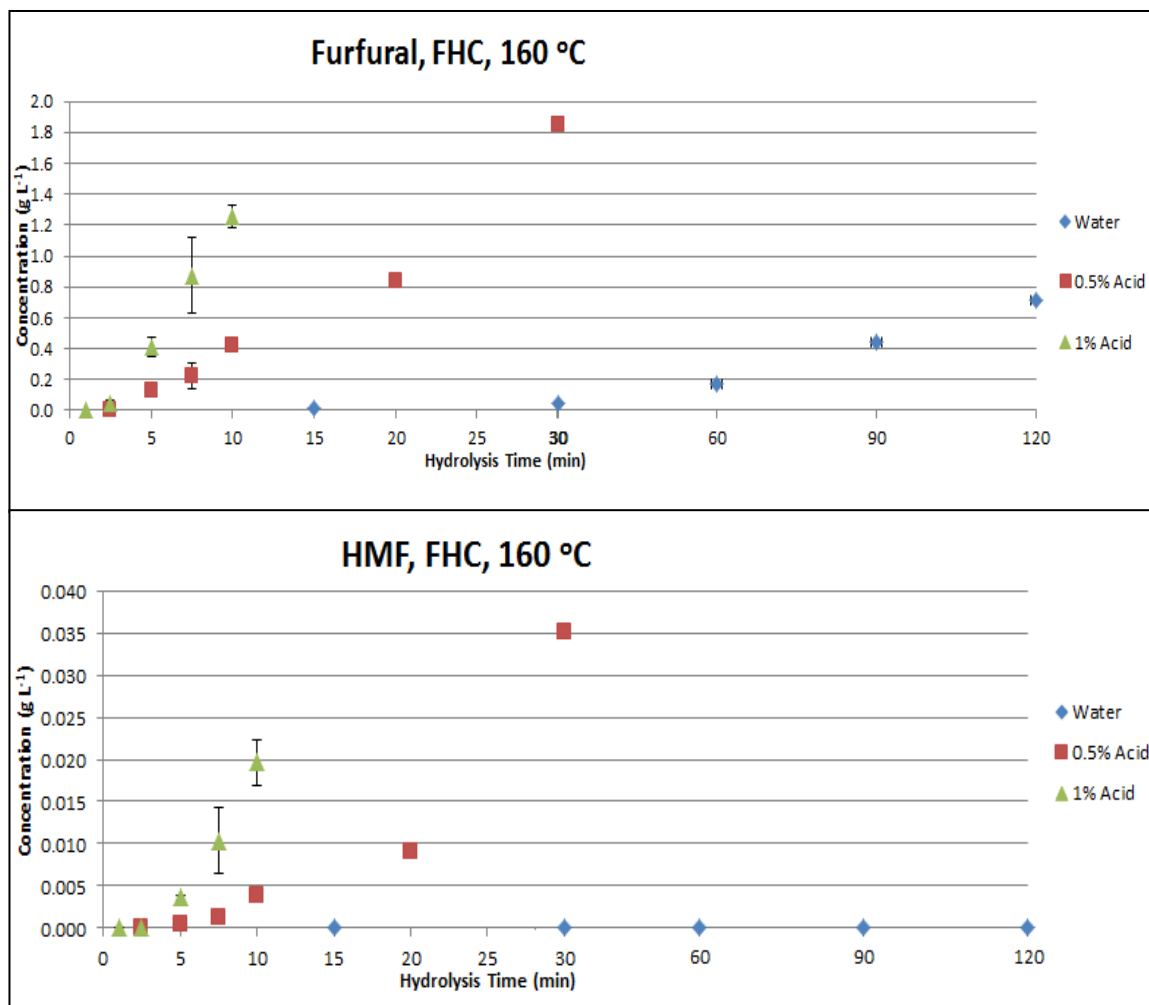
Figure 29: Experimental data for xylose (top), arabinose (middle), and glucose (bottom) yields

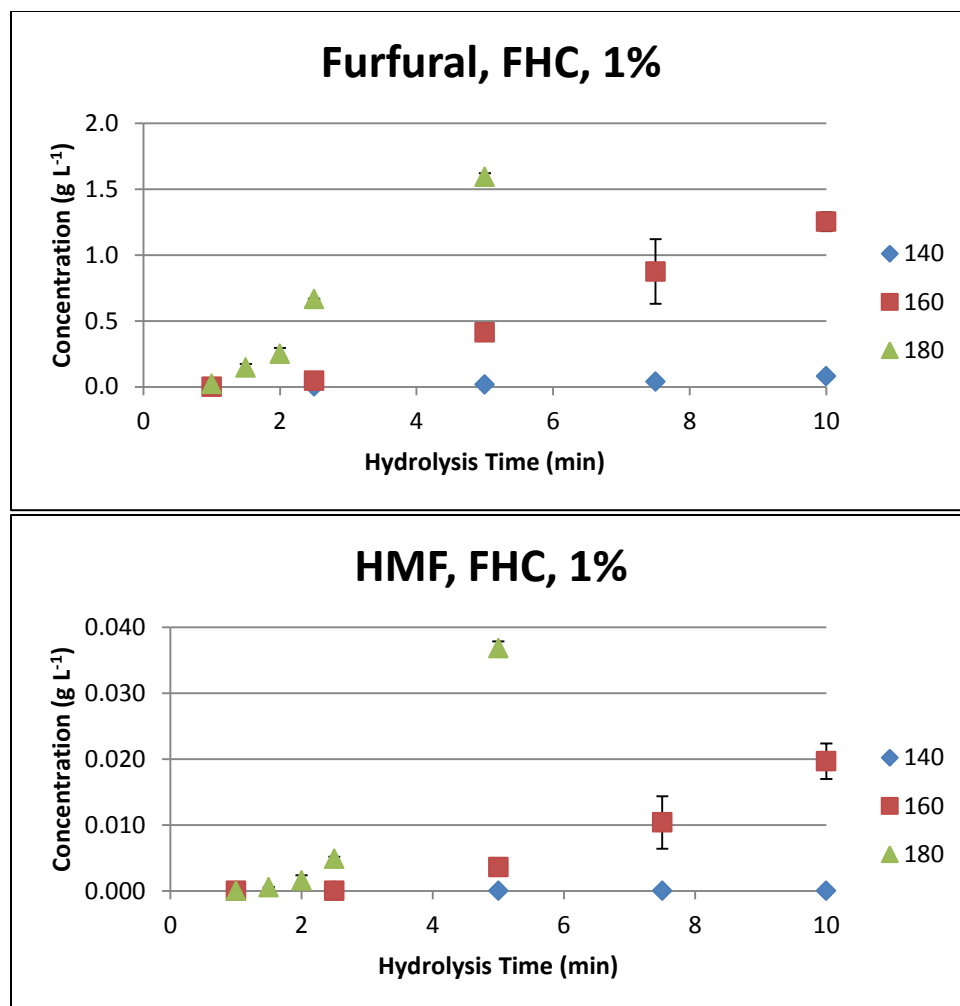from the hydrolysis of February (FHC) and July (JHC) hemicelluloses using 1 % acid at 160 $^{\circ}$C.

94

Figure 30 illustrates the effect of acid concentration on the accumulation of furfural and HMF at 160 ^{o}C. For all three conditions, furfural concentrations continued to increase as hydrolysis proceeded. The same is true for HMF during acid hydrolysis; however, because no glucose was released by water-only hydrolysis at 160 ^{o}C, no HMF was produced at this condition either. It is interesting to note that furfural concentrations were 0.44 g L^{-1} after 90 min of water-only hydrolysis, 0.43 g L^{-1} after 10 min of 0.5 % acid hydrolysis, and 0.41 g L^{-1} after 5 min of 1.0 % acid hydrolysis. Although these furfural concentrations are similar, the corresponding xylose yields for water-only and acid hydrolysis are not. Xylose yields were 12.6 % after 90 min of water-only hydrolysis, 69.9 % after 10 min of 0.5 % acid hydrolysis, and 72.9 % after 5 min of 1.0 % acid hydrolysis.

Figure 31 illustrates the effect of temperature on the accumulation of furfural and HMF for hydrolysis using 1.0 % acid. Much like acid concentration, the accumulation of furfural and HMF increased as hydrolysis proceeded and accelerated as temperature increased. This was especially true for HMF, which increased 925 % when comparing concentrations after 5 min of 1.0 % acid hydrolysis at 180 and 160 ^{o}C. No HMF was produced within the observed hydrolysis time for 1.0 % acid hydrolysis at 140 ^{o}C.

Figure 32 illustrates the effect harvest date on the accumulation of furfural and HMF for hydrolysis at 160 ^{o}C using 1.0 % acid. Like monomeric sugar yield profiles, the furfural and HMF profiles are largely similar for July and February hemicelluloses. It is only after 10 min of hydrolysis that the furfural concentrations begin to differ, with February hemicelluloses producing 0.37 g L^{-1} more furfural than July hemicelluloses.

Figure 30: Experimental data for furfural (top) and hydroxymethylfurfural (HMF) (bottom) concentrations from the hydrolysis of February hemicelluloses (FHC) at 160 $^{\circ}$C at 0.0, 0.5, and 1.0 % acid.

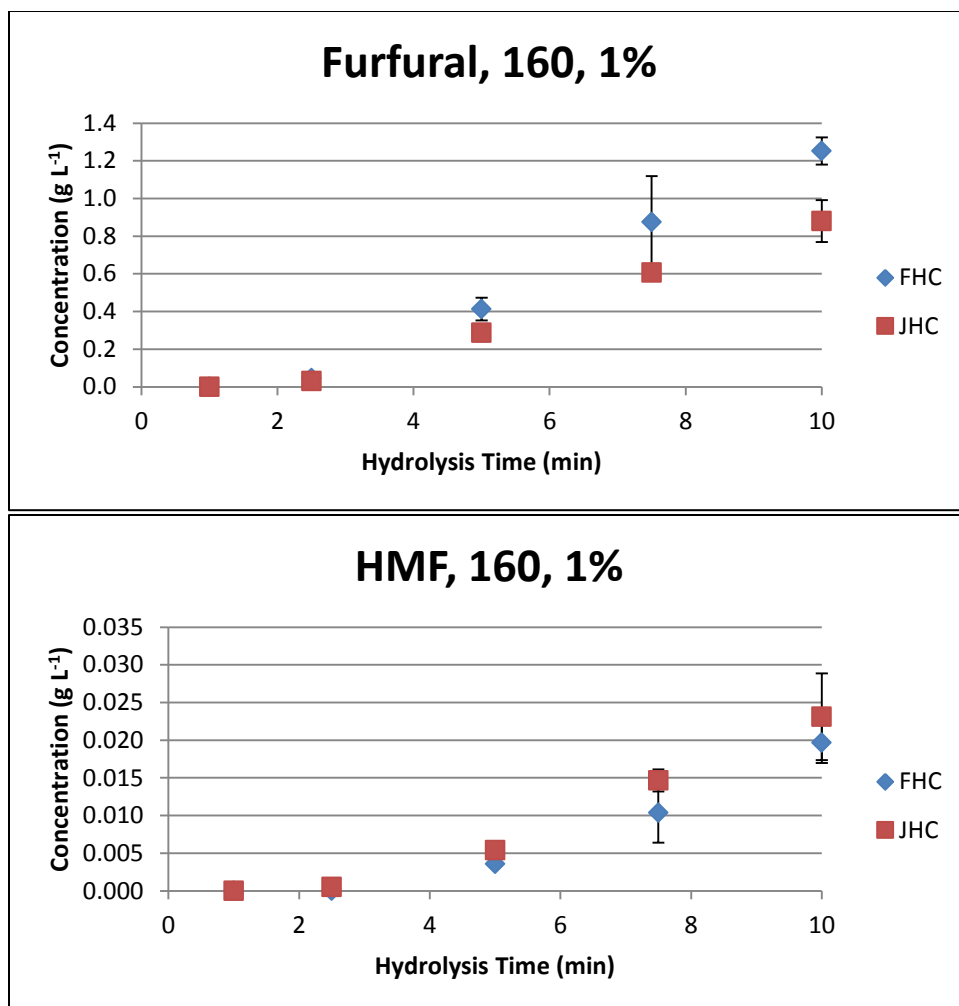**Figure 31:** Experimental data for furfural (top) and hydroxymethylfurfural (HMF) (bottom) concentrations from the hydrolysis of February hemicelluloses (FHC) using 1.0 % acid at 140, 160, and 180 °C.
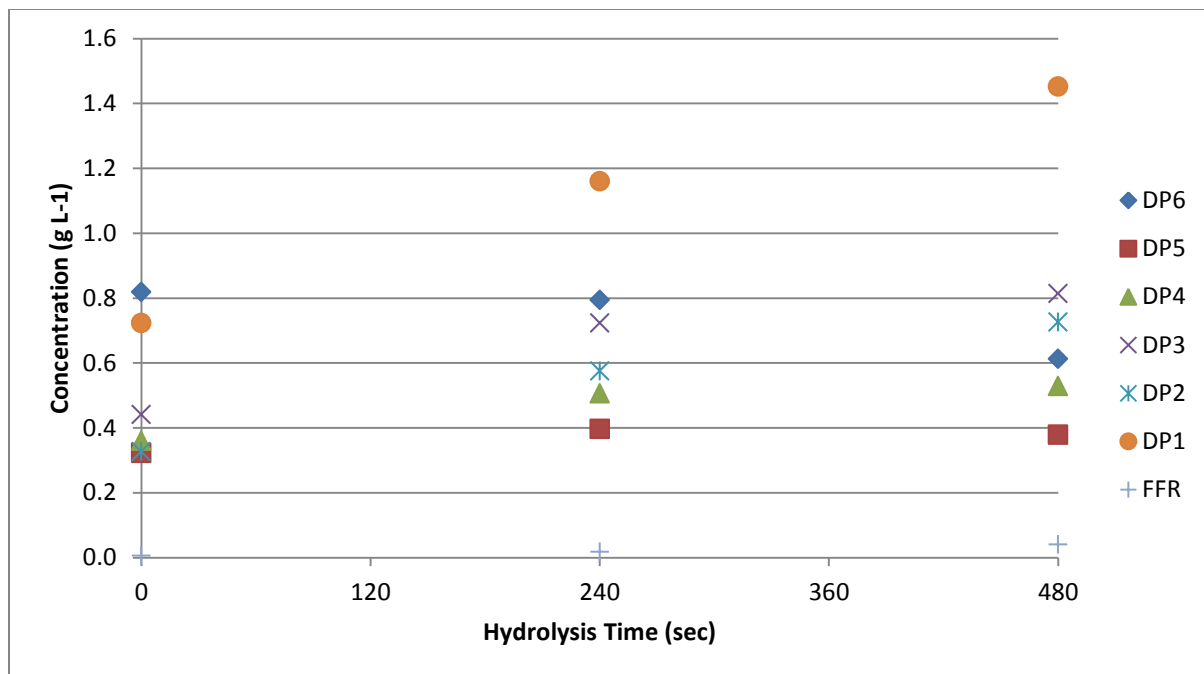
Figure 32: Experimental data for furfural (top) and hydroxymethylfurfural (HMF) (bottom)

concentrations from the hydrolysis of February (FHC) and July (JHC) hemicelluloses using 1.0

% acid at 160 °C.

## 5.10.2 Pretreatment of switchgrass hemicelluloses-derived oligomers

CPC-purified xylose oligomers were pretreated using water at 160 and 180 ^{o}C and 1.0 wt % sulfuric acid at 160 ^{o}C. Experiments were performed with duplicates at these conditions. Hydrolysis data for these experiments can be seen in **Figures 33-35**. For the sake of clarity, only one set of data are shown for each condition in **Figures 33-35**. Experiments were conducted with different batches of purified DP6, thus different initial starting concentrations of oligomers were observed. Experiments were performed on a much shorter time scale than those of Lau (2012) because hydrolysis happened on a time scale of seconds rather than minutes. This further differentiates this work from that performed by Lau (2012).

At 160 ^{o}C using water, 69 % of DP6 remained after 720 sec of hydrolysis. DP6 concentration decreased as hydrolysis proceeded; DP5 concentration increased until 480 sec of hydrolysis before decreasing; and DP4 concentration increased at 240 sec, decreased at 480 sec, and increased again at 720 sec of hydrolysis. DP3 and DP1 concentrations decreased until 480 sec of hydrolysis before increasing at 720 sec of hydrolysis. DP2 concentration initially decreased until 240 sec of hydrolysis before increasing throughout the remaining hydrolysis time. Furfural concentrations increased as hydrolysis proceeded. After 720 sec of hydrolysis, xylose equivalent concentrations for DP6, DP5, DP4, DP3, DP2, DP1, and furfural were 27, 11, 11, 17, 12, 21, and 1 %, respectively.

Figure 33: Experimental data of DP6, DP5, DP4, DP3, DP2, DP1, and furfural concentrations for the hydrolysis of DP6 in water at 160 ^{o}C.

At 160 $^{\circ}$C using 1.0 wt % sulfuric acid, 17 % of DP6 remained after 60 sec of hydrolysis. DP6 and DP5 concentrations decreased as hydrolysis proceeded. DP4 concentration decreased after 20 sec of hydrolysis, increased after 40 sec of hydrolysis, and decreased again after 60 sec of hydrolysis. DP3 concentration increased until 40 sec of hydrolysis before beginning to decrease. DP2, DP1, and furfural concentrations increased as hydrolysis proceeded. After 60 sec of hydrolysis, xylose equivalent concentrations for DP6, DP5, DP4, DP3, DP2, DP1, and furfural were 6, 7, 12, 20, 21, 34, and 0 %, respectively. Likewise to 160 $^{\circ}$C, 0.5 %, the major products from hydrolysis were DP1, DP2, and DP3 (total of 75%).
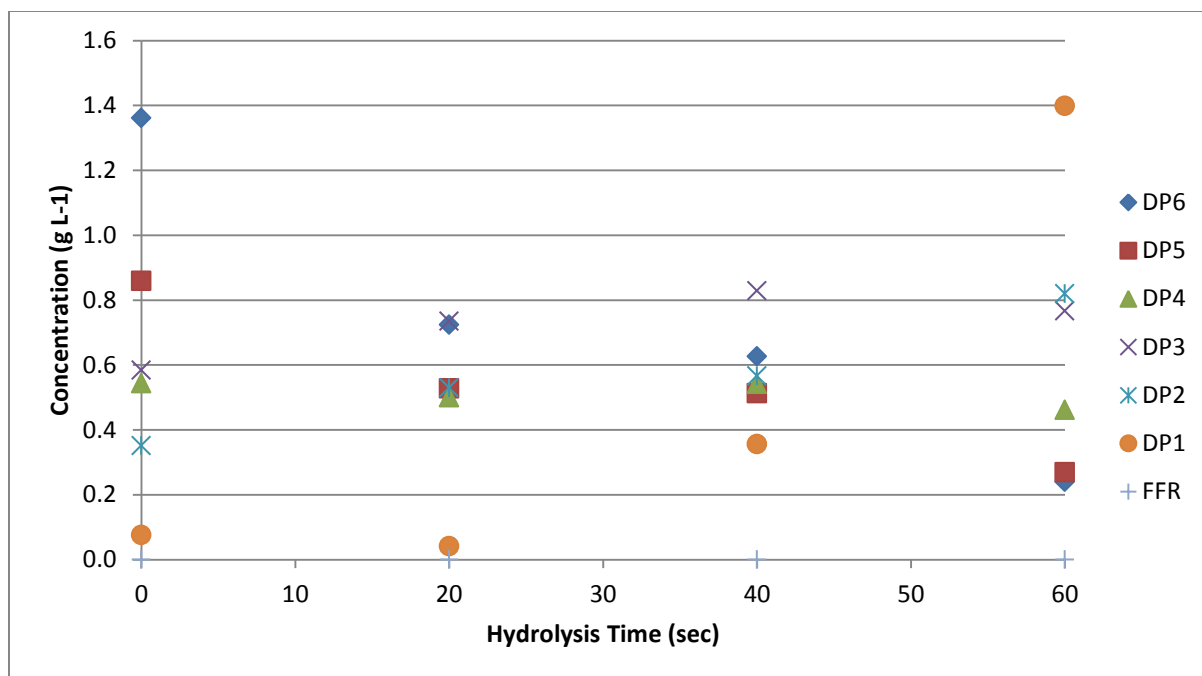
Figure 34: Experimental data of DP6, DP5, DP4, DP3, DP2, DP1, and furfural concentrations for the hydrolysis of DP6 in 1.0 wt % sulfuric acid at 160 $^{\circ}$C.

At 180 ^{o}C, 0.0 %, 47 % of DP6 remained after 540 sec of hydrolysis. DP6 concentration decreased as hydrolysis proceeded. DP5 and DP 4 concentrations increased after 180 sec of hydrolysis before beginning to decrease. DP3 concentration increased until 360 sec of hydrolysis before beginning to decrease. DP2, DP1, and furfural concentrations increased as hydrolysis proceeded. After 540 sec of hydrolysis, xylose equivalent concentrations for DP6, DP5, DP4, DP3, DP2, DP1, and furfural were 11, 8, 12, 11, 15, 40, and 4 %, respectively.
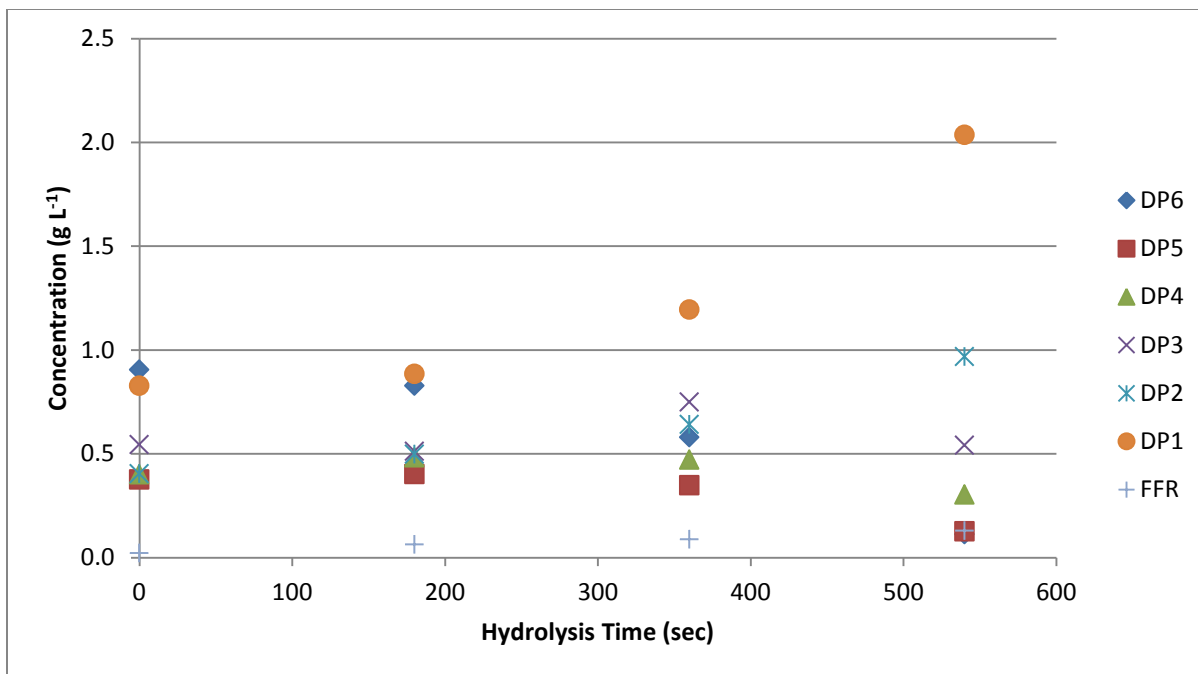
Figure 35: Experimental data of DP6, DP5, DP4, DP3, DP2, DP1, and furfural concentrations for the hydrolysis of DP6 in water at 180 ^{o}C

Several conclusions can be drawn from these experiments. First, acid concentration affected the range of products produced during hydrolysis, with DP1 being the primary product followed by DP2 and DP3 for dilute acid hydrolysis (**Figure 36**). Compared to dilute acid, water-only hydrolysis produced more of a consortium of oligomers rather than monomer. It can also be inferred that hydrolysis time affected the production of furfural. At the acid conditions explored, furfural concentrations were minimal compared to water-only hydrolysis, which was conducted at 9 to 12 times longer residence times than acid hydrolysis. For DP6 degradation, the water-only experiments were the least severe, with an increase in severity as temperature increased. The remaining experiments could be ranked from most severe to least severe by decreasing temperature, with an increase in severity for each temperature as acid concentration increased.
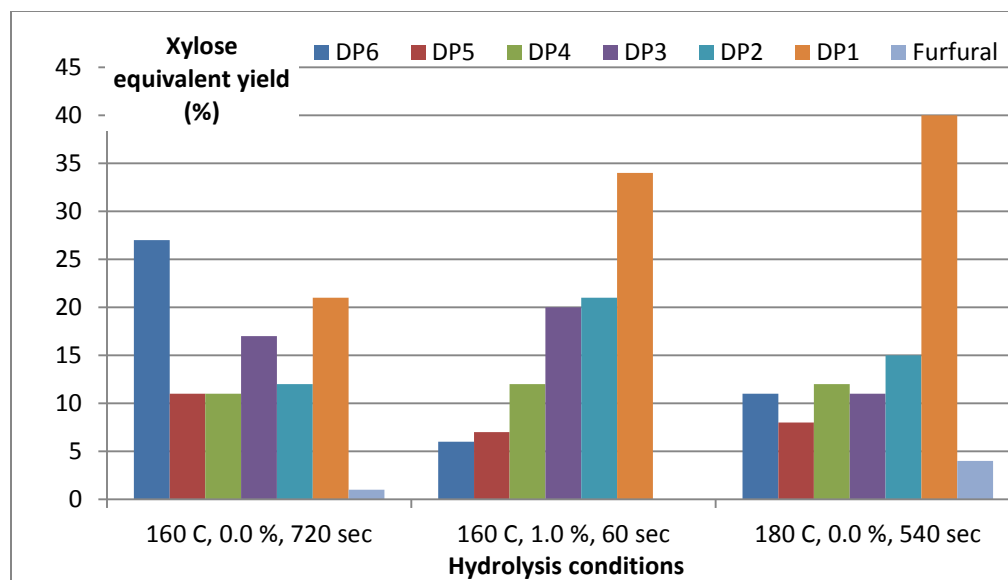
Figure 36: Xylose equivalent yields for DP6, DP5, DP4, DP3, DP2, DP1, and furfural at given hydrolysis conditions.

5.11 Kinetic modeling of switchgrass hemicelluloses-derived oligomers during pretreatment

5.11.1 Modeling degradation rate constants

Degradation rate constants for the experimental data in **Figures 33-35** were generated by the normalized least squares method using the Excel Solver routine and **Equations 1-7**, **9-13**, **18**, and **19**. **Equations 18** and **19** were generated by modifying **Equations 14** and **15**. Because formic acid concentrations were not included in experimental data as originally planned, the k_{1A} term in **Equation 14** and the k_{FA} term in **Equation 15** were eliminated, resulting in **Equations 18** and **19**, respectively.

$$\frac{dX_6}{dt} = -k_6 X_6 \tag{1}$$

$$\frac{dX_5}{dt} = -k_5 X_5 + k_{61} X_6 \tag{2}$$

$$\frac{dX_4}{dt} = -k_4 X_4 + k_{62} X_6 + k_{51} X_5 \tag{3}$$

$$\frac{dX_3}{dt} = -k_3 X_3 + 2k_{63} X_6 + k_{52} X_5 + k_{41} X_4 \tag{4}$$

$$\frac{dX_2}{dt} = -k_2 X_2 + k_{62} X_6 + k_{52} X_5 + 2k_{42} X_4 + k_{31} X_3 \tag{5}$$

$$\frac{dX_1}{dt} = -k_1 X_1 + k_{61} X_6 + k_{51} X_5 + k_{41} X_4 + k_{31} X_3 + 2k_{21} X_2 \tag{6}$$

$$\frac{dF}{dt} = -k_F F + k_{1F} X_1 \tag{7}$$

$$k_6 = k_{61} + k_{62} + k_{63} \tag{9}$$

$$k_5 = k_{51} + k_{52} \tag{10}$$

$$k_4 = k_{41} + k_{42} \qquad \qquad \textbf{(11)}$$

$$k_3 = k_{31} \qquad \qquad \textbf{(12)}$$

$$k_2 = k_{21} \qquad \qquad \textbf{(13)}$$

$$k_1 = k_{1F} \qquad \qquad \textbf{(18)}$$

$$k_F = k_{FL} \qquad \qquad \textbf{(19)}$$

where X_6, X_5, X_4, X_3, X_2, X_1, and F are concentrations of DP6, DP5, DP4, DP3, DP2, DP1, and furfural, respectively, in mmol L^{-1}. k_{61}, k_{62}, k_{63}, k_{51}, k_{52}, k_{41}, k_{42}, k_{31}, k_{21}, k_{1F}, and k_{FL} are the rate constants for the formation of DP1 from DP6, DP2 from DP6, DP3 from DP6, DP1 from DP5, DP2 from DP5, DP1 from DP4, DP2 from DP4, DP1 from DP3, DP1 from DP2, furfural from DP1, and degradation of furfural into unaccounted degradation products, respectively, in min^{-1}. The overall degradation rates for DP6, DP5, DP4, DP3, DP2, DP1, and furfural are k_6, k_5, k_4, k_3, k_2, k_1, and k_F, respectively. The reaction pathway for the degradation of xylose oligomers with accompanying rate constants can be seen in **Figure 37**.

As mentioned previously, reactions were assumed to be irreversible, first-order reactions with degradation rate constants exhibiting Arrhenius-type temperature and acid concentration dependence. Additionally, DP6 and other oligomers were assumed to be linear chains composed solely of xylose (i.e. no xylose or arabinose branches). This assumption is made in part for convenience, but is also supported by total sugar analysis results and HPAEC-PAD results (**Figure 20**) for the CPC-fractionated switchgrass hemicelluloses-derived oligomers that were used as feedstock for the pretreatment studies on which the kinetic modeling is based.
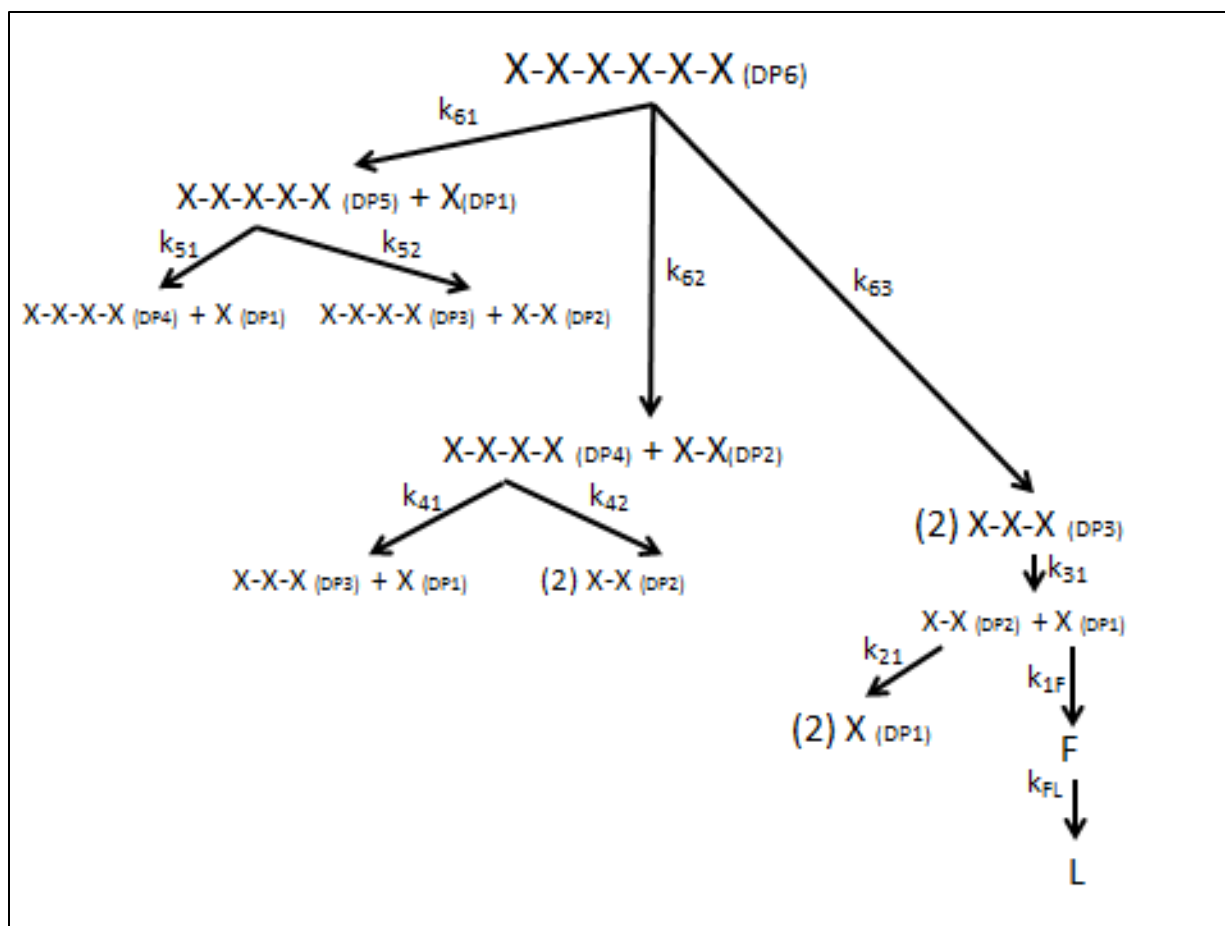
Figure 37: Reaction pathway for degradation of xylose oligomers. k_{61}, k_{62}, k_{63}, k_{51}, k_{52}, k_{41}, k_{42}, k_{31}, k_{21}, and k_{1F} are the rate constants for the formation of DP1 from DP6, DP2 from DP6, DP3 from DP6, DP1 from DP5, DP2 from DP5, DP1 from DP4, DP2 from DP4, DP1 from DP3, DP1 from DP2, furfural from DP1, and degradation of furfural into unaccounted degradation products, respectively, in min^{-1}.

The modeling approach chosen minimized the normalized sum of squares of the differences between experimental concentrations data and model-predicted concentrations data. This approach for modeling prevents biasing towards compounds with higher molar concentrations, such as xylose. Best-fit models and experimental data can be seen in **Figures 38-40**, and model-predicted values for the degradation rate constants can be seen in **Table 5**. Comparison of the degradation rate constants found in this work to those obtained by Kumar and Wyman (2008) and Lau (2012) can be seen in **Table 6**.

Modeling results predicted oligomer and furfural data well for the conditions explored. However, for DP1, model predictions were not as accurate using water and 1.0 wt % acid at 160 ^{o}C as compared to water at 180 ^{o}C. As seen by Lau (2012), model predictions were more accurate as temperature increased. It is also worth noting that xylose oligomers might not follow first order reaction kinetics during water-only hydrolysis conditions. Kumar and Wyman (2008) reported that at low acid concentrations, xylose degradation depends on xylose concentration, thus not following first order reaction kinetics. As mentioned by Kumar and Wyman (2008), this is also supported by research performed at NREL.
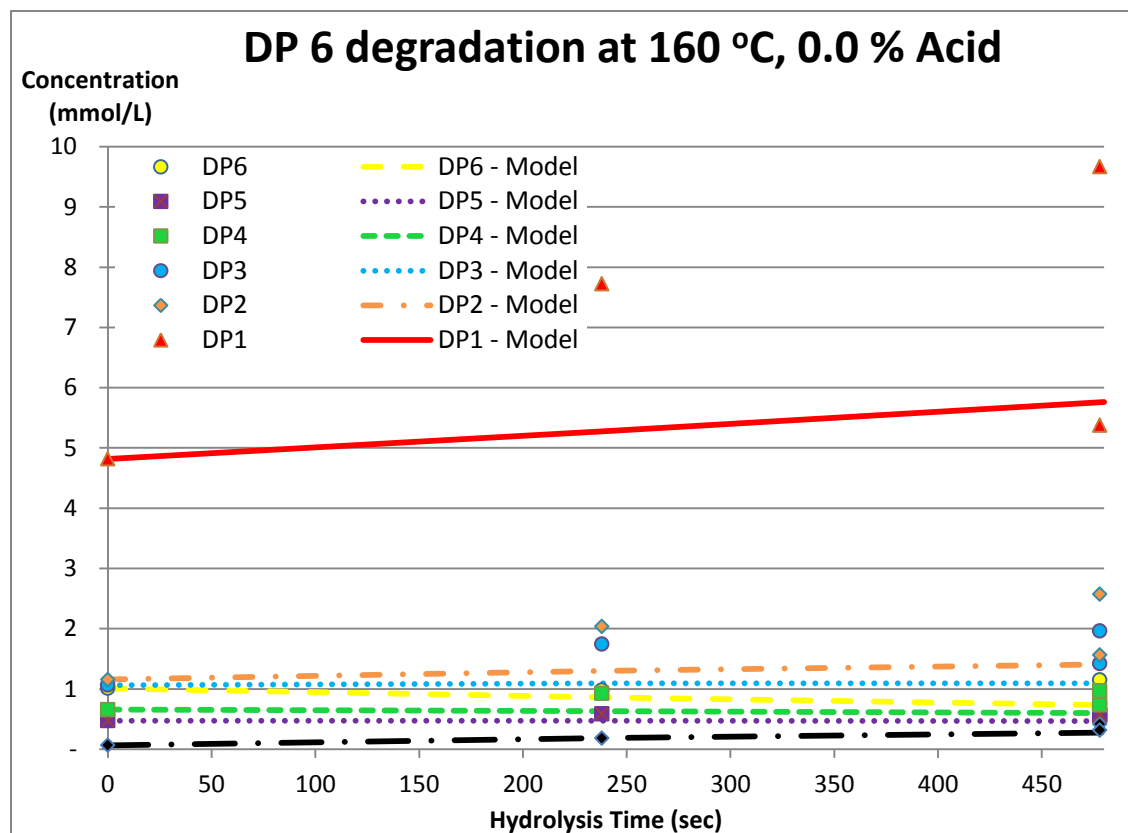
Figure 38: Best-fit model predictions and experimental data for DP6, DP5, DP4, DP3, DP2, DP1, and furfural concentrations for the hydrolysis of DP6 at 160 °C in 0.0 wt % sulfuric acid.
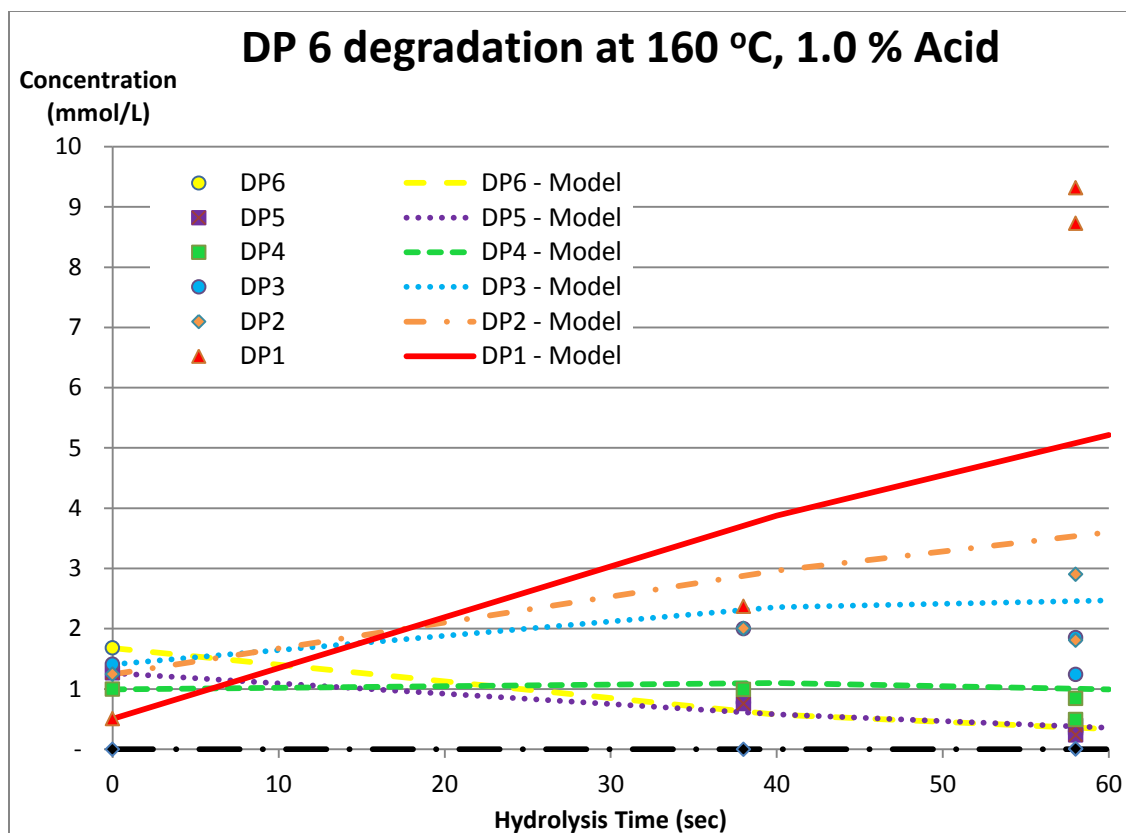
Figure 39: Best-fit model predictions and experimental data for DP6, DP5, DP4, DP3, DP2, DP1, and furfural concentrations for the hydrolysis of DP6 at 160 °C in 1.0 wt % sulfuric acid.
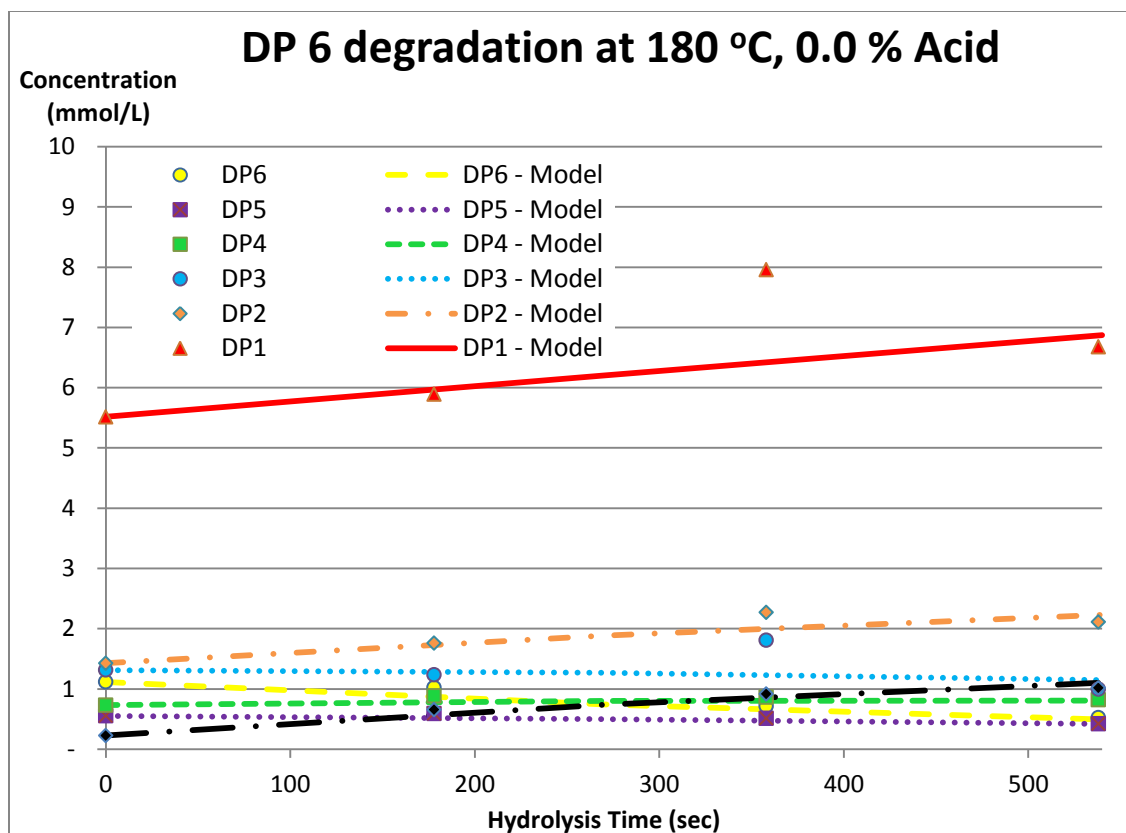
Figure 40: Best-fit model predictions and experimental data for DP6, DP5, DP4, DP3, DP2, DP1, and furfural concentrations for the hydrolysis of DP6 at 180 ^{o}C in 0.0 wt % sulfuric acid.

Table 5: Summary of degradation rate constants as determined using an Excel Solver routine for normalized least sum of squares method

Rate Constant (min -1)	160 ^{o}C Water	160 ^{o}C 1% Acid	180 ^{o}C Water
k6	0.04036	1.613733	0.090559
k61	0.00006	1.613613	0.039285
k62	0.020713	0.00006	0.014639
k63	0.019587	0.00006	0.036634
k5	0.00184	2.979355	0.09049
k51	0.00178	1.152528	0.090006
k52	0.00006	1.826827	0.000483
k4	0.040848	0.804105	0.059999
k41	0.023236	0.804045	0.00006
k42	0.017611	0.00006	0.059939
k3 (k31)	0.040883	0.559812	0.059427
k2 (k21)	0.041288	0.085594	0.04917
k1 (k1F)	0.009288	0.000906	0.029394
kF (kFL)	0.123972	0.137863	0.118176

Table 6: Comparison of rate constants in this study to those of Kumar and Wyman (2008) and Lau (2012) for 160 ^{o}C using water

Rate constant (min -1)	Current study	Kumar and Wyman (2008)	Lau (2012)
k6	0.04036		
k61	6E-05		
k62	0.020713		
k63	0.019587		
k5	0.00184	0.0629	
k51	0.00178	0.04186	
k52	6E-05	0.021	
k4	0.040848	0.0184	0.0032
k41	0.023236	0.0148	0.0001
k42	0.017611	0.0032	0.0031
k3 (k31)	0.040883	0.024	0.0103
k2 (k21)	0.041288	0.0121	0.003
k1 (k1F)	0.009288	0.0059	0.0054
kF (kFL)	0.123972		0.0027

Using the degradation rates from **Table 5**, the effect of acid concentration on the cleavage of different bonds within the oligomers were examined as seen in **Table 7**. These results were in agreement with the general trend seen by Lau (2012), where the addition of acid increased cleavage of end bonds versus interior bonds. As seen with DP6, increased acid concentration increased the rate of cleavage of the end bond, whereas hydrolysis with water-only promoted cleavage of the interior bonds. This effect was more prominent with the 160 $^{\circ}$C hydrolysis data, likely because of the increased autoionization effect of pressurized water at 180 $^{\circ}$C versus 160 $^{\circ}$C.

Table 7: Comparison of bond cleavage rates for DP6 from this study

Rate Constant (min -1)	160 C Water	160 C 1% Acid	180 C Water
k6 (k61+k62+k63)	0.04036	1.613733	0.090559
k61	0.00006	1.613613	0.039285
k62	0.020713	0.00006	0.014639
k63	0.019587	0.00006	0.036634
k61/k62	0.002897	26893.54	2.683534
k61/k63	0.003063	26893.54	1.072381
k62/k63	1.057501	1	0.399615

5.11.2 Modeling temperature and acid concentration effects

Temperature and acid effects were modeled using a modified Arrhenius equation (**Equation 17**). The pre-exponential factor, acid concentration exponent, and activation energy were generated by the least squares method using the Excel Solver routine. This approach minimized the sum of squares of the differences between the degradation rate constants in **Table 6** and model-predicted degradation rate constants using **Equation 17**. A summary of the Arrhenius parameters can be seen in **Table 8**. Using these results, it is possible to predict concentration profiles for xylose oligomers over a broader range of conditions.

$$k_i = k_o(H^+)^m EXP(-E_a/RT) \tag{17}$$

k_i is the rate constant of a given compound in min^{-1}, k_o is the pre-exponential factor in min^{-1}, (H^+) is the hydrogen ion concentration in $mol\ L^{-1}$, m is the unitless acid concentration exponent, E_a is the activation energy in $J\ mol^{-1}$, R is the gas constant in $J\ mol^{-1}\ K^{-1}$ (8.314), and T is the reaction temperature in K.

Acid concentration exponent results were similar for DP3, DP4, DP5, and DP6, showing that acid concentration affects these compounds equally. The acid concentration exponents were much lower for DP2, DP1, and furfural. Activation energies for DP2, DP3, DP4, DP5, and DP6 were comparative, whereas the activation energy of DP1 was much high. The activation energy for furfural was low in comparison to literature values. Thus, all compounds were found to be affected by temperature and acid concentration, but to differing degrees.

Table 8: Summary of Arrhenius parameters for degradation rate constants.

Compound	k_0 (min^{-1})	m (unitless)	E_a (kJ/mol/K)
DP6	2.71E+07	0.249	58.24
DP5	2.71E+07	0.302	55.94
DP4	2.54E+07	0.225	60.88
DP3	9.34E+05	0.193	50.48
DP2	4.45E+03	0.064	38.77
DP1	4.45E+03	0.020	141.91
Furfural	7.11E+02	0.030	30.58

5.12 Implications from pretreatment experiments and kinetic modeling

The impact of acid on the preference of bond cleavage is of great importance for designing pretreatment processing conditions at the commercial scale. As shown in **Table 7**, model-predicted degradation rates showed that acid promoted hydrolysis at end bonds versus interior bonds, as can be seen by the ratio of k_{61} to k_{63} at acid hydrolysis conditions. On the other hand, water-only hydrolysis promoted hydrolysis at interior bonds, as can be seen by the ratio of k_{61} to k_{63} at water-only hydrolysis conditions. The preference of the cleavage of the internal bond during acid hydrolysis was not only supported by this work, but also by Lau (2012).

6.0 CONCLUSIONS

In summary, hemicelluloses were successfully extracted from July- and February-harvested switchgrass samples and subsequently characterized for monomeric composition, size, and glycosyl linkages. Results showed that changes do occur in the physicochemical properties of the hemicelluloses as switchgrass senesces. Using the methods reported here, the physicochemical properties of other bioenergy-destined feedstocks could be examined. It would be interesting to see if the physicochemical properties of other feedstocks such as crop residues, hardwoods, and softwoods change in a manner similar to switchgrass. These results could have major implications for converting biomass into fuels and chemicals, as well as providing insight on the physiological role of hemicelluloses.

Extracted switchgrass hemicelluloses were partially hydrolyzed in water at 160 ^{o}C to produce a range of oligomers. These oligomers were then fractionated using CPC with a butanol:methanol:water solvent system. Although the consolidated oligomer fractions obtained via CPC were not as pure as commercially available oligomers, these CPC-fractionated oligomers are still useful as feedstock for future studies. Because the oligomers eluted the CPC rotor in order of increasing DP, from smallest to largest, these fractions can be tailored such that they do not contain oligomers over a given DP. Thus, the consolidated fractions are suitable feedstock for pretreatment experiments that examine oligomer depolymerization. Also worth noting, the xylose oligomers fractionated in this work did not contain formic acid, which was observed in the xylobiose and xylotetraose samples in Lau *et al.* (2013). This is the first time xylose oligomers have been fractionated from switchgrass or any other bioenergy-destined feedstock using CPC.

121

Pretreatment of extracted switchgrass hemicelluloses and CPC-fractionated switchgrass hemicelluloses-derived oligomers provided new insight into the depolymerization of these compounds during water-only and acid hydrolysis. Particularly interesting was the preference of bond cleavage observed under different pretreatment conditions. Kinetic modeling revealed that acid hydrolysis promotes cleavage of end bonds whereas water-only hydrolysis promotes cleavage of interior bonds.

Together, these results have implications for designing pretreatment processing conditions during the conversion of biomass to fuels and chemicals at the commercial scale. However, other factors must be taken into account, such as mass transport limitations within the cell wall and the digestibility of cellulose-rich solids resulting from pretreatment.

7.0 FUTURE WORK

This work reported on the characterization of extracted switchgrass hemicelluloses, production and fractionation of switchgrass-hemicelluloses-derived xylose oligomers, and the pretreatment of extracted switchgrass hemicelluloses and hemicelluloses-derived oligomers.

From CPC-fractionation experiments, it was observed that the solvent system and operating parameters used were not sufficient for fractionating xylose oligomers of a DP larger than six. Thus, it would be worthwhile to explore additional solvent systems and operating parameters for the fractionation of these larger oligomers. These larger oligomers could be used as feedstock for additional depolymerization, enzymatic inhibition, and prebiotic studies.

There are many additional studies that could be undertaken to improve upon the pretreatment experiments performed in this study. In this study, acid concentration, in terms of g of acid per L solution, was considered as a variable for catalyst loading effects. However, it might be more beneficial to consider a ratio of acid to biomass for determining catalyst loading effects. As previously noted, further investigation into the solids loading should also be explored. As other researchers have reported, xylose degradation at water-only and low acid concentrations is affected by xylose concentration. Thus, not following first order kinetics. This should be further investigated for not only xylose, but xylose oligomers as well.

WORKS CITED

1. Aachary, A.; Prapulla, S. Xylooligosaccharides (XOS) as an emerging prebiotics: Microbial synthesis, utilization, structural characterization, bioactive properties, and applications. *Compr. Rev. Food Sci. Food Saf.* **2010**, *10*, 2-16.

2. Adler, P.; Sanderson, M.; Boateng, A.; Weimer, P.; Jung, H. Biomass yield and biofuel quality of switchgrass harvested in fall or spring. *Agron. J.* **2006**, *98*, 1518-1525.

3. Alvira, P.; Pejo, T.; Ballesteros, M.; Negro, M. Pretreatment technologies for an efficient bioethanol production process based on enzymatic hydrolysis: A review. *Bioresour. Technol*. **2010**, 101, 4851-4861.

4. Arora, A.; Martin, E.; Pelkki, M.; Carrier, D. Effect of formic acid and furfural on the enzymatic hydrolysis of cellulose powder and dilute acid-pretreated poplar hydrolysates. *ACS Sustainable Chem. Eng*. **2013**, *1*, 23-28.

5. Balan, V.; Bals, B.; Sousa, L.; Garlock, R.; Dale, B. A short review on ammonia-based lignocellulosic biomass pretreatment. In *Chemical and biochemical catalysis for next generation biofuels*, Simmons, B., Ed. RSC Publishing: Cambridge, UK, 2011; 89-114.

6. Bowman, M.; Dien, B.; O'Bryan, P.; Sarath, G.; Cotta, M. Selective chemical oxidation and depolymerization of (*Panicum virgatum* L.) xylan with switchgrass oligosaccharide product analysis by mass spectrometry. *Rapid Commun.Mass Spectrom.* **2011**, *25*, 941-950.

7. Buckeridge, M.; Rayon, C.; Urbanowicz, B.; Tine, M.; Carpita, N. Mixed linkage (1_3),(1_4)-_-D-glucans of grasses. *Cereal Chem*. **2004**, *81*, 115-127.

8. Bunnell, K.; Rich, A.; Luckett, C.; Wang, Y.; Martin, E.; Carrier, D. Plant maturity effects on the physicochemical properties and dilute acid hydrolysis of switchgrass (*Panicum virgatum*, L.) hemicelluloses. *ACS Sustainable Chem. Eng*. **2013a**, DOI: 10.1021/sc4000175.

9. Bunnell, K.; Lau, C.; Lay, J.; Gidden, J.; Carrier, D. Production and fractionation of xylose oligomers from switchgrass hemicelluloses using centrifugal partition chromatography. *Ind. Eng. Chem. Res.***2013b**, (*In review*).

10. Cazes, J.; Nunogaki, K. Centrifugal partition chromatography. *Am. Lab.* **1987**, *19*, 126-132.

11. Chevolot, L.; Jouault, S.; Foucault, A.; Ratiskol, J.; Sinquin, C. Preliminary report on fractionation of fucans by ion-exchange displacement centrifugal partition chromatography. *J. Chromatogr. B* **1998**, *706*, 43-54.

12. Ciucanu, I.; Kerek, F. A simple and rapid method for the permethylation of

carbohydrates. *Carbohydr. Res.* **1984**, *131*, 209-217.

13. Claassen, P.; Lier, J.; Contreras, A.; Niel, E.; Sijtsma, L.; Stams, J.; Vries, S.; Weusthuis, R. Utilisation of biomass for the supply of energy carriers. *Appl. Microbiol. Biotechnol.* **1999**, *52*, 741-755.

14. David, K.; Ragauskas, A. Switchgrass as an energy crop for biofuel production: A review of its ligno-cellulosic chemical properties. *Energy Environ. Sci.* **2010**, *3*, 1182-1190.

15. Dien, B.; Jung, H.; Vogel, K.; Casler, M.; Lamb, J.; Iten, L.; Mitchell, R.; Sarath, G. Chemical composition and response to dilute-acid pretreatment and enzymatic saccharification of alfalfa, reed canarygrass, and switchgrass. *Biomass Bioenergy.* **2006**, *30*, 880-891.

16. Du, B.; Sharma, L.; Becker, C.; Chen, S.; Mowery, R.; Walsum, P.; Chambliss, C. Effect of varying feedstock-pretreatment chemistry combinations on the formation and accumulation of potentially inhibitory degradation products in biomass hydrolysates. *Biotechnol. Bioeng.* **2010**, *107*, 430-440.

17. Ebringerova, A.; Hromadkova, Z.; Heinze, T. Hemicellulose. *Adv. Polym. Sci.* **2005**, *186*, 1-67.

18. Eggeman, T.; Elander, R. Process and economic analysis of pretreatment technologies. *Bioresour. Technol.* **2005**, *96*, 2019-2025.

19. Energy independence and security act of 2007, Public Law 110-140, 2007, http://www.gpo.gov/fdsys/pkg/PLAW-110publ140/pdf/PLAW-110publ140.pdf.

20. Fan, L.; Lee, Y.; Gharpuray, M. The nature of lignocellulosics and their pretreatments for enzymatic hydrolysis. *Adv. Biochem. Eng.* **1982**, *23*, 158-187.

21. Fenske, J.; Griffin, D.; Penner, M. Comparison of aromatic monomers in lignocellulosic biomass prehydrolysates. *J. Ind. Micriobiol. Biotechnol.* **1998**, *20*, 364-368.

22. Garlock, R.; Balan, V.; Dale, B.; Pallapolu, V.; Lee, Y.; Kim, Y.; Mosier, N.; Ladisch, M.; Holtzapple, M.; Falls, M.; Sierra, R.; Shi, J.; Ebrik, M.; Redmond, T.; Yang, B.; Wyman, C.; Donohoe, B.; Vinzant, T.; Elander, R.; Hames, B.; Thomas, S.; Warner, R. Comparative material balances around pretreatment technologies for the conversion of switchgrass to soluble sugars. *Bioresour. Technol.* **2011**, *102*, 11063-11071.

23. Hendriks, A.; Zeeman, G. Pretreatments to enhance the digestibility of lignocellulosic biomass. *Bioresour. Technol.* **2009**, *100*, 10-18.

24. Himmel, M.; Ding, S.; Johnson, D.; Adney, W.; Nimlos, M.; Brady, J.; Foust, T. Biomass recalcitrance: Engineering plants and enzymes for biofuels production. *Sci.* **2007**, *315*, 804-807.

25. Hoch, G. Cell wall hemicelluloses as mobile carbon stores in non-reproductive plant tissues. *Funct. Ecol.* **2007**, *21*, 823-834.

26. Hodge, D.; Karim, M.; Schell, D.; and McMillan, J. Soluble and insoluble solids contributions to high-solids enzymatic hydrolysis of lignocellulose. *Bioresour.Technol*. **2008**, *99*, 8940-8948.

27. Jorgensen, H.; Kristensen, J.; Felby, C. Enzymatic conversion of lignocellulose into fermentable sugars: Challenges and opportunities. *Biofuels, Bioprod. Biorefin.* **2007**, *1*, 119-134.

28. Kamiyama, Y.; Sakai, Y. Rate of hydrolysis of xylo-oligosaccharides in dilute sulfuric acid. *Carbohydr. Res.* **1979**, *73*, 151-158.

29. Kim, Y.; Kreke, T.; Hendrickson, R.; Parenti, J.; Ladisch, M. Fractionation of cellulase and fermentation inhibitors from steam pretreated mixed hardwood. *Bioresour. Technol.* **2013a**, *135*, 30-38.

30. Kim, Y.; Kreke, T.; Ladisch, M. Reaction mechanisms and kinetics of xylo-oligosaccharide hydrolysis by dicarboxylic acids. *AIChE J*. **2013b**, 59, 188-199.

31. Klinke, H.; Thomsen, A.; Ahring, B. Inhibition of ethanol-producing yeast and bacteria by degradation products produced during pre-treatment of biomass. *Appl. Biochem. Biotechnol.* **2004**, *66*, 10-26.

32. Kothari, U.; Lee, Y. Inhibition effects of dilute-acid prehydrolysate of corn stover on enzymatic hydrolysis of Solka Floc. *Appl. Biochem. Biotechnol.* **2011**, 165, 1391-1405.

33. Kumar, G.; Pushpa, A.; Prabha, H. A review on xylooligosaccharides. *Int. Res. J. Pharm.* **2012**, *3*, 71-74.

34. Kumar, R.; Wyman, C. Effect of xylanase supplementation of cellulase on digestion of corn stover solids prepared by leading pretreatment technologies. *Bioresour. Technol.* **2009**, *100*, 4203-4213.

35. Kumar, R.; Wyman, C. The impact of dilute sulfuric acid on the selectivity of xylooligomer depolymerization to monomers. *Carbohydr. Res*.**2008**, *343*, 290-300.

36. Kumar, P.; Barrett, D.; Delwiche, M.; Stroeve, P. Methods for pretreatment of lignocellulosic biomass for efficient hydrolysis and biofuel production. *Ind. Eng. Chem. Res.* **2009**, *48*, 3713-3729.

37. Larsson, S.; Palmqvist, E.; Hahn-Hagerdal, B.; Tengborg, C.; Stenberg, K.; Zacchi, G.; Nilvebrant, N. The generation of fermentation inhibitors during dilute acid hydrolysis of softwood. *Enzyme Microb.Technol*. **1999**, *24*, 151-159.

38. Lau, C.; Clausen, E.; Lay, J.; Gidden, J.; Carrier, J. Separation of xylose oligomers using centrifugal partition chromatography with a butanol-methanol-water system. *J. Ind. Microbiol. Biotechnol*. **2013**, *40*, 51-62.

39. Lau, C. 2012. Characterization and quantification of monomers, oligomers, and by-products from xylan during biomass pretreatment. Ph.D. Dissertation, University of Arkansas, Fayetteville, AR.

40. Lau, C.; Bunnell, K.; Clausen, E.; Thoma, G.; Lay, J.; Gidden, J.; Carrier, J. Separation and purification of xylose oligomers using centrifugal partition chromatography. *J. Ind. Microbiol. Biotechnol*. **2011**, *38*, 363-370.

41. Laureano-Perez, L.; Teymouri, F.; Alizadeh, H.; Dale, B. Understanding factors that limit enzymatic hydrolysis of biomass. *Appl. Biochem. Biotechnol.* **2005**, *121-124*, 1081-1099.

42. Li, X.; Converse, A.; Wyman, C. Characterization of molecular weight distribution of oligomers from autocatalyzed batch hydrolysis of xylan. *Appl. Biochem. Biotechnol.* **2003**, *105-108*, 515-520.

43. Lloyd, T.; Wyman, C. Application of a depolymerization model for predicting thermochemical hydrolysis of hemicellulose. *Appl. Biochem. Biotechnol.* **2003**, *105-108*, 53-67.

44. Lynd, L.; Laser, M.; Bransby, D.; Dale, B.; Davison, B.; Hamilton, R.; Himmel, M.; Keller, M.; McMillan, J.; Sheehan, J.; Wyman, C. How biotech can transform biofuels. *Nat. Biotechnol.* **2008**, *26*, 169-172.

45. Mazumder, K.; York, W. Structural analysis of arabinoxylans isolated from ball-milled switchgrass biomass. *Carbohydr. Res.* **2010**, *345*, 2183-2193.

46. McKendry, P. Energy production from biomass (Part 1): Overview of biomass. *Bioresour. Technol.* **2002**, 83, 37-46.

47. Methacanon, P.; Chaikumpollert, O.; Thavorniti, P.; Suchiva, K. Hemicellulose polymer from Vetiver grass and its physicochemical properties. *Carbohydr. Polym.* **2003**, *54*, 335-342.

48. Morinelly, J.; Jensen, J.; Browne, M.; Co, T.; Shonnard, D. Kinetic characterization of xylose monomer and oligomer concentrations during dilute acid pretreatment of lignocellulosic biomass from forests and switchgrass. *Ind. Eng. Chem. Res.* **2009**, *48*,

9877-9884.

49. Mosier, N.; Wyman, C.; Dale, B.; Elander, R.; Lee, Y.; Holtzapple, M. Ladisch, M. Features of promising technologies for pretreatment of lignocellulosic biomass. *Bioresour. Technol.* **2005**, *96*, 673-686.

50. Moure, A.; Gullon, P.; Dominguez, H.; Parajo, J. Advances in the manufacture, purification and applications of xylo-oligosaccharides as food additives and nutraceuticals. *Process Biochem.* **2006**, *41*, 1913-1923.

51. Nabarlatz, D.; Farriol, X.; Montane, D. Kinetic modeling of the autohydrolysis of lignocellulosic biomass for the production of hemicellulose-derived oligosaccharides. *Ind. Eng. Chem. Res.* **2004**, *43*, 4124-4131.

52. Nimlos, M.; Qian, X.; Davis, M.; Himmel, M.; Johnson, D. Energetics of xylose decomposition as determined using quantum mechanics modeling. *J. Phys. Chem.* **2006**, *110*, 11824-11838.

53. Padmore, J. Protein (crude) in animal feed Dumas method. In *Official methods of analysis of association of official analytical chemists,* 15th ed.; Herlich, K., Ed.; Arlington, VA. 1990.

54. Palmqvist, E.; Hahn-Hagerdal, B. Fermentation of lignocellulosic hydrolysates I: inhibition and detoxification. *Bioresour. Technol.* **2000**, *74*, 17-24.

55. Palmqvist, E.; Hahn-Hagerdal, B. Fermentation of lignocellulosic hydrolysates II: inhibitors and mechanisms of inhibition. *Bioresour. Technol.* **2000**, *74*, 25-33.

56. Panagiotou, G.; Olsson, L. Effect of compounds released during pretreatment of wheat straw on microbial growth and enzymatic hydrolysis rates. *Biotechnol. Bioeng.* **2007**, *96*, 250-258.

57. Puls, J.; Schuseil, J. Chemistry of hemicelluloses: Relationship between hemicellullose structure and enzymes required for hydrolysis. *Hemicellulose and Hemicellulases*. **1993**, *4*, 1-27.

58. Qian, X.; Nimlos, M. Mechanisms of xylose and xylo-oligomer degradation during acid pretreatment. In *Biomass recalcitrance: Deconstructing the plant cell wall for bioenergy*, Himmel, M., Ed. Blackwell Publishing Ltd.: Oxford, UK, 2009; 331-351.

59. Qing, Q.; Wyman, C. Supplementation with xylanase and β-xylosidase to reduce xylo-oligomer and xylan inhibition of enzymatic hydrolysis of cellulose and pretreated corn stover. *Biotechnol. Biofuels*. **2011**, *4:18*.

60. Qing, Q.; Yang, B.; Wyman, C. Xylooligomers are strong inhibitors of cellulose hydrolysis by enzymes. *Bioresour. Technol.* **2010**, *101*, 9624-9630.

61. Saha, B. Hemicellulose bioconversion. *J. Ind. Microbiol. Biotechnol.* **2003**, *30*, 279-291.

62. Sanchez, O.; Cardona, C. Trends in biotechnological production of fuel ethanol from different feedstocks. *Biorsour. Technol.* **2008**, *99*, 5270-5295.

63. Sanderson, M.; Reed, R.; McLaughlin, S.; Wullschleger, S.; Conger, B.; Parrish, D.; Wolf, D.; Taliaferro, C.; Hopkins, A.; Ocumpaugh, W.; Hussey, M.; Read, J.; Tischler, C. Switchgrass as a sustainable bioenergy crop. *Bioresour. Technol.* **1996**, *56*, 83-93.

64. Schell, D.; Farmer, J.; Newman, M.; McMillan, J. Dilute-sulfuric acid pretreatment of corn stover in pilot-scale reactor. *Appl. Biochem. Biotechnol.* **2003**, *105*, 69-85.

65. Sharara, M.; Clausen, E.; Carrier, J. An overview of biorefinery technology. In *Biorefinery co-products: Phytochemicals, primary metabolites and value-added biomass processing*, Bergeron, C., Carrier, D., Ramaswamy, S., Eds. John Wiley & Sons, Ltd. West Sussex, UK, 2012; 1-18.

66. Sims, R.; Mabee, W.; Saddler, J.; Taylor, M. An overview of second generation biofuel technologies. *Bioresour. Technol.* **2010**, *101*, 1570-1580.

67. Sluiter, A.; Hames, B.; Ruiz, R.; Scarlata, C.; Sluiter, J.; Templeton, D. Determination of ash in biomass. Technical Report NREL/TP- 510-42622. National Renewable Energy Laboratory: Golden, CO, 2008a; http://www.nrel.gov/biomass/pdfs/42622.pdf.

68. Sluiter, A.; Ruiz, R.; Scarlata, C.; Sluiter, J.; Templeton, D. Determination of extractives in biomass. Technical Report NREL/TP- 510-42619. National Renewable Energy Laboratory: Golden, CO, 2008b; http://www.nrel.gov/biomass/pdfs/42619.pdf.

69. Sluiter, A.; Hames, B.; Ruiz, R.; Scarlata, C.; Sluiter, J.; Templeton, D.; Crocker, D. Determination of structrual carbohydrates and lignin in biomass. Technical Report NREL/TP- 510-42618. National Renewable Energy Laboratory: Golden, CO, 2008c; http://www.nrel.gov/biomass/pdfs/42618.pdf.

70. Sweet, M.; Winandy, J. Influence of degree of polymerization of cellulose and hemicellulose on strength loss in fire-retardant-treated souther pine. *Holzforschung*. **1999**, *53*, 311-317.

71. Ulbricht, R.; Northup, S.; Thomas, J. A review of 5-hydroxymethylfurfural (HMF) in parental solutions. *Fundam. Appl. Toxicol.* **1984**, *4*, 843-853.

72. Vazquez, M.; Alonso, J.; Dominguez, H.; Parajo, J. Xylooligosaccharides: manufacture and applications. *Trends Food Sci. Technol.* **2000**, *11*, 387-393.

73. Williams, D.; Dunlop, A. Kinetics of furfural destruction in acidic aqueous media. *J. Ind. Eng. Chem.* **1948**, *40*, 239-241.

74. Wyman, C.; Dale, B.; Elander, R.; Holtzapple, M.; Ladisch, M.; Lee, Y. Coordinated development of leading biomass pretreatment technologies. *Bioresour. Technol.* **2005a**, *96*, 1959-1966.

75. Wyman, C.; Dale, B.; Elander, R.; Holtzapple, M.; Ladisch, M.; Lee, Y. Comparative sugar recovery data from laboratory scale application of leading pretreatment technologies to corn stover. *Bioresour. Technol.* **2005b**, *96*, 2026-2032.

76. Ximenes, E.; Kim, Y.; Mosier, N.; Dien, B.; Ladisch, M. Deactivation of cellulases by phenols. *Enzyme Microb. Technol.* **2011**, *48*, 54-60.

77. Ximenes, E.; Mosier, K.; Dien, B.; Ladisch, M. Inhibition of cellulases by phenols. *Enzyme Microb. Technol*. **2010**, *46*, 170-176.

78. Yan, J.; Hu, Z.; Pu, Y.; Brummer, E.; Ragauskas, A. Chemical compositions of four switchgrass populations. *Biomass Bioenergy.* **2010**, *34*, 48-53.

79. Yang, B.; Wyman, C. Pretreatment: The key to unlocking low-cost cellulosic ethanol. *Biofuels, Bioprod. Biorefin.* **2008**, *2*, 26-40.

80. York, W.; Darvill, A.; McNeil, M.; Stevenson, T.; Albersheim, P. Isolation and characterization of plant cell walls and cell wall components. *Methods Enzymol.* **1985**, *118*, 3-40.

81. Yuan, Q.; Zhang, H.; Qian, Z.; Yang, X. Pilot-plant production of xylo-oligosaccharides from corncob by steaming, enzymatic hydrolysis and nanofiltration. *J. Chem. Technol. Biotechnol.* **2004**, *79*, 1073-1079.